# ATP-activated channels in rat superior cervical ganglion neurones and their modulation by extracellular zinc

A thesis submitted for the Doctorate of Philosophy

University of London

by

Robin Cloues

Department of Pharmacology

University College London

Gower Street

London WC1E 6BT

ProQuest Number: 10017739

All rights reserved

INFORMATION TO ALL USERS
The quality of this reproduction is dependent upon the quality of the copy submitted.

In the unlikely event that the author did not send a complete manuscript
and there are missing pages, these will be noted. Also, if material had to be removed,
a note will indicate the deletion.



ProQuest 10017739

Published by ProQuest LLC(2016). Copyright of the Dissertation is held by the Author.

ProQuest LLC
789 East Eisenhower Parkway
P.O. Box 1346
Ann Arbor, MI 48106-1346

# Abstract

It has recently been shown that adenosine 5'-triphosphate (ATP) can act as a fast excitatory transmitter at neuro-neuronal synapses in both the central and the peripheral nervous systems. I have examined the ATP-activated inward current ($I_{ATP}$) in cultured rat superior cervical ganglion (SCG) neurones and its modulation by extracellular zinc ions ($Zn^{2+}$). ATP activated a non-specific cation conductance and caused a transient rise in intracellular $Ca^{2+}$ which was dependent on extracellular $Ca^{2+}$. The current was activated specifically by ATP and was reversibly blocked by the $P_2$-purinoceptor antagonist, suramin. Low concentrations of extracellular $Zn^{2+}$ rapidly and reversibly potentiated both $I_{ATP}$ and the intracellular $Ca^{2+}$ rise. Higher concentrations of $Zn^{2+}$ reduced and prolonged the current. Other divalent cations mimicked the effect of $Zn^{2+}$ with an order of potency of: $Cu^{2+} > Zn^{2+} > Ni^{2+} > Cd^{2+} > Co^{2+} > Mn^{2+}$. The potentiation by $Zn^{2+}$ was dependent on the concentration of agonist; $Zn^{2+}$ increased the apparent affinity of the receptor for ATP without potentiating the maximum response. Single channels activated by ATP, and reversibly blocked by suramin, were recorded using excised outside-out patches. The channels were small (conductance at -80 mV = 11 pS). Both single channel conductance and opening probability increased with hyperpolarization. Low concentrations of $Zn^{2+}$ significantly increased the frequency of ATP-evoked channel opening and burst duration without altering the unitary conductance. Higher concentrations of $Zn^{2+}$ further increased channel burst duration but also decreased unitary current amplitude. These results are consistent with two sites of action for $Zn^{2+}$: a positively acting allosteric site which enhances macroscopic current amplitude and a site, possibly within the pore, which blocks conductance through the channel. In conclusion, the $P_{2x}$-purinoceptor in rat SCG neurones is allosterically regulated by changes in concentration of extracellular $Zn^{2+}$, increasing both $I_{ATP}$ amplitude and ATP-evoked changes in intracellular $Ca^{2+}$.

# Table of Contents

**Table of Contents (cont.)**

**Table of Contents (cont.)**

# Table of Contents (cont.)

## List of Figures and Tables

**List of Figures (cont.)**

**List of Figures (cont.)**

## Acknowledgements

---

-in memory of my grandmother-

**<u>Chapter 1:  Introduction</u>**

The importance of adenosine 5'-triphosphate (ATP) as a source of energy for cell metabolism is well established. In recent years, it has become apparent that ATP is also used externally by a variety of different tissues. Pioneering work by Burnstock and colleagues in the early 1970's showed that ATP is released from sympathetic nerves innervating various smooth muscle tissues and acts as a neurotransmitter or a neuromodulator at these synapses. Since that time it has been shown that ATP is a transmitter at neuro-neuronal synapses in the central and peripheral nervous systems as well.

## Historical Background

The study of the biological activity of adenine compounds began in the late 1920's. In these early studies, a compound isolated from heart muscle, termed adenylic acid, was shown to negatively influence cardiac activity when injected intravenously into animals (Drury & Szent-Gyorgyi, 1929; Bennet & Drury, 1931). The effects of adenylic acid were not specific to cardiac tissue but could also affect smooth muscle from blood vessels and the intestinal tract. It was proposed that the compound isolated from the heart was adenosine since injection of adenosine mimicked the effects of adenylic acid.

Hints that ATP could also have biological activity came from studies on sensory innervation of rabbit ear artery. As early as 1953 it was suspected that ATP was responsible for capillary vasodilation caused by antidromic stimulation of dorsal root fibres (Holton & Holton, 1953). ATP mimicked the effect of stimulation, extracts of dorsal root neurones had similar chemical characteristics to ATP, and application of the substance isolated from dorsal roots caused vasodilation (Holton & Holton, 1954). Using a specific assay for ATP, it was demonstrated that ATP was released during stimulation of sensory nerves innervating the blood vessels (Holton, 1959).

Although the above studies clearly demonstrated that ATP was a transmitter in the rabbit ear artery, the broader hypothesis of purinergic transmission was not put

forward until the 1970's. The hypothesis was based on studies of parasympathetic or enteric innervation of intestinal tissue in guinea pigs and toad (Burnstock *et al.*1970). Nerve stimulation elicited inhibitory junction potentials (IJPs) which caused relaxation of the smooth muscle. These responses were not blocked by antagonists to either cholinergic or adrenergic receptors (Burnstock *et al.*1963; Burnstock *et al.*1964) and were therefore placed into the generic category of non-adrenergic, non-cholinergic (NANC) transmission. The muscle relaxations could be mimicked, however, by application of ATP (Burnstock *et al.*1970). Effects of exogenously applied ATP (both contractions and relaxations) have been demonstrated in other smooth muscle preparations including urinary bladder, vas deferens, and numerous blood vessels (for review see Hoyle, 1992).

Evidence supporting ATP as a transmitter in smooth muscle tissue accumulated over the following years. It was demonstrated that ATP was stored in vesicles in sympathetic nerves (Aberer *et al.*1979), that ATP was released from nerve terminals during stimulation (Su *et al.*1971; Burnstock *et al.*1978b; Cunnane & Stjarne, 1984; Stjarne & Astrand, 1984), and that responses to both nerve stimulation and exogenously applied ATP could be blocked by specific antagonists (Fedan *et al.*1981; Sneddon & Burnstock, 1984; Sneddon & Westfall, 1984). With these findings, it became generally accepted that ATP mediated transmisssion at many peripheral synapses. In 1971 in a letter to Nature (Burnstock, 1971), Burnstock coined the term "purinergic" to refer to ATP-mediated transmission.

## Co-transmission

ATP is frequently released together with other transmitters such as noradrenaline (NA) and acetylcholine (ACh). This has been clearly demonstrated in the vas deferens where the contractile response to nerve stimulation is biphasic: an early fast twitch contraction is mediated by ATP and a slower, longer lasting contraction is mediated by NA (French & Scott, 1983; Meldrum & Burnstock, 1983; Kirkpatrick & Burnstock, 1987). Both responses can be blocked by chemical sympathectomy, indicating that the

transmitters are released from the same set of nerves (Allcorn *et al.* 1986). Co-release has been substantiated by studies at the single cell level: sympathetic cells grown individually in co-cultures with cardiac myocytes release ACh, ATP, and NA, with the proportion of each varying between cells (Potter *et al.* 1983). It has also been suggested that ATP can be co-released with other transmitters such as neuropeptide Y (NPY) in sympathetic nerves innervating blood vessels (Morris & Gibbins, 1992) and ACh in motoneurones (Silinsky & Hubbard, 1973) (for review on co-transmission see Morris & Gibbins, 1992).

## Effect of ATP on neurones

In addition to smooth muscles, a variety of neuronal preparations also respond to exogenously applied ATP. The first demonstration of an action of ATP on nerve cells was in spinal cord neurones from the dorsal horn (Jahr & Jessel, 1983). In these cells ATP caused depolarization and enhanced excitability. Since that time a variety of neurones have been shown to respond to ATP, including sensory neurones (Jahr & Jessel, 1983; Krishtal *et al.* 1988; Bean, 1990b), sympathetic neurones (Akasu *et al.* 1983a; Evans *et al.* 1992), intracardiac neurones (Allen & Burnstock, 1990), and parasympathetic cells (Fieber & Adams, 1991) in the peripheral nervous system; and in the central nervous system (CNS) neurones from the locus coeruleus (Harms *et al.* 1992; Shen & North, 1993), supraoptic nucleus (Day *et al.* 1993), nucleus solitarii (Ueno *et al.* 1992b), medial habenula (Edwards *et al.* 1992), and caudal trigeminal nucleus (Salt & Hill, 1983). In all of these preparations ATP opens non-specific cation channels which allow $Na^+$ into the cell thus depolarizing the neurone.

ATP-gated channels are also permeable to $Ca^{2+}$, which can have important physiological consequences. $Ca^{2+}$ entry can activate second messenger cascades, $Ca^{2+}$-dependent enzymes such as protein kinase C, and other ion channels. Indeed, it has been demonstrated that in rat nucleus solitarii neurones, $Ca^{2+}$ entry through ATP-gated channels can activate a $K^+$ conductance (Ueno *et al.* 1992a). In addition, $Ca^{2+}$ influx through ATP-gated channels can modulate transmitter release in

pheochromochytoma PC12 cells (Nakazawa & Inoue, 1992). It has been postulated that ATP-mediated $Ca^{2+}$ entry could be important in long-term potentiation (LTP)-like phenomena, which are dependent on $Ca^{2+}$ entry (Edwards & Gibb, 1993). Unlike the NMDA receptor, which requires both transmitter (glutamate) and concomitant depolarization to relieve the voltage-dependent $Mg^{2+}$ block (Nowak et al. 1984), ATP-gated channels are opened at resting membrane potential. ATP is released from hippocampal cells during stimulation in a $Ca^{2+}$-dependent manner (Wieraszko et al. 1989a; Wieraszko & Seyfried, 1989b) and can induce LTP in hippocampal slices (Wieraszko & Seyfried, 1989). These findings make the characterization and study of ATP receptor-channels in different neuronal preparations all the more pertinent.

It was recently demonstrated that neurones can form purinergic synapses with each other in both the central and the peripheral nervous systems. Guinea pig coeliac ganglion cells (sympathetic neurones) will form purinergic synapses when grown in culture (Evans et al. 1992; Silinsky & Gerzanich, 1993). Spontaneous excitatory postsynaptic potentials in these cells are blocked by the ATP-receptor antagonist, suramin, and mimicked by application of exogenous ATP. Neurones in intact sympathetic ganglia also respond to ATP (Silinsky & Gerzanich, 1993), suggesting that expression of ATP receptors is not an artifact of tissue culture.

In the CNS, ATP mediates synaptic transmission in the medial habenula (Edwards et al. 1992). Both spontaneous and evoked synaptic currents recorded in slice preparations are specifically blocked by suramin but are not affected by antagonists of other transmitters. ATP therefore joins the short list of fast neurotransmitters in the CNS. In the brain, only glutamate and ATP have been unequivocally demonstrated to mediate fast excitatory transmission.

## Receptor classification

The recognition that ATP activated a receptor distinct from the adenosine receptor came in 1978 with the division of purinergic receptors into two families (Burnstock, 1978a). $P_1$-purinoceptors are preferentially activated by adenosine (see

Reddington & Lee, 1991 for review) and will not be discussed in this report. $P_2$-purinoceptors are activated by ATP and have been futher divided into 5 major subclasses based on agonist selectivity and transduction mechanisms. Three of the receptors are G protein-linked ($P_{2y}$, $P_{2u}$, $P_{2t}$), one ($P_{2x}$) is a ligand-gated ion channel, and one ($P_{2z}$) is present on mast cells, macrophages and fibroblasts, but its signaling mechanism is not well understood (for review of classification see Gordon, 1986; Hoyle, 1992; Abbracchio & Burnstock, 1993; Dubyak & El-Moatassim, 1993). $P_{2u}$ receptors are classified by their activation by both UTP and ATP (Davidson et al.1990; O'Connor et al.1991). A $P_{2u}$ receptor has recently been cloned from NG108-15 cells (Lustig et al.1993). The $P_{2t}$ receptor is located on platelets and is preferentially activated by ADP; ATP is a competitive antagonist at this receptor (Cusack et al.1979).

$P_{2x}$- and $P_{2y}$-purinoceptors are the two main classes of ATP-activated receptors. They differ in their agonist potency profiles in addition to their signalling mechanisms (Burnstock & Kennedy, 1985). Like other transmitter substances in the nervous system (GABA, glutamate, and ACh), ATP can activate either a ligand-gated ion channel ($P_{2x}$) which mediates fast transmission or a G protein-linked receptor ($P_{2y}$) which is neuromodulatory. The $P_{2y}$ receptor has recently been cloned from whole chick brain and displays the characteristic topology of G protein-linked receptors (Webb et al.1993). However, there is only limited sequence identity (27%) with other G protein-linked receptors, suggesting that this receptor is a member of a new subfamily. The $P_{2x}$ receptor has not been cloned at this time.

A complete classification of $P_2$-purinoceptors has been limited by the lack of specific antagonists, radioligands, and cloned receptor cDNAs. Reactive Blue 2 is a $P_{2y}$ receptor antagonist in some preparations (Burnstock & Warland, 1987), but the effects are variable and the dye is toxic and difficult to use. Neomycin is a $P_{2x}$ receptor antagonist in outer hair cells (Lin et al.1993) but has not been studied in neuronal preparations. $\alpha,\beta$-methyleneATP selectively desensitizes $P_{2x}$ receptors in smooth muscle tissue (Kasakov & Burnstock, 1983) but is not consistent between

preparations. The most commonly used antagonist for $P_2$-purinoceptors is the trypanocidal drug, suramin, which blocks responses to ATP but not other transmitters (Dunn & Blakeley, 1988). However, this drug does not distinguish between $P_{2x}$- and $P_{2y}$-purinoceptors (Hoyle *et al.* 1990), making its usefulness for classification limited. With the recent cloning of the $P_{2u}$ and $P_{2y}$ receptors (Lustig *et al.* 1993; Webb *et al.* 1993), new methods to study the classification, as well as the distribution of purinoceptors, will be available. At the present time, electrophysiological and biochemical methods remain the best means for ATP receptor classification.

## Statement of purpose

The responses to ATP in most neuronal preparations examined are mediated by ionotropic $P_{2x}$ receptors. In these various preparations, ATP opens non-specific cation channels, resulting in depolarization of the cell membrane. ATP is therefore described as an excitatory transmitter (Jahr & Jessel, 1983) as opposed to a neuromodulator. In some neuronal preparations, however, the G protein-linked (either $P_{2y}$ or $P_{2u}$) receptor is activated. These include sympathetic and sensory neurones from bullfrog (Akasu *et al.* 1983a; Morita *et al.* 1984; Tokimasa & Akasu, 1990), as well as glial cells (Magoski & Walz, 1992; Walz *et al.* 1993) and various neuronal cell lines (PC12 cells: Clementi *et al.* 1992; NCB-20 cells: Aberer *et al.* 1979; Garritsen *et al.* 1992; NG108-15 cells: Lustig *et al.* 1993). The aim of this thesis was to examine the responses of sympathetic neurones cultured from rat SCG to exogenously applied ATP, both at the whole-cell and single channel level, and to classify the receptor subtype present in these cells. In addition, modulation of the responses by extracellular $Zn^{2+}$ is described, and a mechanism for this effect is proposed.

Two reports have recently been published which pertain directly to the work presented here. Nakazawa & Inoue (1993) briefly describe ATP-activated channels in excised patches from rat SCG neurones. Li and coworkers (1993) have shown $Zn^{2+}$ modulation of ATP-evoked whole-cell currents in rat sympathetic neurones. These papers were published after completion of the experiments presented in this thesis.

**<u>Chapter 2:  Methods</u>**

## I. Tissue culture

Cultured rat superior cervical ganglion (SCG) neurones were used for all studies. Cells were cultured using methods previously described (Marrion *et al.* 1987). Briefly, 15-19 day Sprague-Dawley rats were killed using carbon dioxide and the ganglia surgically removed. The ganglia were mechanically desheathed and cut into four pieces. The pieces were incubated 15 minutes in collagenase (390 units/ml), washed three times in Hank's Balanced Salt Solution (HBSS; no $Ca^{2+}$, no $Mg^{2+}$) containing 10 mM HEPES, and then incubated 30 minutes in trypsin (type XII-S; 10,000 units/ml). Both the collagenase and the trypsin were diluted in HBSS containing bovine serum albumin (6 mg/ml). Following trypsin incubation, the neurones were triturated using a fire-polished glass pipette, centrifuged (3 min; 900 revolutions per minute), and resuspended in incubation medium containing: Leibovitz L15 medium, fetal calf serum (10%), glucose (0.7%), penicillin (50 units/ml), streptomycin (50 $\mu$g/ml), L-glutamine (2 mM), bicarbonate, and nerve growth factor (50 ng/ml). Cells were plated onto laminin-coated dishes and maintained 1-4 days in an incubator (37° C, 95% $O_2$/5% $CO_2$).

## II. Electrophysiology

### Whole-cell recording

For electrophysiological recording, plates of cultured rat SCG neurones were placed on the stage of an inverted microscope (Nikon TMS) and superfused with a bicarbonate buffered Krebs' solution of the following composition (mM): NaCl 120; KCl 3; $MgCl_2$ 1.2; $NaHCO_3$ 22.6; $CaCl_2$ 2.5; D-glucose 11.1; HEPES 5. The Krebs' solution was superfused by gravity at a rate of 6-12 ml/min at room temperature. The plate contained 1-2 ml of solution. The pH was maintained around 7.4 by constantly gassing with 95% $O_2$/5% $CO_2$.

Voltage-clamp experiments were performed using single patch-clamp pipettes in the whole-cell recording configuration (Hamill *et al.* 1981). The patch pipettes (5-10 MOhm) were pulled on a Kopf vertical pipette puller using thin-walled filament glass (Clark Electromedical). Electrodes were coated with a thin layer of Sylgard and fire-polished. For recording, the patch pipettes were filled with a solution of the following composition (mM): potassium or caesium acetate 102.4; KCl 15.6; HEPES 40; $MgCl_2$ 1; NaOH 12; EGTA 1; $CaCl_2$ 0.420 (buffered with EGTA = 100 nM); pH 7.2.

For recording, patch electrodes were held in a Perspex holder attached to a Narishige mechanical micromanipulator. Constant voltage pulses (-2 mV, 10 ms) were applied through an Axopatch 1-D amplifier (Axon Instruments) and the conductance monitored on a storage oscilloscope (Tektronix). Before sealing onto the cell, the pipette current was adjusted so that I = 0; the reference ground was a silver wire coated with silver chloride. Using the manipulator, the electrode was lowered onto the cell until a small decrease in the conductance was detected. Gentle suction was applied to the patch electrode until a high resistance (5-50 GOhm) seal was obtained. The fast capacity transients were compensated, and the holding potential was set at -60 mV. A quick application of stronger suction was then used to rupture the underlying membrane and obtain access to the interior of the cell. The series resistance was usually compensated 60-70%.

In a few experiments, the nystatin perforated-patch technique was used to record $I_{ATP}$ (Horn & Marty, 1988). Nystatin was dissolved 50 mg/ml in dimethyl sulphoxide (DMSO), sonicated for 30 seconds and diluted 1/250 in intracellular solution containing no EGTA or $CaCl_2$. Patch electrodes were dipped in filtered intracellular solution for 2-10 seconds and then backfilled with the nystatin solution. After obtaining a high resistance seal, the gradual development of slow capacity transients was monitored; this generally took 5-10 minutes. Cells in which there occurred a fast jump in whole-cell capacitance were excluded as this was assumed to be breakthrough into the whole-cell mode (this was also indicated by a developing inward current). Recording began

when the uncompensated series resistance reached $<50$ MOhm. As in whole-cell

recording, series resistance was usually compensated 60-70%. The maximum series

resistance was, therefore, 20 MOhm, giving a $V_{error}$ of 20 mV/nA current. However,

because ATP-activated currents were usually 100-200 pA, no correction was made.

Adenosine 5'-triphosphate (ATP; $Mg^{2+}$ salt) was applied to the cells either in

the bath or by pressure ejection (20-100 ms, 70-100 KPa) through a second pipette

placed 10-50 $\mu$m from the cell soma (estimated by eye). ATP-evoked currents were

monitored on a thermal array chart recorder (Gould TA240 EasyGraf).

Pharmacological agents and divalent cation solutions were applied via the bath. Data

was recorded and analyzed on a Ness PC-486 computer using the pClamp acquisition

and analysis programs, Clampex, Clampan, and Clampfit (Axon Instruments).

Integration of current records was performed using software developed by Dr. S.J.

Marsh (University College London).

In some experiments, the ionic composition of the external medium was

changed. Low $Na^+$ solution contained (mM): N-methyl-D-glucamine 144.6; KCl 3;

$MgCl_2$ 1.2; $CaCl_2$ 2.5; glucose 11.1; $NaHCO_3$ 22.6; HEPES 5; pH 7.4. High

$Ca^{2+}$ solution contained (mM): $CaCl_2$ 120; HEPES 3.2; glucose 3.6; pH 7.4 with

$Ca(OH)_2$. For these experiments, ATP was applied diluted in the respective external

solution. The change in potential at the bath ground during solution changes was

measured as described in Neher (1992). A saturated KCl (3 M) wide-bore patch pipette

was used as the reference electrode and zeroed in standard Krebs solution. With high

KCl, the liquid junction potential should not alter substantially during solution changes.

The potential seen by a chlorided silver ground wire, identical to the usual ground

electrode in the experimental setup, was then measured in different external solutions.

For the low $Na^+$ solution the junction potential was -6 mV and for the high $Ca^{2+}$

solution it was -9 mV. These values were not subtracted from the data.

The liquid junction potential between the pipette solution (caesium acetate based

solution) and the normal extracellular solution was also measured as described in Barry

& Lynch (1991) and Neher (1992). Again using a wide-bore patch pipette filled with 3

M KCl as the reference electrode, the amplifier voltage was zeroed with internal solution in both the bath and the recording electrode. The bath solution was then exchanged for normal extracellular Krebs. The junction potential between the internal and external solutions was -2.1 mV (n=3). This value was not subtracted from the experimental data.

## Series resistance errors

In whole-cell experiments, the measured series resistance ($R_s$) was 10-20 MOhm. This was compensated 60-70%, giving a final series resistance of 3-8 MOhm. For current-voltage relation experiments, the holding potential was corrected for by subtracting the voltage error, calculated from the equation $V_{error} = IR_s$, from the nominal holding current. In most other experiments the membrane voltage of the cell was held constant at -60 mV, $I_{ATP}$ was small, and the error was calculated to be <3 mV; no correction of holding potential was made for these experiments.

During activation of $I_{ATP}$ the resistance of the cell membrane changed from 455 ± 84 MOhm to 170 ± 63 MOhm (n=6; measured using conductance pulses of -10 mV). In whole-cell recording mode, $R_s$ would still be significantly less than the resistance of the cell membrane ($R_m$; 8 MOhm vs 170 MOhm), so it can be safely assumed that $V_{error}$ was small even at peak $I_{ATP}$ amplitude and that the voltage of the cell did not vary from the command potential.

The specific capacitance of SCG cell membranes was estimated by measuring the membrane time constant ($\tau$). $\tau$ was determined from the exponential fit of the decay following a 10 mV step change in voltage. Average capacity (calculated using the equation $\tau = R_m C$) was 56.8 ± 7.5 pF (n=11). $C_m$ is assumed to be 1 $\mu F/cm^2$ giving an average membrane area of approximately 5500 $\mu m^2$. This would be equivalent to the area of a sphere with a diameter of 42 $\mu m$, which accords well with the average size of SCG neurones (Gabella, 1985).

## Single channel recording

Currents through single ATP-activated channels were recorded using excised outside-out patches (Hamill *et al.* 1981). High resistance patch pipettes (10-15 MOhm) were used to minimize the number of channels in the patch. The patches were also more stable and had a lower baseline noise if the pipette resistance was high. The pipette solution contained (mM): Cs Gluconate 86; CsCl 9; HEPES 7; EGTA 1; $CaCl_2$ 0.420 (buffered with EGTA = 100 nM); pH 7.3. To form outside-out patches, the whole-cell recording configuration was obtained, and the patch pipette was slowly withdrawn from the cell until a high resistance seal had been formed. The resistance was monitored using -2 mV, 10 ms pulses. Only patches with a stable baseline noise <0.5 pA and low spontaneous channel activity were used. ATP was applied to the patch either by pressure ejection (10-100 $\mu$M) or, more commonly, in the bath. Using the gluconate-based pipette solution, ATP channels could be recorded for up to 40 minutes without significant rundown. $Zn^{2+}$ (3-100 $\mu$M) was included in the bath. In some experiments, $Zn^{2+}$ was added to the bath 1 minute prior to application of ATP. All recordings were performed at room temperature.

In some experiments, single channel currents were recorded using nystatin perforated vesicles (Levitan & Kramer, 1990). After reaching a whole-cell series resistance <50 MOhm with nystatin in the pipette solution, as described above, the pipette was slowly withdrawn from the cell. ATP was applied to the patch as described for outside-out patches. Single channel currents activated by ATP were recorded onto a DTR-1202 Digital Tape Recorder (Biologic) and stored for later analysis.

## Single channel analysis

Single channel currents were low-pass filtered at 250-1000 Hz (-3 dB Bessel filter, Barr and Stroud) and digitized using either the PAT single channel analysis program (J. Dempster, University of Strathclyde) or pClamp software (Fetchex). Records were sampled at 5 times the filter frequency. Channel openings were identified using the 50% threshold-crossing method, and an ideal record of openings

was made. The open and closed levels were determined by Gaussian distributions fitted to the all point histogram of the record (see below). In some patches a large channel with low spontaneous activity, not correlated with the presence of ATP, was seen. Openings of this channel were omitted from the idealized record.

For amplitude histograms, the distribution was plotted as a percentage of the total recording time. Three points were excluded at the start and end of each state so that only complete openings were included. The minimum resolvable channel opening was 2 ms. Gaussian curves were fitted to the histogram using a non-linear least squares routine. These were then used to determine the mean current amplitude of each open state. The area under the curve was used to determine the relative time the channel resided in each state.

Channel open probability was estimated as nPo, the product of the number of channels in the patch times the percent time the channel resided in the open state.

To estimate channel burst duration, closed time distributions were made for each record using software created by D. Colquhoun and A. Gibb (University College London). Records were chosen which had a low density of events to avoid the problem of overlap of several channels. Records were filtered at 750 Hz and digitized at 3.3 KHz. Fitting of exponentials was done by the method of maximum likelihood. The distributions were usually fitted with 2 or 3 well-separated exponentials, the shortest of which was assumed to be intraburst closures. A value of 5 times this shortest mean closure was used as a critical gap length ($T_{crit}$) to define the burst, i.e. closures shorter than this value were omitted.

## III. Intracellular $Ca^{2+}$ measurements

Intracellular $Ca^{2+}$ was estimated using Indo-1 fluorescence by dual wavelength emission. For these experiments, SCG cells were grown on laminin-coated glass coverslips and the coverslips placed on the stage of an inverted microscope (Nikon 'Diaphot'). Cells were illuminated by a 75 W Xenon arc lamp (Osram XBO-75) via a

quartz lens and 360 nm excitation filter (330-380 nm bandwidth). UV light was reflected by a 400 nm dichroic mirror and passed through an oil immersion objective (Nikon x 40 fluorite, NA 1.3). To avoid photobleaching, neutral density filters reduced illumination by 0.6 log units, and illumination was restricted to the cell recorded using a field diaphragm. Emitted light was collected from an aperture-limited field just greater than the area of the cell and split by a 430 nm dichroic mirror to two photomultipliers (Thorn EMI QL 30; power source PM 28B, 900 V DC) at 407 and 488 nm. Anodal currents were converted to voltage and fed into a differential amplifier providing continuous outputs of individual wavelength emissions and the ratio of emissions at 407 and 488 nm ( = R).

Intracellular $Ca^{2+}$ levels during application of ATP were measured in voltage-clamped cells. Indo-1 (200 $\mu$M) was included in the patch pipette solution and the 407/488 emission ratio (R) and membrane current were simultaneously recorded. The pipette solution contained (mM): Cs Acetate 108; CsCl 30; HEPES 10; $MgCl_2$ 1; BAPTA 0.1. For each cell, autofluorescence was measured under cell-attached configuration (before breakthrough) and amplifier outputs offset to zero. $Ca^{2+}$ concentrations were determined using the equation (Grynkiewicz et al. 1985):

$$[Ca^{2+}] = K_d(F_o/F_s)(R-R_{min})/(R_{max}-R)$$

where $R_{min} = 0.38$, $R_{max} = 4$, and $K_d(F_o/F_s) = 1400$ nM (Robbins et al. 1992). For $Ca^{2+}$-free experiments, $CaCl_2$ was omitted from the extracellular solution and $MgCl_2$ (5 mM) was added to compensate for surface charge effects and maintain seal stability. ATP was applied by pressure application or via the bath; $Zn^{2+}$ was applied via the bath.

## IV. Chemicals

Tissue culture media were purchased from Sigma with the exception of
collagenase (Worthington Biochemical Corporation). Standard laboratory chemicals
used for making solutions were purchased from BDH Limited. Suramin was purchased
from Bayer. Adenosine 5'-triphosphate ($Mg^{2+}$ salt), other nucleotides and nucleosides
and nystatin were purchased from Sigma. ATP was stored at -20° C in 100 mM
aliquots in $dH_2O$ until needed. Nystatin was kept at -20° C and made fresh before use.
2-methylthioadenosine triphosphate tetrasodium salt (2-methylthioATP) was purchased
from Research Biochemicals Inc. 1,1-dimethyl-4-phenylpiperazinium iodide (DMPP)
was purchased from Aldrich. Indo-1 pentasodium salt was purchased from
Calbiochem.

# Chapter 3:  Characterization of $I_{ATP}$ in SCG cells

# I. Introduction

As discussed in Chapter 1, ATP affects neurones from a variety of areas of the central and peripheral nervous sytems. In most cases, ATP activates a $P_{2x}$ receptor, causing rapid depolarization, similar to other fast neurotransmitters. Indeed it has been demonstated that ATP mediates synaptic transmission in the medial habenula (Edwards et al. 1992) and in guinea pig coeliac ganglion (Evans et al. 1992; Silinsky & Gerzanich, 1993).

ATP has been reported to have several different actions on sympathetic neurones. In superior cervical ganglion cells from the bullfrog, ATP acts on a G protein-linked receptor to depolarize neurones by inhibiting a potassium current (Akasu et al. 1983a) and also increases the sensitivity of nicotinic ACh receptors (Akasu et al. 1983b; Akasu & Koketsu, 1985). In mammalian coeliac ganglion sympathetic cells, ATP acts on a $P_{2x}$ receptor, activating a non-specific cation channel (Evans et al. 1992; Silinsky & Gerzanich, 1993). In addition, ATP can reduce transmitter release from frog (ACh; Silinsky & Ginsborg, 1983) and rat (noradrenaline; von Kûgelgen et al. 1993) sympathetic neurones. This effect appears to be mediated by a G protein-linked receptor and not the $P_{2x}$ receptor (at least in rats) as the action is blocked by pertussis toxin (von Kûgelgen et al. 1993). While it has been established that superior cervical ganglion neurones store (Richards & Prada, 1977; Tolkovsky & Suidan, 1987) and release (Wolinsky & Patterson, 1985; Furshpan et al. 1986; McCaman & McAfee, 1986) ATP, the action of exogenously applied ATP on rat SCG cells has only recently been described (Cloues et al. 1993; see Supplementary Material). This chapter characterizes the action of exogenously applied ATP on cultured sympathetic cells from the rat SCG. Li and coworkers (Li et al. 1993) have recently reported comparable observations to some of those described in the following account, after the experiments presented in this report were completed.

## II. Results

Membrane effects of ATP on SCG cells

Application of extracellular ATP depolarized rat SCG neurones. Figure 1A (top trace) shows the voltage response of one cell in response to a short application of ATP. ATP caused a rapid depolarization of the cell membrane potential with a corresponding decrease in input resistance. In some cells the depolarization was large enough to initiate action potentials. Figure 1A (bottom trace) shows the current underlying the ATP-induced depolarization. ATP evoked an inward current ($I_{ATP}$) accompanied by an increase in conductance. Inward currents were recorded in response to ATP in all cells tested, though the current amplitude varied between cells (mean current at Vm -60 mV: -145 ± 94 pA (SD); n = 39).

The current response in SCG cells declined during prolonged exposure to ATP (Figure 1B). The decline in amplitude in the presence of agonist was accompanied by a decrease in conductance and was relatively slow (half time 11.5 ± 0.9 s SEM; n=7). In addition to this slow waning, ATP currents tended to run down with repeated applications of ATP, particularly with long exposures. For three cells in which ATP was applied once every 30 seconds (30 ms applications), the rate of rundown was 3.2 ± 1.6% per exposure. The current rundown was not prevented by inclusion of ATP (2 mM) and GTP (0.5 mM) in the recording solution nor by altering the intracellular anions or $Ca^{2+}$ buffering. Rundown was decreased in cells recorded using the nystatin perforated-patch technique, which minimally alters the intracellular constituents. However, in most experiments, the whole-cell recording method was used. ATP applications were usually kept to a short duration (< 100 ms) to minimize the decline in current amplitude.

Concentration-response relationship

The concentration/response relationship for $I_{ATP}$ is shown in Figure 2. Different concentrations of ATP were bath applied to the cell, with the order of

concentrations randomized. A 3 minute wash followed each application to minimize current rundown. Current responses were normalised by reference to the average of an initial and a final response to 100 $\mu$M ATP for a given cell. 100 $\mu$M ATP was taken to be maximum as higher concentrations did not substantially increase current amplitude but did result in greater current rundown. The threshold for activation of $I_{ATP}$ under these conditions was 10 $\mu$M. The $EC_{50}$ value was estimated to be 45 $\mu$M (curve fit by eye).

## Voltage dependence of $I_{ATP}$

Figure 3 shows the voltage dependence for $I_{ATP}$ in one cell, recorded using caesium in the pipette solution. $I_{ATP}$ was evoked by pressure application of ATP at holding potentials between -120 mV and +20 mV. The current amplitude increased as the potential was held more negative and decreased closer to 0 mV. During the course of the experiment, there was approximately 15% rundown of $I_{ATP}$, measured from the initial and final responses at -60 mV. The measurements at more positive potentials are therefore slightly underestimated. However, the general shape of the I/V curve was confirmed in other experiments in which the membrane potential was held at positive potentials first.

The current/voltage curve showed strong inward rectification; outward currents were very small at holding potentials positive to 0 mV. In some cells, there was no reversal of the current direction; the term "null potential" will therefore be used in place of "reversal potential". The null potential in 6 experiments using $K^+$ in the intracellular solution was -7 $\pm$ 4 mV. This null potential does not correspond to the equilibrium potential of any individual cation present in the intra- and extracellular solutions, suggesting that $I_{ATP}$ is carried through non-selective ion channels. When intracellular $K^+$ was replaced with $Cs^+$ the measured null potential was +8.5 $\pm$ 3.8 mV (n=4). There was no significant change in the rectification.

## Permeability of ATP-gated channels

To examine the permeability of ATP-gated channels, external $Na^+$ was replaced with the large cation NMDG. Under low $Na^+$ conditions (external $Na^+$ = 22.6 mM), ATP (pressure application, ATP dissolved in low $Na^+$ solution) activated only a small inward current compared to control (Figure 4A)($I_{ATP}$ = 21 ± 7% of control, Vm -60 mV; n=4). Increasing the duration of the ATP application from 50 ms to 150 ms (which presumably increases the concentration of ATP reaching the cell) increased both control and low-$Na^+$ $I_{ATP}$ amplitude, but the low-$Na^+$ current remained small compared to control (45% of control; n=2)(i.e. the reduction in current amplitude could not be overcome by increasing ATP concentration).

$I_{ATP}$ in low $Na^+$ was reduced at all potentials measured and showed an apparent shift in the extrapolated null potential of approximately -20 mV (Figure 4B; n=2). This is consistent with NMDG acting as an impermeant ion as opposed to a receptor antagonist. Replacement of external $Na^+$ with another large cation, choline, also reduced $I_{ATP}$ amplitude by 79% and 85% for 2 cells. In one other cell, there was an outward current in response to ATP in the choline chloride solution. Due to the rectifying nature of $I_{ATP}$, detailed examination of channel permeability (usually based on shifts in reversal potential) could not be adequately completed.

## Effect of ATP on intracellular $[Ca^{2+}]$

The effect of ATP on intracellular $Ca^{2+}$ levels was estimated using Indo-1 fluorescence. In voltage-clamped cells, ATP elicited a transient rise in $[Ca^{2+}]_i$ of 88 ± 14 nM (n=5; Figure 5, control column) which closely followed the time course of the inward current. No increase in $[Ca^{2+}]_i$ was observed in $Ca^{2+}$-free solution (n=4; Figure 5, middle column), indicating that the rise is dependent on extracellular $Ca^{2+}$. Replacement of $Ca^{2+}$ immediately restored the ATP-mediated $Ca^{2+}$ rise. For $Ca^{2+}$-free experiments, extracellular $Mg^{2+}$ was raised (to 5 mM) to compensate for surface charge effects. Under these conditions, current amplitude was decreased by 30 ± 13%

(n=4); in the presence of control $Ca^{2+}$ levels, addition of 5 mM $Mg^{2+}$ also reduced $I_{ATP}$ by 62 $\pm$ 10% (n=3; see Chapter 4).

The intracellular $Ca^{2+}$ rise could be expressed as a ratio of moles of free $Ca^{2+}$ per litre per coulomb of charge transfer during $I_{ATP}$ (M/q ratio). Charge transfer was calculated from the integral of the whole-cell current activated by pressure application of ATP (1 mM). For 6 cells, the M/q ratio was 114 $\pm$ 10 nmoles of free $Ca^{2+}$ $1.^{-1}$ $nC.^{-1}$. This was compared to the M/q ratio for responses to the nicotinic ACh receptor agonist DMPP recorded under the same conditions. The M/q ratio for ATP channels was two times greater than the ratio calculated from the response to DMPP (48 $\pm$ 12 nmoles of free $Ca^{2+}$ $1.^{-1}$ $nC.^{-1}$; n=6). Interestingly, when the agonists were bath applied instead of pressure ejected, the M/q ratios were significantly lower. For $I_{ATP}$, the ratio was 40.5 $\pm$ 15.0 (n=6) and for $I_{DMPP}$ the ratio was 19.6 (n=2). Both sets of results strongly suggest that ATP-gated channels have a higher permeability to $Ca^{2+}$ than nicotinic AChR channels in SCG cells.

To confirm that the ATP-gated channels were directly permeable to $Ca^{2+}$, currents were activated in a solution containing $Ca^{2+}$ as the only external cation (Figure 6). ATP was applied by pressure ejection dissolved in the high $Ca^{2+}$ solution. In three cells, ATP evoked inward currents in 120 mM $CaCl_2$ which were 13 $\pm$ 5% the amplitude of currents recorded under control conditions. While $I_{ATP}$ was greatly reduced in high $Ca^{2+}$, there was a current none-the-less, confirming that $Ca^{2+}$ permeates ATP-gated channels in these cells.

## Pharmacology of $I_{ATP}$

$I_{ATP}$ was reversibly antagonized by the $P_2$-purinoceptor antagonist suramin (Figure 7A). Suramin at 10-50 $\mu$M blocked the response to ATP (n=6) while the $P_1$-purinoceptor antagonist theophylline (0.03-3 mM; n=5) did not reduce the current amplitude. Antagonists to other ligand-gated cation channels such as the non-NMDA receptor antagonist DNQX (30 $\mu$M; n=2) did not affect $I_{ATP}$. Likewise, the nicotinic receptor antagonist mecamylamine at concentrations up to 100 $\mu$M (Figure 7B; n=3)

did not inhibit the current. This is in contrast to the inward current activated by the nicotinic ACh receptor agonist DMPP (1 mM; n=3) which was completely blocked by 10 $\mu$M mecamylamine (Figure 8). $I_{DMPP}$ showed rapid rundown so that there was an apparent reduction in current amplitude in the presence of 10 $\mu$M suramin; however, increasing the suramin concentration to 100 $\mu$M did not further reduce current amplitude.

The inhibition of $I_{ATP}$ by suramin was examined in more detail. $I_{ATP}$ was activated by pressure application of 1 mM ATP, and suramin (0.3-300 $\mu$M) was applied via the bath (Figure 9A). The percentage current remaining in the presence of suramin with respect to the previous control current was plotted as a function of suramin concentration (Figure 9B). The curve was fitted by eye and gave an estimated $IC_{50}$ value of 3 $\mu$M. The threshold for inhibition was 300 nM, and $I_{ATP}$ was maximally inhibited by 100 $\mu$M suramin. Interestingly, low concentrations of suramin (0.3-1 $\mu$M) slightly potentiated $I_{ATP}$ amplitude in 2 out of 6 cells.

The specificity of ATP in evoking the inward current was examined. No inward currents were evoked by up to 100 $\mu$M adenosine, ADP (n=4), AMP (n=4), or UTP (n=2; bath application; Figure 10A). $I_{ATP}$ was activated by the poorly-hydrolyzable ATP analogue, ATP-gamma-S (100 $\mu$M; n=3) indicating that the response to ATP is not due to a breakdown product or to a phosphorylation reaction.

The ATP-derivative, adenosine 5'-[$\alpha$,ß-methylene]-triphosphate (100 $\mu$M) evoked a small inward current in some cells (3/6) cells but did not antagonize the response to ATP (up to 1 mM; n=2). 2-methylthioATP activated an inward current which was reversibly antagonized by suramin (Figure 10B; n=3). However, this compound was less effective than ATP, activating currents 80% smaller than ATP at the same concentration (50 $\mu$M, bath application; n=2).

## III. Discussion

This chapter demonstrates that cultured rat SCG cells express a $P_{2x}$-purinoceptor which is activated by exogenously applied ATP. Binding of ATP to the receptor causes opening of non-specific cation channels, resulting in depolarization and a rise in intracellular $Ca^{2+}$ which is dependent on extracellular $Ca^{2+}$. This is in contrast to reported actions of ATP on $P_{2y}$ receptors, which activates phospholipase C and causes a rise in $Ca^{2+}$ mediated via $IP_3$ sensitive stores (Hirano et al. 1991; Clementi et al. 1992; Garritsen et al. 1992; Kitanaka et al. 1992; Henning et al. 1993). SCG cells may express other purinoceptor subtypes which cannot be detected by the assays used in this report.

### Dose-response relationship

The dose-response curve in Figure 2 shows the concentration range over which ATP activates the inward current in rat SCG neurones. The threshold for activation was 10 $\mu$M and the $EC_{50}$ was about 45 $\mu$M. The slow speed of the perfusion system (time to peak = 2.5 s) means that the current will have desensitized by approximately 20% during this time, and the peak amplitude of $I_{ATP}$ will therefore be underestimated. This problem, coupled with the slow rundown of the current, makes the dose-response relationship only a rough estimate. Even with these limitations, however, it can be concluded that the $P_{2x}$-purinoceptor in rat SCG cells is unlikely to be greatly different from the measured values ($EC_{50}$ taking into account a 20% desensitization = 36 $\mu$M). This falls into the sensitivity range of $EC_{50}$ = 30-60 $\mu$M observed for ATP-receptors in nucleus solitarii neurones (Ueno et al. 1992b), locus coeruleus neurones (Shen & North, 1993), PC12 cells (Nakazawa & Inoue, 1992) and atrial muscle (Friel & Bean, 1988). In some tissues, such as vas deferens (Friel, 1988), rat sensory neurones (Bean, 1990b), and guinea-pig coeliac neurones (Silinsky & Gerzanich, 1993), the sensitivity of the receptor is much higher, $EC_{50}$ = 3-7 $\mu$M.

Voltage-dependence

The current/voltage curve of $I_{ATP}$ showed strong inward rectification. The null potential was reached near 0 mV, but only small outward currents were recorded above this potential.

In cardiac atrial cells (Friel & Bean, 1988), rabbit ear artery smooth muscle (Benham et al. 1987a), and uterine smooth muscle (Hornore et al. 1989), $I_{ATP}$ is linear, but in other preparations, including rat vas deferens (Friel, 1988), coeliac ganglia (Evans et al. 1992; Silinsky & Gerzanich, 1993), nucleus solitariius (Ueno et al. 1992b), and PC12 cells (Nakazawa et al. 1990; Nakazawa et al. 1991) the current shows strong inward rectification similar to that seen in SCG neurones. The most extensive examination of the voltage-dependence of $I_{ATP}$ has been done in bullfrog sensory neurones (Bean et al. 1990a). In bullfrog neurones, the rectification is reduced but not entirely abolished when both internal and external $Mg^{2+}$ is removed. Rapid voltage jumps during activation of $I_{ATP}$ do not reveal any obvious voltage dependent gating of the channels. This suggests that the rectification in these cells is an instantaneous property of ion permeation in the channel or the result of very fast voltage-dependent gating that is complete within the resolution of the voltage clamp (tens of microseconds). The nature of the rectification in rat SCG neurones is not clear from the whole-cell experiments presented in this chapter. However, the mechanism will be discussed further in Chapter 5.

Permeability

The null potential of approximately 0 mV does not correspond to the equilibrium potential of any individual ion present in the intra- and extracellular solutions, indicating that the conductance underlying $I_{ATP}$ is not selective for any one ionic species. The reduced current amplitude in low $Na^+$ conditions, as well as the shift in the null potential, suggest that the current is carried predominantly by $Na^+$, with the channels also permeable to $K^+$. The null potential remained around 0 mV when intracellular $K^+$ was replaced with $Cs^+$, indicating approximately equal

permeability of these ions. While a comprehensive study of permeability ratios of the different ions was not undertaken, these results are consistent with the permeability characteristics of ATP-gated channels in other neuronal preparations (Krishtal *et al.*1983; Allen & Burnstock, 1990; Bean *et al.*1990a; Fieber & Adams, 1991; Harms *et al.*1992; Ueno *et al.*1992b; Shen & North, 1993; Silinsky & Gerzanich, 1993). It should be noted that in chick skeletal muscle (Thomas & Hume, 1990) ATP-gated channels appear to be permeable to both cations and anions. Permeability to $Cl^-$ was not examined in the present experiments.

In rat SCG neurones, application of ATP caused an elevation in intracellular $Ca^{2+}$ which was dependent on extracellular $Ca^{2+}$. No release of $Ca^{2+}$ from internal stores was observed in nominally $Ca^{2+}$-free external solutions, consistent with ATP acting on a $P_{2x}$ receptor. The action of ATP on SCG cells is distinct from the response in NCB-20 cells (Garritsen *et al.*1992) and NG108-15 cells (Hirano *et al.*1991), in which ATP causes a $Ca^{2+}$ rise via release from intracellular stores. These cells are presumed to express a G protein-linked purinoceptor. It is likely that the ATP-evoked rise in intracellular $Ca^{2+}$ in SCG cells is due entirely to $Ca^{2+}$ entry through the ATP-gated channels; there is no evidence of $Ca^{2+}$-induced $Ca^{2+}$ release in SCG cells (Trouslard *et al.*1993).

That $Ca^{2+}$ was directly permeant through ATP-gated channels in SCG cells was confirmed by the presence of an ATP-induced current when $Ca^{2+}$ was the only charge carrier. This current was much smaller than control $I_{ATP}$ and may be due to $Ca^{2+}$ blocking its own permeation through the conductance pathway (Nakazawa *et al.*1990; Fieber & Adams, 1991; Ueno *et al.*1992b). Alternatively, the extremely high $Ca^{2+}$ concentration may alter either the receptor or the ATP molecule such that binding of ATP is affected.

While $P_{2x}$-purinoceptors in a range of preparations show approximately equal permeability to $Na^+$, $K^+$, and $Cs^+$ ions, the permeability of ATP-gated channels to $Ca^{2+}$ varies widely. In rabbit ear artery, the $Ca^{2+}:Na^+$ permeability ratio is as high as 3:1 (Benham & Tsien, 1987b), whereas in rat sensory neurones it is only 1:3 (Bean

*et al.* 1990a). Because reversal potential measurements of $I_{ATP}$ were not examined in this report, the $Ca^{2+}$ permeability of ATP-gated channels in these cells remains unknown. However, comparison of the M/q ratios between ATP-gated channels and nicotinic AChR channels indicate that the permeability of the former is substantially higher than the latter when recorded under the same conditions. The exact values for these M/q ratios should be taken lightly as it is clear that they can vary with recording conditions. The much lower M/q ratio during bath application of ATP may reflect buffering of intracellular $Ca^{2+}$ during the slower activation of the current.


Pharmacology

The nomenclature of $P_2$-purinoceptors is in a state of transition at the present time (G. Burnstock, personal communication). Previously, ATP receptors were divided into two main categories, $P_{2x}$ and $P_{2y}$, based on the rank order of agonist potency of structural analogues of ATP in smooth muscle (see Burnstock & Kennedy, 1985 for review). $P_{2x}$ receptors had the potency order: $\alpha,\beta$-methyleneATP > ATP > 2-methylthio ATP, and $P_{2y}$ receptors had the potency order: 2-methylthio ATP > > ATP > $\alpha,\beta$-methyleneATP (Burnstock & Kennedy, 1985). The potency order determined in this report for the purinoceptor in SCG neurones is: ATP > 2-methylthio ATP > > $\alpha,\beta$-methyleneATP. This sequence does not match either of the two categories and may indicate a distinct $P_2$-purinoceptor subtype. The receptor in SCG cells is clearly distinct from the $P_{2u}$ receptor, as UTP had no effect on the cells.

Recently it has been suggested that the nomenclature of ATP receptors be changed to a more functional definition (Abbracchio & Burnstock, 1993; Edwards & Gibb, 1993). In the new scheme, $P_{2x}$ receptors are ligand-gated ion channels, and $P_{2y}$ receptors are members of the family of G protein-coupled receptors, as described in several neuronal and glial cell lines (Hirano *et al.* 1991; Garritsen *et al.* 1992; Kitanaka *et al.* 1992). Using this definition, the $P_2$-purinoceptor in rat SCG neurones is classified as a $P_{2x}$ receptor. This is consistent with reports of ligand-gated ion channels in other excitable cells (Krishtal *et al.* 1983; Allen & Burnstock, 1990; Bean, 1990b; Fieber &

Adams, 1991; Edwards *et al.* 1992; Harms *et al.* 1992; Ueno *et al.* 1992b; Shen & North, 1993; Silinsky & Gerzanich, 1993).

ATP is clearly acting on a receptor distinct from other fast transmitter receptors. There is evidence that ATP can activate nicotinic ACh receptors in skeletal muscle (Kolb & Wakelam, 1983; Hume & Thomas, 1988; Igusa, 1988; Lu & Smith, 1991; Mozrzymas & Ruzzier, 1992) and possibly bullfrog sympathetic ganglion cells (Akasu & Koketsu, 1985); however, the data from SCG cells indicates that the receptors activated by nicotinic agonists and ATP have a distinct pharmacology and calcium permeability. This has been confirmed in other preparations (Bean, 1990b; Nakazawa *et al.* 1991). Interestingly, Nakazawa and colleagues have shown that in PC12 cells, the receptors activated by ACh and ATP differ in their pharmacology, desensitization, and single channel conductances (Nakazawa *et al.* 1991), but they postulate that ATP activates the same population of channels as ACh. This would require a distinct binding site affected by different agonists and antagonists and opening the channel in a distinct conformation. While it is impossible to eliminate this hypothesis without having amino acid sequences for the two receptors (the $P_{2x}$ receptor has not been cloned), this scenario seems highly unlikely.

Recently, two $P_2$ receptors were cloned, a $P_{2u}$ receptor from neuroblastoma cells (Lustig *et al.* 1993) and a $P_{2y}$ receptor from whole chick brain (Webb *et al.* 1993). These receptors are both G protein-linked. Interestingly, G protein-linked ATP receptors have not been described electrophysiologically in mammalian neurones, with the exception of one report (von Kûgelgen *et al.* 1993). In this study, block of $P_2$-purinoceptors with suramin increased release of NA from sympathetic nerves innervating the vas deferens. Exogenously applied ATP inhibits release of NA from these same terminals (von Kûgelgen *et al.* 1989). The effect of ATP is mediated via a $P_{2y}$ G protein-linked receptor as the effect was blocked by incubation in pertussis toxin, and ATP was more potent than UTP. ATP, therefore, can act on presynaptic receptors, resulting in negative feedback of transmitter release. This resembles the pattern described for other transmitters where presynaptic modulatory receptors are G

protein-linked (see Starke *et al.* 1989, for review), and the postsynaptic receptors responsible for fast transmission are ligand-gated.

## Conclusion

In conclusion, rat SCG neurones express a $P_{2x}$-purinoceptor which is selectively activated by ATP. It is unlikely that the expression of $P_{2x}$ receptors is a culture artifact as depolarizing responses to ATP have been reported in intact SCG ganglia (G. Burnstock, personal communication). The $P_{2x}$ receptor is expressed at least on the cell soma, as this is where ATP was applied to activate the inward currents. While there was no indication of a $P_{2y}$-mediated response these responses may have been either too small to measure or masked by the $P_{2x}$-mediated response. $P_{2y}$ receptor activation may also affect intracellular processes which cannot be measured electro-physiologically. Work by others suggests that $P_{2y}$ receptors are expressed at least on the presynaptic endings of sympathetic neurones where they can modulate transmitter release (von Kûgelgen *et al.* 1993). There may therefore be a distinct pattern of expression of $P_2$-purinoceptors in rat SCG cells with $P_{2x}$ purinoceptors located on the cell body and $P_{2y}$ receptors located on the terminals.
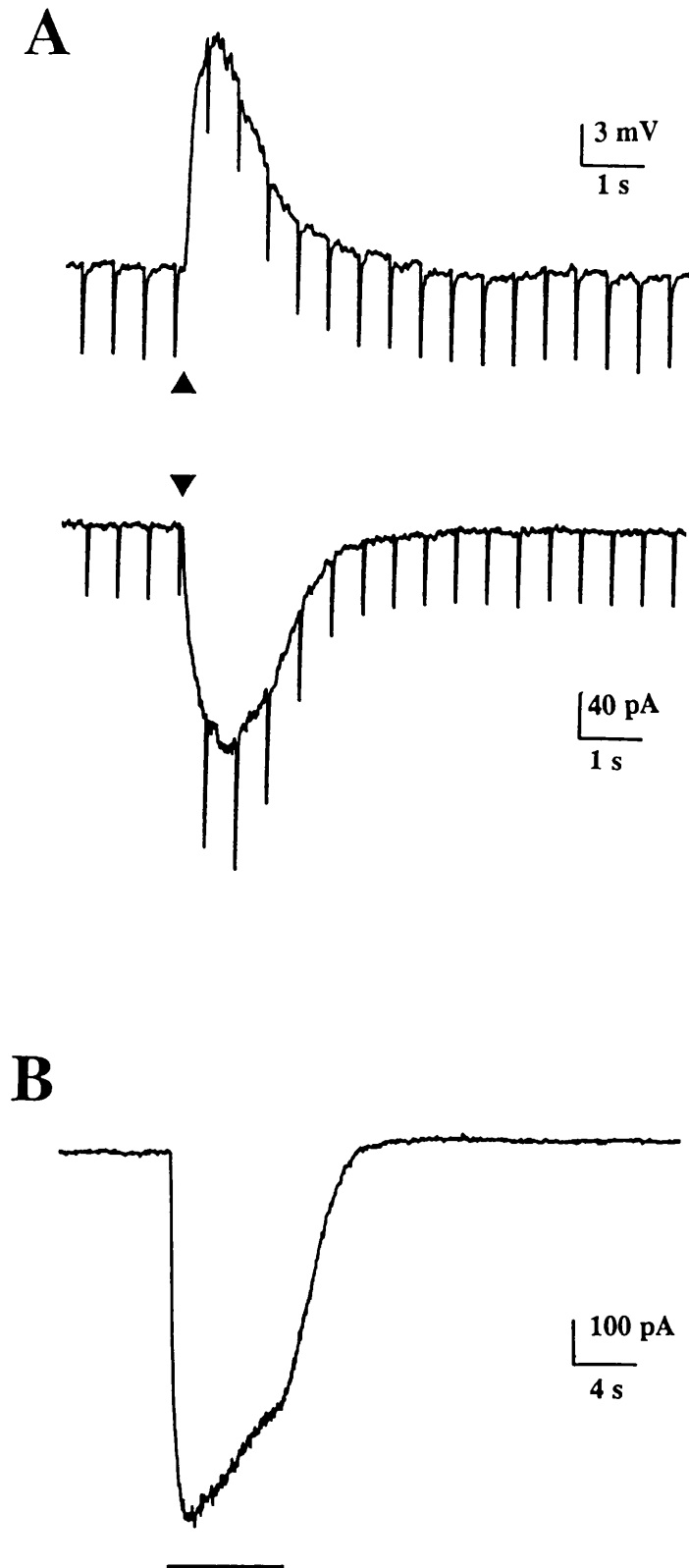
**Figure 1** ATP-evoked responses in SCG cells. **A.** Membrane voltage response recorded in current-clamp (top trace) and underlying current response recorded in voltage clamp (bottom trace) to 1 mM ATP in the same cell. ATP was applied by pressure ejection (50 ms), indicated at the arrows. Downward deflections represent responses to -10 pA/-15 mV pulses (15 ms) to monitor changes in conductance. Membrane potential for both traces = -60 mV. Current trace has been digitally filtered (100 Hz) to eliminate capacity transients. **B.** Voltage-clamp record of response to prolonged application of 1 mM ATP (pressure ejection; 5 s). Holding potential = -60 mV.
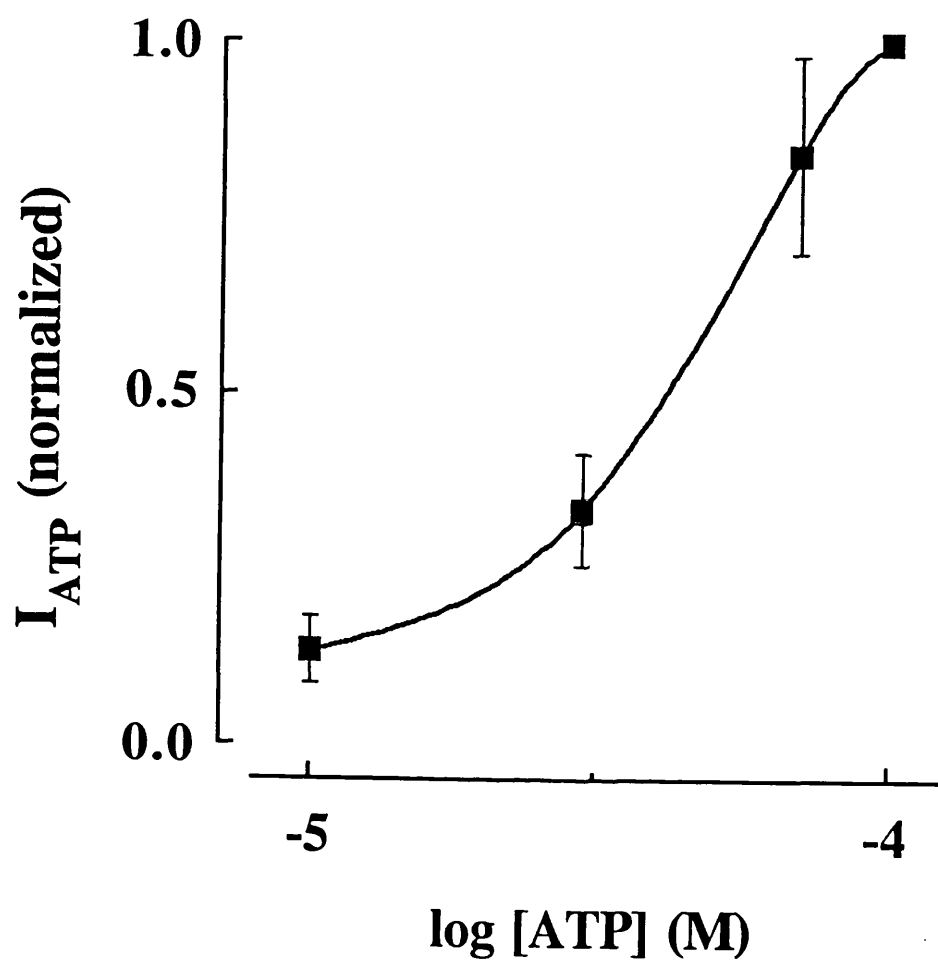
**Figure 2** ATP concentration-response curve. Current responses were normalised to the average of an initial and final response to 100 $\mu$M ATP (bath application). ATP was applied to the cell once every 3 minutes to minimize rundown. The curve was fit by eye and gave an estimated $EC_{50}$ of 45 $\mu$M. Error bars are SEM (n=4 for each point).
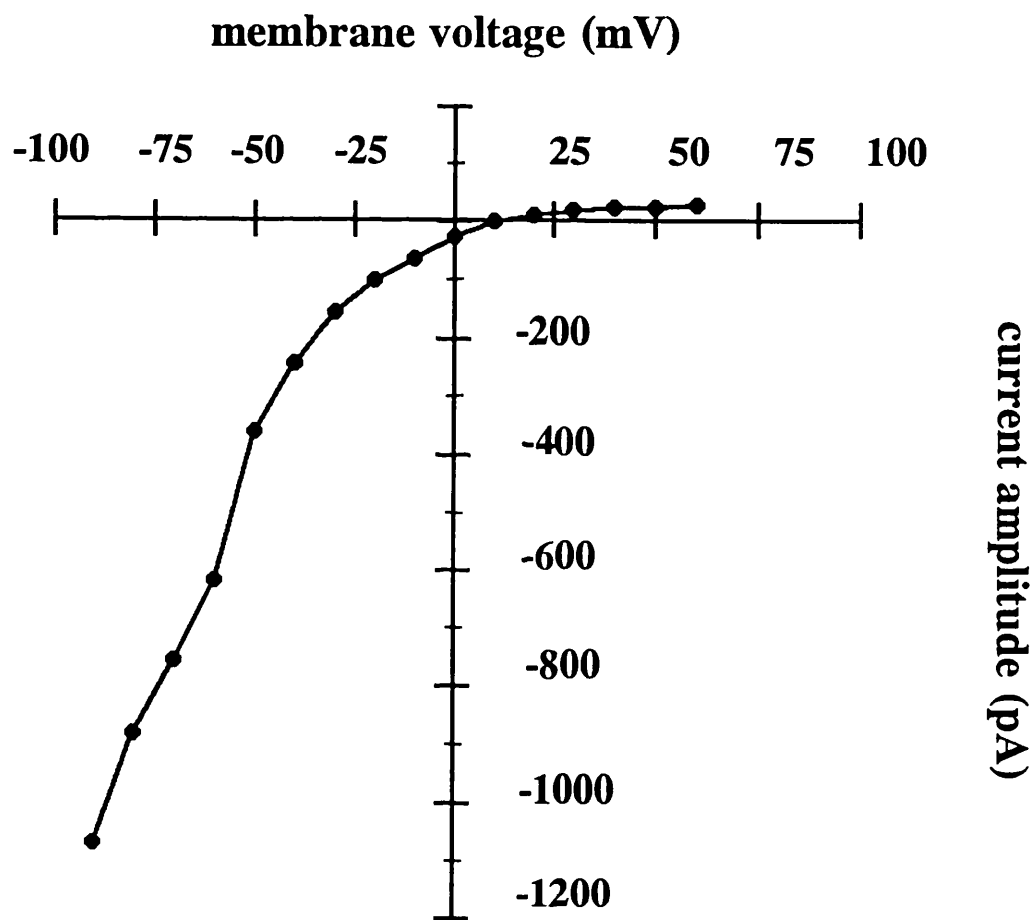
**Figure 3** Current-voltage relationship of $I_{ATP}$. Current amplitude in one cell measured at the peak response to 1 mM ATP at different holding potentials. ATP was applied by pressure ejection (50 ms) once per 30 seconds. A caesium-based recording solution was used.
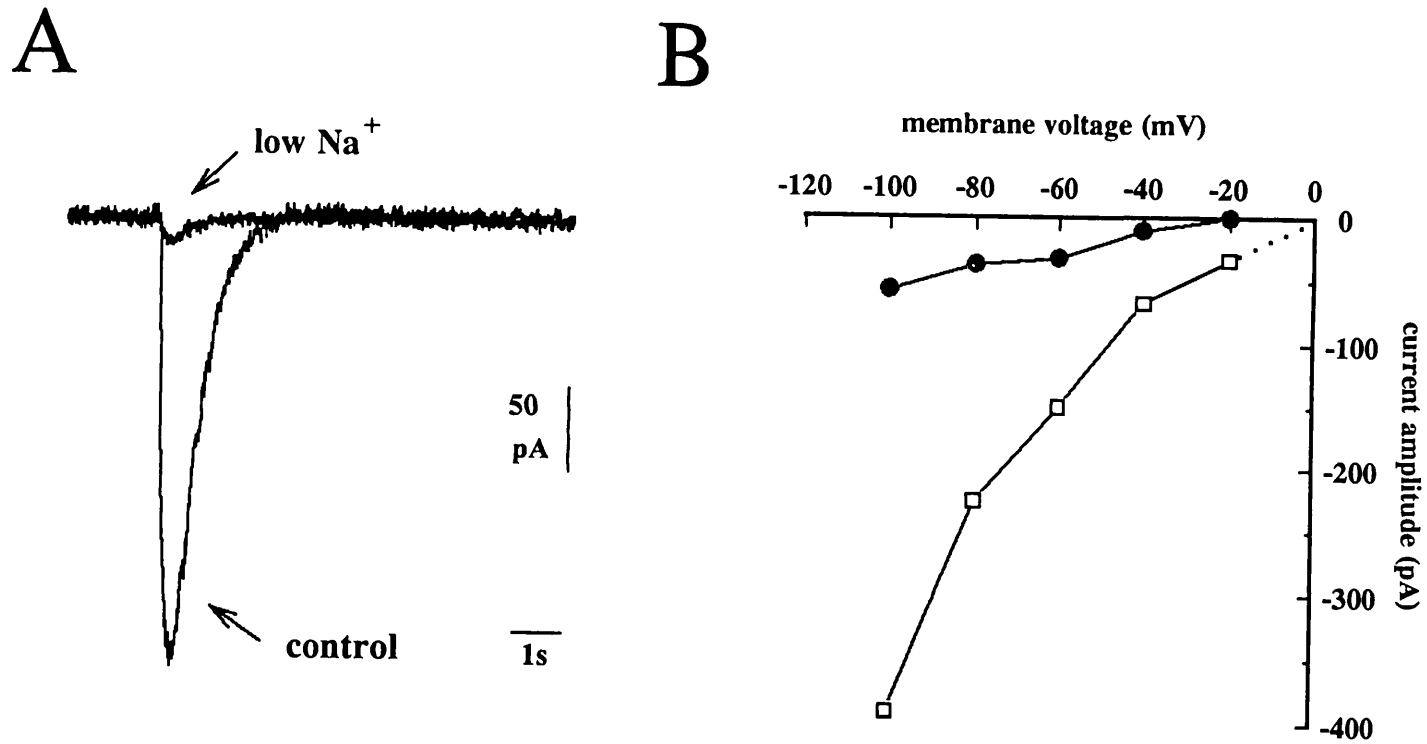
**Figure 4** Effect of low Na$^+$ on I$_{ATP}$  **A.** Superimposed traces of I$_{ATP}$ evoked by 1 mM ATP (pressure ejection; 50 ms) in control conditions and low Na$^+$ (22.6 mM) solutions in one cell. Holding potential = -60 mV.  **B.** Current voltage relation of peak I$_{ATP}$ in one cell under control (open squares) and low-Na$^+$ (filled circles) conditions. Notice the shift in extrapolated null potential (dashed line). Currents were evoked by pressure application of 1 mM ATP (50 ms) every 30 s.
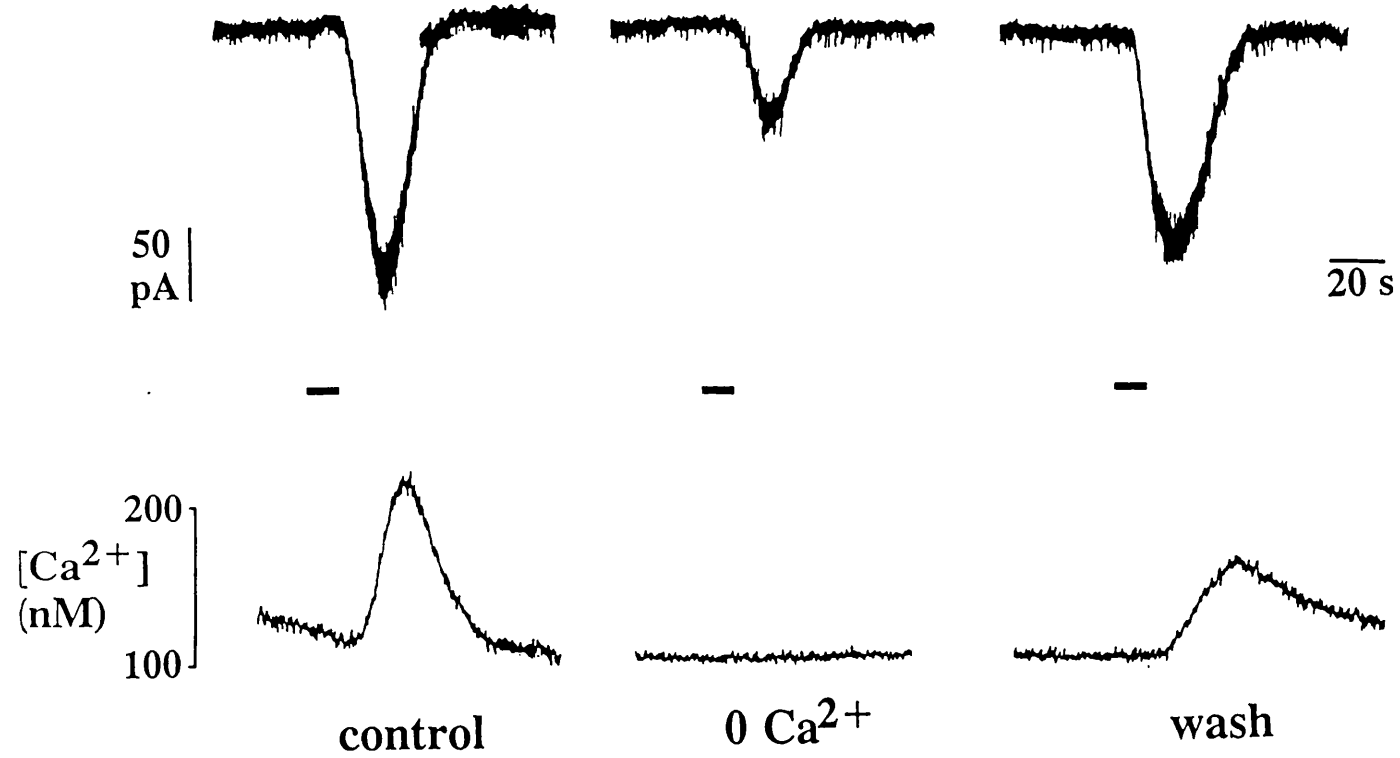
**Figure 5** ATP-evoked rises in intracellular $Ca^{2+}$. $I_{ATP}$ (top traces) was evoked by bath application of 100 $\mu$M ATP (12 s exposure at the bar) and intracellular $Ca^{2+}$ levels monitored (bottom traces). In the absence of external $Ca^{2+}$ (middle column), no rise in $Ca^{2+}$ was observed. Holding potential = -60 mV.
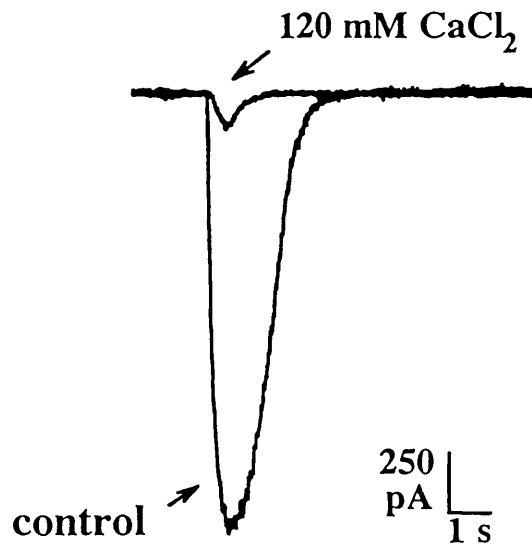
**Figure 6** Permeability of $Ca^{2+}$ through ATP-gated channels. Comparison of currents evoked by 1 mM ATP in control solution and with $Ca^{2+}$ as the only external cation (120 mM $CaCl_2$, 3.2 mM HEPES, 3.6 mM glucose) in the same cell. Holding potential = -90 mV. ATP was evoked by pressure application (500 ms). ATP was dissolved in high $Ca^{2+}$ solution for the measurements in isotonic $Ca^{2+}$.

# A

### control    suramin    wash

# B

### control    mecamylamine    wash

25
pA
1 s
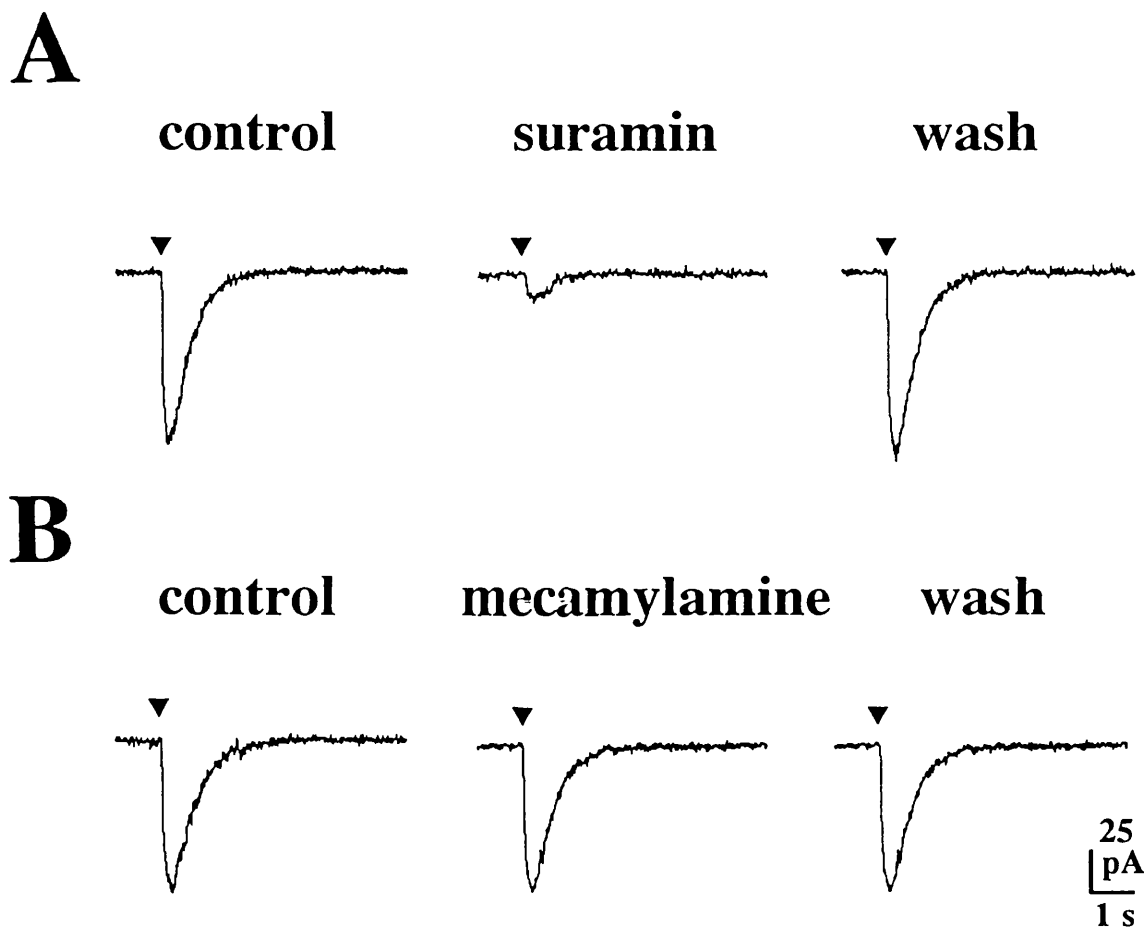
**Figure 7** Pharmacology of $I_{ATP}$. A. The $P_2$-purinoceptor antagonist suramin reversibly blocked the current response to 1 mM ATP (pressure ejection, 20 ms). $I_{ATP}$ was evoked by pressure application (20 ms) once every 30 seconds, allowing 1 minute for solution changes. Suramin (10 $\mu$M) was included in the bath. Current traces are an average of three responses. B. The nicotinic ACh receptor antagonist, mecamylamine (100 $\mu$M), had no effect on $I_{ATP}$ (same conditions as A). Holding potential = -60 mV.

CONTROL

10 $\mu$ M
SURAMIN

100 $\mu$ M
SURAMIN

10 $\mu$M
MECA.

WASH

200
pA
2 s
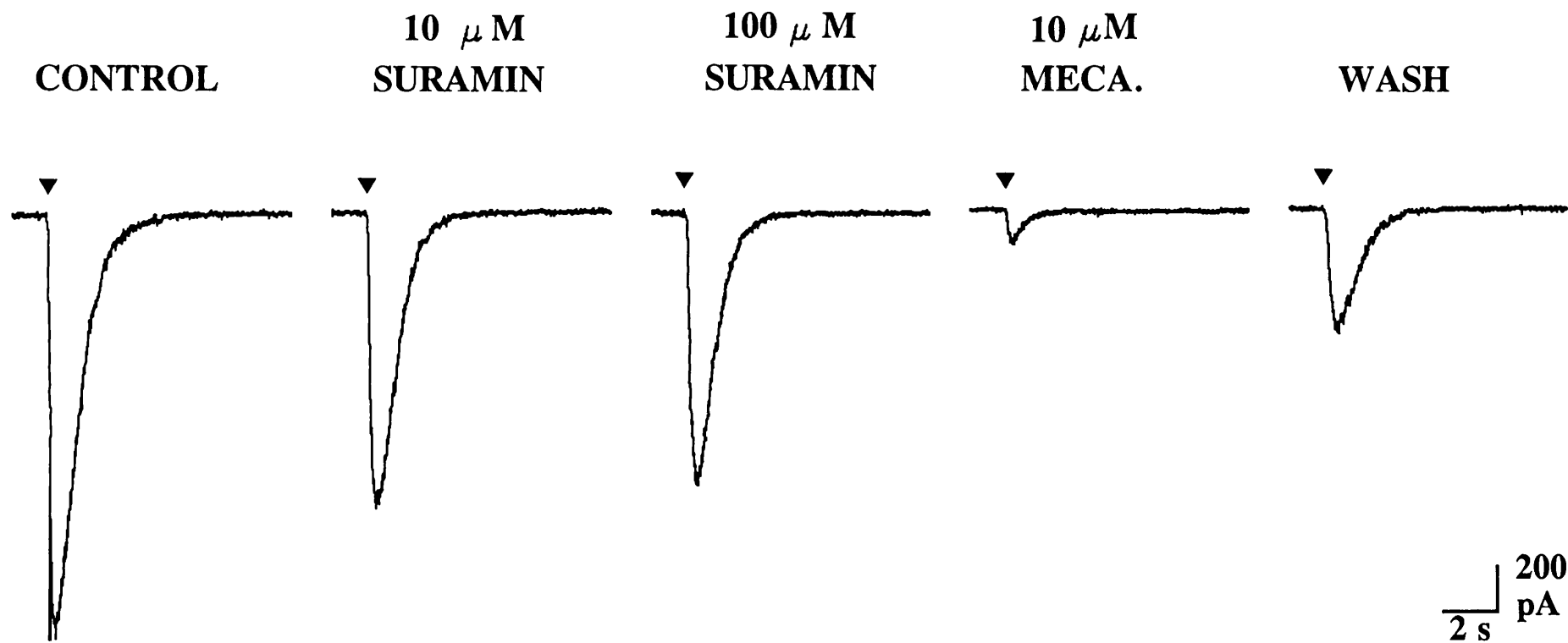
Figure 8 Pharmacology of $I_{DMPP}$. Currents activated by the nicotinic agonist DMPP (1 mM, pressure application, 50 ms). 10-100 $\mu$M suramin did not block the current, while the nicotinic antagonist mecamylamine (10 $\mu$M) almost completely abolished the current. All drugs were bath applied. Holding potential = -60 mV.
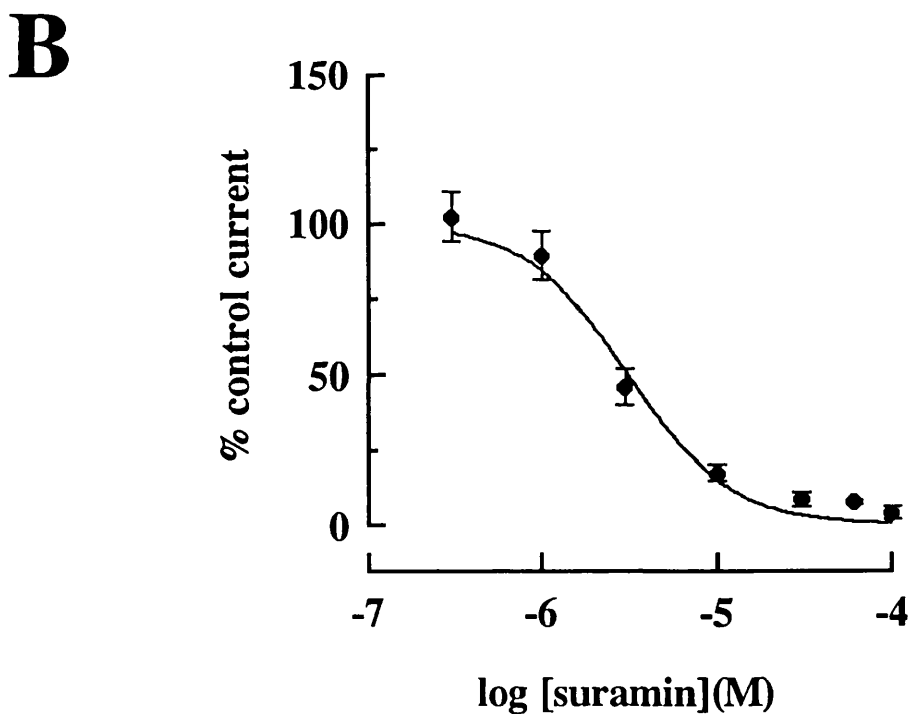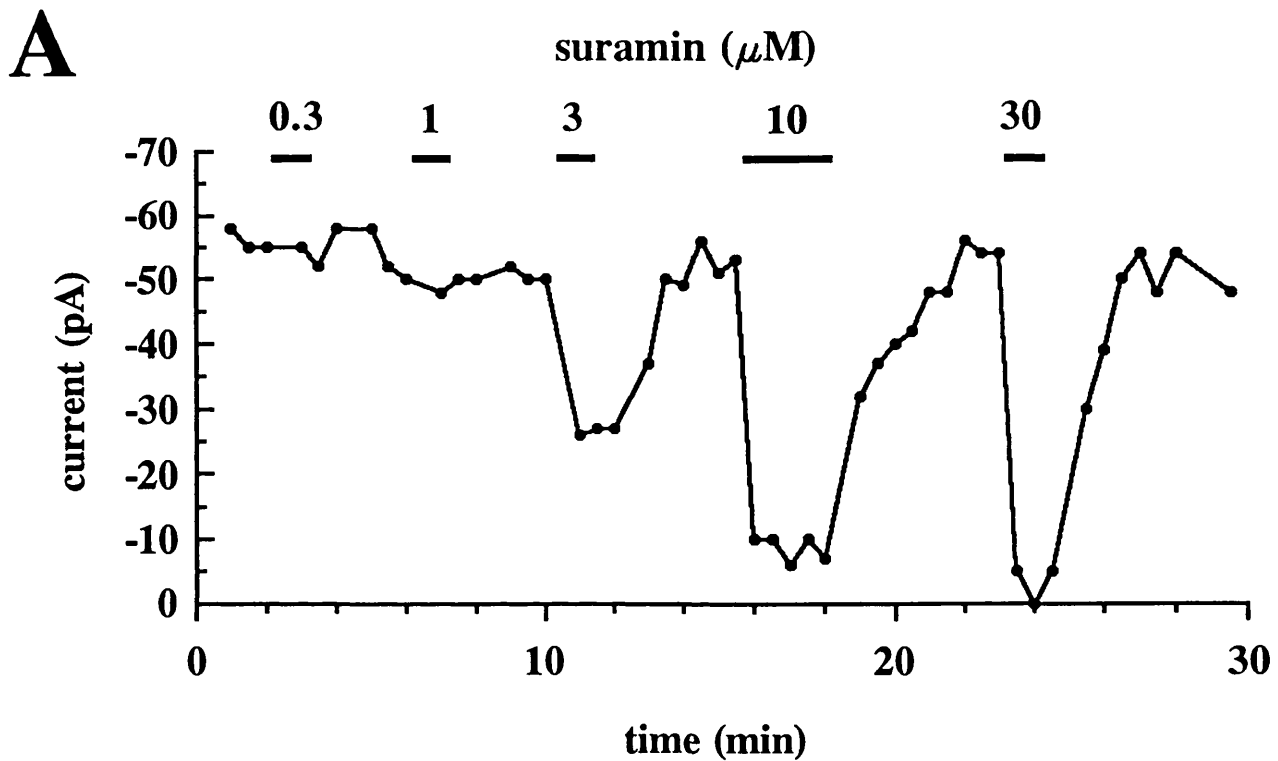
**Figure 9** Suramin dose-response relationship for $I_{ATP}$. **A.** Current amplitude of $I_{ATP}$ evoked once per minute in different concentrations of suramin. ATP was applied by pressure ejection (1 mM; 70 ms). **B.** Dose-response curve for the effect of suramin on $I_{ATP}$. $I_{ATP}$ was evoked as in A and the percent current remaining in the presence of suramin with respect to the previous wash was plotted. The curve was fitted by eye. Each point represents mean and SEM of at least 3 cells. Holding potential for all cells = -60 mV.

A



B

ATP                    2MT-ATP
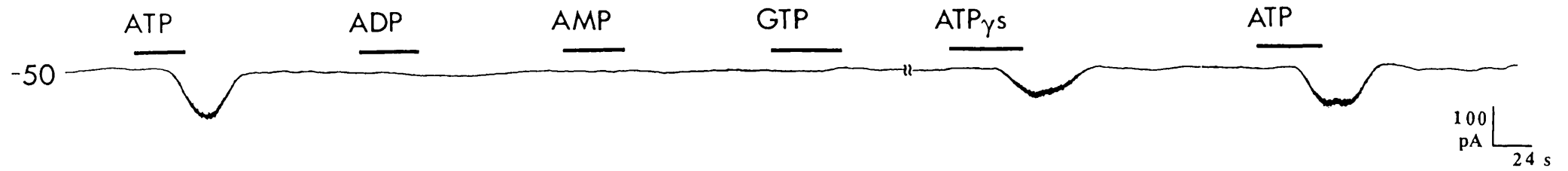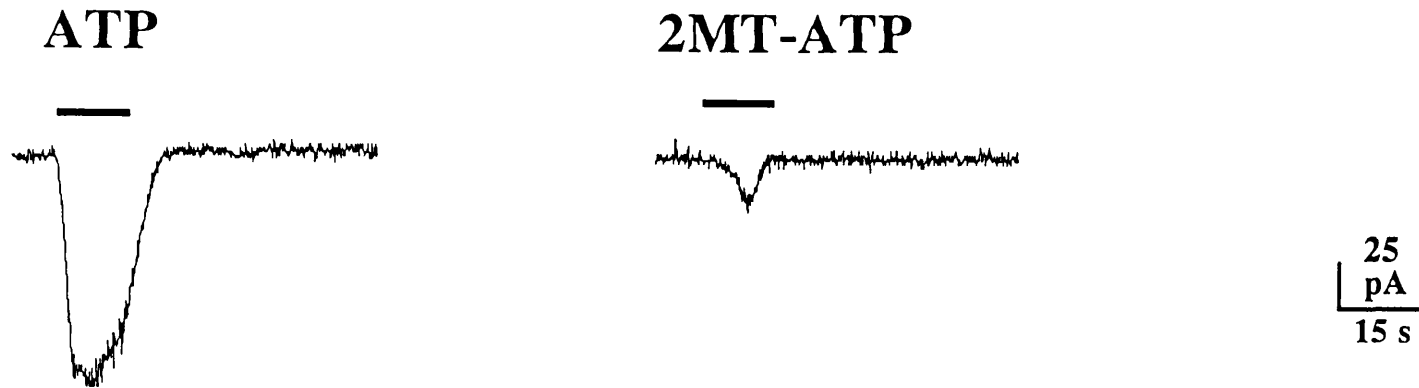
Figure 10 Effect of ATP analogues. A. Current responses to bath application of ATP, ADP, AMP, GTP, and ATP-gamma-S in one cell (100 $\mu$M each case). Double hash-marks represent a break of 2 minutes. Holding potential: -60 mV. B. Currents evoked by ATP (50 $\mu$M, bath application at the bar) and the ATP-derivative, 2methylthio-ATP (50 $\mu$M) in the same cell. Holding potential = -60 mV.

48

# Chapter 4:  Modulation of $I_{ATP}$ by extracellular $Zn^{2+}$

## I. Introduction

Reports on modulation of ionic currents by changes in external divalent cation concentration are common. Many voltage- and ligand-gated ion channels are blocked by high concentrations of divalent cations: $K^+$ channels such as the M-channel (Robbins *et al.* 1992a) and delayed rectifier (Taglialatela *et al.* 1993) are blocked by a variety of divalent cations, $Ca^{2+}$ channels are blocked by $Zn^{2+}$ ions (Busselberg *et al.* 1992), and NMDA-gated channels are blocked by external $Mg^{2+}$ (Nowak *et al.* 1984; Ascher & Nowak, 1988). In these examples, the cations interfere with permeation through the channel pore to reduce the apparent current amplitude. Divalent cations can also interact allosterically with receptors to alter binding properties and channel kinetics. This type of modulation can be positive or negative. For example, nicotinic receptor responses can be potentiated by external $Ca^{2+}$ (Mulle *et al.* 1992); in contrast, $GABA_A$-mediated currents are inhibited by $Zn^{2+}$ (Smart & Constanti, 1991; Smart, 1992). In the one case, the divalent cation increases the frequency of channel opening, while in the latter example, channel opening frequency is decreased.

There has been particular interest in the effects of the divalent transition metal, $Zn^{2+}$, on ionic currents. $Zn^{2+}$ is critical for normal development of the nervous system; deficiency results in congenital malformation of many brain structures (Hurley & Shrader, 1972) and impaired proliferation of neurones (Dvergsten *et al.* 1983). Firing patterns can also be altered by changes in $Zn^{2+}$ concentration (Hesse, 1979; Wright, 1984), and increasing intraventricular $Zn^{2+}$ induces epileptic seizures (Itoh & Ebadi, 1982). $Zn^{2+}$ is toxic to cortical neurones (Yokoyama *et al.* 1986; Choi *et al.* 1988) and possibly to other neuronal preparations as well. Clearly, an appropriate balance of $Zn^{2+}$ is essential for normal neuronal functioning.

The changes in neuronal activity under conditions of altered $Zn^{2+}$ homeostasis suggest that $Zn^{2+}$ could be important in normal neuronal activity. Indeed, there is much evidence to support a role of $Zn^{2+}$ as a neuromodulator. $Zn^{2+}$ is found localized

in synaptic vesicles in several brain regions including the cortex and hippocampus

(Crawford & Connor, 1972; Friedman & Price, 1984). This endogenous $Zn^{2+}$ can be

released during excitatory stimulation (Assaf & Chung, 1984; Howell et al. 1984;

Charton et al. 1985) in a $Ca^{2+}$-dependent manner. Reuptake of $Zn^{2+}$ has also been

observed in response to stimulation (Howell et al. 1984), suggesting that the rise in

extracellular $Zn^{2+}$ is transient. It has been estimated that concentrations could reach as

high as 300 $\mu M$ in the extracellular space during periods of high activity. Released

$Zn^{2+}$ would thus be available in the synaptic cleft where it could influence

neurotransmission.

$Zn^{2+}$ has previously been reported to modulate ionic currents gated by

excitatory and inhibitory amino acids. The NMDA receptor is inhibited by $Zn^{2+}$ in the

micromolar range (Peters et al. 1987; Westbrook & Mayer, 1987). The $GABA_A$

receptor is also inhibited by $Zn^{2+}$ at similar concentrations (Smart & Constanti, 1981;

Westbrook & Mayer, 1987; Celentano et al. 1991; Smart, 1992). At both receptors,

$Zn^{2+}$ acts noncompetitively to decrease channel open probability (Christine & Choi,

1990; Legendre & Westbrook, 1991; Smart & Constanti, 1991; Kilic et al. 1993).

Non-NMDA receptors, on the other hand, are positively affected by $Zn^{2+}$: low

concentrations of $Zn^{2+}$ potentiate currents elicited by kainate and AMPA by interacting

allosterically with the receptor (Peters et al. 1987; Westbrook & Mayer, 1987;

Rassendren et al. 1990; Xie et al. 1993). Higher concentrations of $Zn^{2+}$ inhibit these

same currents. Thus, $Zn^{2+}$ has distinct actions on different transmitter receptors and,

in some cases, may also produce multiple effects on a single receptor type.

With the recent discovery that ATP is a fast transmitter in both the CNS

(Edwards et al. 1992) and the periphery (Evans et al. 1992; Silinsky & Gerzanich,

1993), it seemed pertinent to examine whether $Zn^{2+}$ modulated ATP-gated currents

$(I_{ATP})$. In this chapter, the effects of extracellular $Zn^{2+}$ on $I_{ATP}$ are examined. These

results have been previously described for SCG cells (Cloues et al. 1993, see

supplementary material) and for rat nodose ganglia (Li et al. 1993).

## II. Results

Effect of $Zn^{2+}$ on macroscopic current amplitude

Application of submillimolar concentrations of $Zn^{2+}$, applied via the bath, had marked effects on whole-cell currents elicited by ATP. Figure 11 shows the effect of two concentrations of $Zn^{2+}$ on $I_{ATP}$: 10 $\mu$M $Zn^{2+}$ reversibly enhanced the amplitude of the peak current; 30 $\mu$M $Zn^{2+}$ did not potentiate the current but in fact inhibited it.

The effect of a range of concentrations of $Zn^{2+}$ on $I_{ATP}$ amplitude is summarized in Figure 12. $I_{ATP}$ was evoked by pressure ejection of 1 mM ATP in the presence of different concentrations of $Zn^{2+}$. The peak current amplitude was measured and the percent enhancement by $Zn^{2+}$ plotted with respect to the previous control ATP-evoked current (no added $Zn^{2+}$). Because no $Zn^{2+}$ was included in the puffer pipette, these values are likely to be underestimated. Potentiation was detected with 500 nM $Zn^{2+}$ and could be elicited repeatedly. The maximum potentiation by $Zn^{2+}$ was observed at 10 $\mu$M. Raising the concentration of $Zn^{2+}$ beyond 100 $\mu$M reduced the current amplitude to below control levels. This was accompanied by a marked increase in the current duration (see below). $I_{ATP}$ was completely blocked by 300 $\mu$M $Zn^{2+}$.

The onset of potentiation of $I_{ATP}$ by $Zn^{2+}$ was rapid, as illustrated in Figure 13. In this cell $I_{ATP}$ was evoked by bath application of ATP and $ZnCl_2$ (100 $\mu$M) was applied by pressure ejection at the peak of the inward current. The amplitude of $I_{ATP}$ increased rapidly upon exposure to $Zn^{2+}$ and declined again as $Zn^{2+}$ was washed away. $Zn^{2+}$ alone, in the absence of ATP, did not activate a current, though in some cells there was a small ($<$ 10 pA) shift in holding current, inconsistent in direction, when $Zn^{2+}$ was added to the bath.

The potentiation of $I_{ATP}$ by extracellular $Zn^{2+}$ was accompanied by an increase in conductance, indicating that the enhancement was not due to $Zn^{2+}$ blocking an outward current (for example a $Ca^{2+}$-activated $K^+$ current). Also, blockers of outward currents such as TEA (1 mM; n=2), apamin (100 nM; n=2), d-tubocurarine

(100 $\mu$M; n=1) and charybdotoxin (10 nM; n=1) did not enhance $I_{ATP}$. Moreover, it is unlikely that $Zn^{2+}$ is altering hydrolysis of ATP because the response to the poorly-hydrolyzable ATP analogue, ATP-gamma-S, was also potentiated by $Zn^{2+}$ (469% and 92% in two cells). Inclusion of 10 $\mu$M $Zn^{2+}$ in the patch pipette solution slightly reduced the mean amplitude of $I_{ATP}$ (-83 $\pm$ 14 pA; n=3); $I_{ATP}$ recorded under these conditions could still be potentiated by extracellular $Zn^{2+}$, suggesting that $Zn^{2+}$ acts at an external site to potentiate $I_{ATP}$. The mean potentiation by 10 $\mu$M $Zn^{2+}$ with $Zn^{2+}$ also included in pipette solution was 85 $\pm$ 42% (n=3). This is not significantly different from potentiation by 10 $\mu$M $Zn^{2+}$ under control conditions (118 $\pm$ 24%; n=6).

Effect of $Zn^{2+}$ on macroscopic current kinetics

In addition to increasing current amplitude, extracellular $Zn^{2+}$ altered the kinetics of $I_{ATP}$. Figure 14A shows $I_{ATP}$ in the absence and presence of 10 $\mu$M $Zn^{2+}$, normalized to illustrate the increase in current duration with $Zn^{2+}$. The rate of rise of $I_{ATP}$ varied between ATP applications for a given cell and did not change in a consistent direction in the presence of $Zn^{2+}$. This variability is most likely due to the method of ATP application, and the onset kinetics were therefore not examined further.

The decay kinetics were more consistent and could be fitted with a single exponential (Figure 14B). The time constant of the decay increased with increasing concentrations of $Zn^{2+}$. Table 1 shows the decay time constant for one cell in different concentrations of $Zn^{2+}$. For each concentration, 2-3 traces were averaged. Curves wre fitted 300-400 ms after the peak of the current to the baseline. Because of the variation in decay time constant between cells (range = 200-700 ms in control solution), the time from peak $I_{ATP}$ amplitude to half recovery (baseline) was measured with increasing concentrations of $Zn^{2+}$ (Figure 15). As the concentration of extracellular $Zn^{2+}$ increased, the duration of the current continued to increase despite the decrease in current amplitude.

## Desensitization

Changes in the rate of 'desensitization' of $I_{ATP}$ by $Zn^{2+}$ were examined. Currents were evoked with 5 second applications of ATP in the presence and absence of $Zn^{2+}$, and the half time of decay back to baseline was measured. The half time was determined by extrapolating a line along the slope of the decay. Applications longer than 5 seconds were not used to avoid problems of current rundown. The half time of decay did not appear to change significantly (Figure 16), indicating that the potentiation of $I_{ATP}$ is distinct from an effect on the slow desensitization. For a 5 second application of 100 $\mu$M ATP, the half time of decay was 7.4 and 8.1 s in two cells under control conditions and 7.2 and 7.3 s in the presence of 10 $\mu$M $Zn^{2+}$. In another cell, there was no desensitization in either condition. It is possible that $Zn^{2+}$ affects a fast component of desensitization which is not resolved within the time course of our application.

Currents evoked with repeated applications of ATP continued to run down. Currents were activated once per 30 seconds in control solution and with 10 $\mu$M $Zn^{2+}$. The rate of rundown was actually faster in the presence of $Zn^{2+}$ (7.6 $\pm$ 1.2% /exposure; n=3) than under control conditions (3.2 $\pm$ 1.6% /exposure).

## Current-voltage relationship

The current-voltage relationship of $I_{ATP}$ was examined to see if $Zn^{2+}$ caused a shift in the null potential of the current (Figure 17). A fast I/V protocol was used to minimize the problem of current rundown. The membrane potential was jumped for 50 ms every 100 ms over the range of -60 mV to +30 mV in 10 mV increments during activation of $I_{ATP}$, either in control solution or in the presence of 10 $\mu$M $Zn^{2+}$. The extracellular solution was nominally $Ca^{2+}$-free and contained the $Na^+$ channel blocker tetrodotoxin (0.5 $\mu$M) to block contaminating inward, voltage-activated currents. Even under these conditions, large inward currents were often activated at strong depolarizing potentials and reliable current-voltage curves were obtained in only two cells. The current-voltage relation of $I_{ATP}$ was determined by subtracting the current at the end of

the 50 ms jump in the presence of ATP (1 mM; or ATP + $Zn^{2+}$) from that in the absence of ATP. As can be seen in Figure 17, $Zn^{2+}$ potentiated $I_{ATP}$ at all potentials but did not change the null potential of the current.

Dependence on agonist concentration

The potentiation of $I_{ATP}$ by $Zn^{2+}$ was dependent on the concentration of agonist used to elicit the current. Figure 18 shows the current evoked by two concentrations of ATP (bath application) in the presence and absence of $Zn^{2+}$. The potentiation was greater for currents activated by low concentrations of ATP. Figure 19 shows the percent enhancement by $Zn^{2+}$ of currents evoked by increasing concentrations of ATP. Because of the rundown of $I_{ATP}$, a full dose-response curve for control and potentiated currents was not feasible. Cells were therefore exposed to only one concentration of ATP in the presence and absence of $Zn^{2+}$ and the data pooled. In 4 cells, ATP (6-10 $\mu$M) elicited a response in the presence of $Zn^{2+}$ while there was no response under control conditions.

To determine whether the maximum of the dose-response curve was potentiated, a supramaximal concentration of ATP (100 mM) was applied by pressure ejection to the cell. The duration of application was increased until the current amplitude reached a plateau and this was taken to be the maximal response of the cell. The maximum amplitude did not significantly change in the presence of $Zn^{2+}$ (control: -397 $\pm$ 61 pA; 10 $\mu$M $Zn^{2+}$: -389 $\pm$ 53 pA; n=6).

Effect of $Zn^{2+}$ on the ATP-evoked $Ca^{2+}$ rise

In addition to potentiating $I_{ATP}$, extracellular $Zn^{2+}$ also potentiated the accompanying rise in intracellular $Ca^{2+}$. Cells were voltage clamped and the $Ca^{2+}$-sensitive dye Indo-1 included in the patch pipette. ATP was applied via the bath. Figure 20 shows the changes in $[Ca^{2+}]_i$ for an ATP-evoked current that was strongly potentiated by $Zn^{2+}$. Data from 4 cells showed that $Zn^{2+}$ enhanced both $I_{ATP}$

amplitude (128 $\pm$ 78%) and peak $Ca^{2+}$ rise (132 $\pm$ 45%) to the same degree compared to control conditions.

The amount of $Ca^{2+}$ entry per charge transfer (M/q ratio, as measured in Chapter 3) of $I_{ATP}$ did not change in the presence of $Zn^{2+}$. For four cells, the M/q ratio under control conditions (bath application) was 30.9 $\pm$ 7 nmoles of free $Ca^{2+}$ $l.^{-1}$ $nC.^{-1}$ and in the presence of 10 $\mu M$ $Zn^{2+}$ was 34.2 $\pm$ 8 nmoles $l.^{-1}$ $nC.^{-1}$.

## Concanavalin A

It has been reported that for particular splice variants of the NMDA receptor, the lectin concanavalin A (Con A) can inhibit $Zn^{2+}$-induced potentiation of these currents (Hollmann et al.1993). To see if Con A acted comparably on the $Zn^{2+}$-induced potentiation of $I_{ATP}$, SCG cells were incubated 10-15 minutes in 10 $\mu M$ Con A. $I_{ATP}$ was evoked in the presence and absence of $Zn^{2+}$ (10 $\mu M$). $I_{ATP}$ showed no obvious differences in current characteristics following incubation in Con A (mean current amplitude = -117 $\pm$ 35 pA; n=3). Extracellular $Zn^{2+}$ was still able to potentiate the current in three cells tested (mean potentiation = 70 $\pm$ 30%).

## Other divalent cations

The effect of $Zn^{2+}$ on $I_{ATP}$ was mimicked by some other divalent cations. The potencies of different cations varied considerably, however. Figure 21 shows the dose-response curves for the three most potent divalent cations (including $Zn^{2+}$) on $I_{ATP}$. $Cu^{2+}$ was the most effective in potentiating $I_{ATP}$, followed by $Zn^{2+}$, $Ni^{2+}$, $Co^{2+}$, $Cd^{2+}$, $Mn^{2+}$, and $Ba^{2+}$. Example traces from one cell are shown in Figure 22. All of the cations inhibited $I_{ATP}$ at higher concentrations.

In addition to the above listed cations, $I_{ATP}$ was also sensitive to changes in external $Mg^{2+}$ and $Ca^{2+}$. As mentioned in Chapter 3, raising extracellular $Mg^{2+}$ concentrations from 1.2 mM to 5 mM reduced $I_{ATP}$ amplitude by 63 $\pm$ 10% (n=3). Conversely, lowering extracellular $Mg^{2+}$ to nominally 0 mM increased current amplitude by 31 $\pm$ 4% (n=4). The low $Mg^{2+}$ experiments were done in the presence

of raised extracellular $Ca^{2+}$ to maintain seal stability. In three cells, removing $Mg^{2+}$ in nominally $Ca^{2+}$-free solution also potentiated current amplitude by 30 $\pm$ 13% (n=4). Addition of low concentrations of $Mg^{2+}$ (10-100 $\mu M$) in nominally $Mg^{2+}$-free solution did not affect $I_{ATP}$ amplitude (n=3).

Reducing external $Ca^{2+}$ from control conditions (2.5 mM) to nominally zero $Ca^{2+}$ (no added $Mg^{2+}$) increased $I_{ATP}$ amplitude by 54 $\pm$ 11% (n=11). Addition of low concentrations of $Ca^{2+}$ did not potentiate $I_{ATP}$ and in fact slightly inhibited the current (1 $\mu M$ reduced $I_{ATP}$ by 21 $\pm$ 4% in 3 cells; 100 $\mu M$ reduced the current by 37% in another cell). The peak potentiation of $I_{ATP}$ by all the divalent cations tested is shown in Figure 23.

## III. Discussion

Extracellular $Zn^{2+}$ had two distinct effects on $I_{ATP}$ in rat SCG neurones. Low concentrations of $Zn^{2+}$ potentiated the response to ATP, including the rise in intracellular $Ca^{2+}$, while higher concentrations reduced the current amplitude. The dose-response curve for the effect of $Zn^{2+}$ on $I_{ATP}$ is therefore bell-shaped with a peak around 10 $\mu$M. In this chapter, I have investigated the potentiating effect of $Zn^{2+}$ in greater detail.

Potentiation of $I_{ATP}$ by $Zn^{2+}$

Several possible mechanisms for the potentiating effect of $Zn^{2+}$ on $I_{ATP}$ were eliminated in initial experiments:

1) $Zn^{2+}$ did not augment current amplitude by blocking an outward $K^+$ current. It has been reported that $Ca^{2+}$ entering through ATP-gated channels can activate a $Ca^{2+}$-dependent $K^+$ conductance (Ueno et al.1992a), which would cause an apparent reduction in $I_{ATP}$ amplitude. This does not appear to be the case for SCG cells. While $Zn^{2+}$ can, in fact, block some $K^+$ channels (Sim & Cherubini, 1990; Harrison et al.1993a; Harrison et al.1993b), the effect of $Zn^{2+}$ on $I_{ATP}$ was not mimicked by other $K^+$ channel blockers, either internal (caesium) or external (TEA, apamin, charybdotoxin).

2) It is unlikely that the potentiation by $Zn^{2+}$ resulted from effects of $Zn^{2+}$ on proteins extraneous to the ATP receptor. Two potential enzymes can be excluded: protein kinase C (PKC) and ectoATPase. PKC can be activated directly by $Zn^{2+}$ (Zalewski et al.1990; Baba et al.1991) or by acting via a divalent cation receptor (Miledi et al.1989), but the rapid reversibility of the potentiation of $I_{ATP}$ argues against PKC involvement. In addition, the effect of $Zn^{2+}$ can be reproduced in excised patches (see Chapter 5), suggesting that no diffusable second messenger is required for modulation.

EctoATPases hydrolyze extracellularly released ATP to AMP and adenosine

(Nagy *et al.* 1986). Inhibition of these enzymes (by $Zn^{2+}$) could theoretically enhance

ATP-evoked currents by increasing the amount of ATP available for binding to the

receptor. However, currents activated by the slowly hydrolyzable analogue of ATP,

ATP-gamma-S, were also potentiated by $Zn^{2+}$, making this explanation unlikely.

3) The potentiation could not be explained by a reduction in either

desensitization or rundown of $I_{ATP}$. In fact, the rundown appeared to be accelerated in

the presence of $Zn^{2+}$.

4) Several experiments argue against $Zn^{2+}$ affecting the permeability pathway

of ATP-gated channels. First, there was no shift in the apparent null potential of $I_{ATP}$

in the presence of $Zn^{2+}$. Second, if $Zn^{2+}$ were increasing the conductance of the

ATP-gated channels, $Zn^{2+}$ should increase the maximum current response of $I_{ATP}$. In

contrast to this, the effect of $Zn^{2+}$ could be overcome by increasing the concentration

of ATP. Finally, it will be demonstrated in Chapter 5 that there is no change in unitary

current amplitude in the presence of $Zn^{2+}$.


Dose-response relationship of $I_{ATP}$

In the presence of $Zn^{2+}$, there was a decrease in the threshold of activation of

$I_{ATP}$ but no potentiation of the maximum current response. This is consistent with a

leftward shift in the dose-response curve and an increase in the apparent affinity of the

receptor for ATP. Due to limitations in the experimental setup, it was not possible to

accurately determine the full dose-response relationship of $I_{ATP}$ in the presence and

absence of $Zn^{2+}$. It is therefore not known whether the slope of the $I_{ATP}$ dose-

response curve changes in the presence of $Zn^{2+}$.

The data presented in this chapter suggest that $Zn^{2+}$ produces its effect by

acting at the level of the ATP receptor. $Zn^{2+}$ may therefore be classified as an

allosteric modulator of the $P_{2x}$-purinoceptor in SCG cells (Monod *et al.* 1965). Several

mechanistic interpretations of the results are possible and can be illustrated using a

simple scheme of a ligand-gated channel first proposed by del Castillo and Katz (del Castillo & Katz, 1957):

$$R \underset{k_{-1}}{\overset{\overset{\displaystyle A}{\overset{\displaystyle |}{\diagdown}} k_1}{\rightleftharpoons}} AR \underset{\alpha}{\overset{\beta}{\rightleftharpoons}} AR^*$$

(closed channel)      (closed channel)      (open channel)
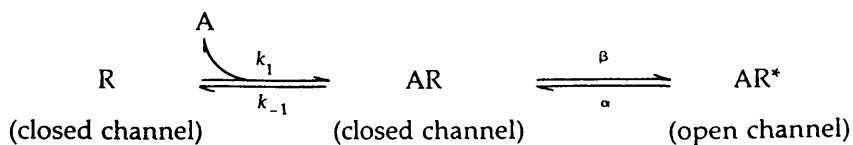
R is the receptor in this scheme and A is the agonist. The open channel-receptor complex is $AR^*$. The rate constants are denoted by the symbols on the arrows. $Zn^{2+}$ could alter either of the two steps (binding or channel opening) to cause an increase in the apparent affinity of the receptor for ATP. First, the microscopic affinity of the receptor for ATP ($k_{-1}/k_{+1}$) may actually increase either by an enhanced rate of binding or a reduced rate of unbinding. Alternatively, $Zn^{2+}$ may affect the second part of the scheme, either increasing the probability of channel opening once the receptor is occupied (increasing ß) or decreasing the probability of the channel closing (decreasing $\alpha$). Mechanistically, $Zn^{2+}$ could bring about these changes by altering the 3-dimensional structure of the receptor-channel protein. For example, $Zn^{2+}$ could increase the accessibility of the ATP binding site. At this time it is not possible to distinguish between these various mechanisms.

ATP-activated currents in rat nodose ganglia are also potentiated by $Zn^{2+}$ (Li *et al.* 1993). In these cells, there is a parallel leftward shift in the ATP dose-response curve with no change in the slope. 10 $\mu$M $Zn^{2+}$ shifts the $EC_{50}$ from 30 $\mu$M to 8 $\mu$M. From the results in Figure 19, it can be estimated that in SCG neurones, 10 $\mu$M $Zn^{2+}$ shifts the $EC_{50}$ from 45 $\mu$M to about 20 $\mu$M. These results are consistent with $Zn^{2+}$ increasing the sensitivity of the receptor for ATP by 2-3 times. In addition, they suggest that the mechanism for potentiation in sympathetic cells from SCG and nodose ganglia is the same.

## Kinetics

The slowed rate of decay of $I_{ATP}$ in the presence of $Zn^{2+}$ is also consistent with an increase in the apparent affinity of the receptor. Higher affinity agonists have been

shown to increase channel burst duration for many ligand-gated ion channels (Adams, 1974; Colquhoun, 1975; Neher & Sakmann, 1975), resulting in a slowing of the time constant of decay. This lengthening of the decay also occurs if the apparent affinity of the receptor for agonist is increased. For example, barbiturates have been observed in binding experiments to enhance binding of [$^3$H]GABA in synaptosomal preparations (Willow & Johnston, 1980) by reducing the dissociation rat constant of GABA (Willow & Johnston, 1981). In addition, barbiturates have many of the same effects on GABA responses as $Zn^{2+}$ does on $I_{ATP}$, including potentiation of current amplitude and duration (Nicoll et al. 1975; Ransom & Barker, 1976; Barker & Ransom, 1978; Macdonald & Barker, 1979; Higashi & Nishi, 1982). By analogy, therefore, an increase in the apparent affinity of the $P_{2x}$-receptor for ATP by $Zn^{2+}$ would be accompanied by a reduction in the rate of current decay.

At higher $Zn^{2+}$ concentrations, channel block may also contribute to the reduced decay rate of $I_{ATP}$. The current amplitude was decreased by high concentrations of $Zn^{2+}$, an effect most likely due to $Zn^{2+}$ blocking conductance through the channels (this will be discussed further in Chapter 5). During fast channel block, the current decay can often be resolved into two time constants, one fast and one slow, representing unblocked and blocked channels closing, respectively (Adams, 1977; Neher & Steinbach, 1978; Colquhoun & Sheridan, 1981). For $I_{ATP}$, however, only a single exponential decay was observed in the presence of $Zn^{2+}$. The mechanism for the increase in the decay is probably more complex than channel block alone and most likely reflects a combination of increased burst duration (from the increased receptor affinity) and channel block.

Interestingly, in rat nodose ganglia, where $Zn^{2+}$ also potentiates $I_{ATP}$, there is no inhibition of the current with high concentrations of $Zn^{2+}$ (Li et al. 1993). Assuming that $P_{2x}$ receptors are composed of multiple subunits like other ligand-gated ion channels (Betz, 1990), this difference may reflect a variation in receptor subunit composition. Expression may differ either between tissue type (nodose vs SCG ganglion) or with developmental age (adult vs 17-day rats). There are many examples

of subunit composition causing differences in functional properties of receptor-channel complexes. For example, expression of the gamma-subunit in $GABA_A$ receptors confers an insensitivity to extracellular $Zn^{2+}$ ions; receptors that do not contain the gamma-subunit are potently inhibited by $Zn^{2+}$ (Draguhn *et al.* 1990; Smart *et al.* 1991). Knowledge of the properties of $I_{ATP}$ may similarly be useful in determining subunit composition of $P_{2x}$ receptors in different tissues.

## Effect of other divalent cations

The effect of $Zn^{2+}$ on $I_{ATP}$ was mimicked by some, but not all, divalent cations. The order of potency for divalent cations potentiating the current was: $Cu^{2+} > Zn^{2+} > Ni^{2+} > Cd^{2+} > Co^{2+} > Mn^{2+} > Ba^{2+}$. This order was determined by the maximally effective concentration of the cation which potentiated $I_{ATP}$. All of the cations inhibited $I_{ATP}$ as their concentration was increased.

The order of potency of divalent cations modulating receptor-ionophore complexes varies for different receptors. For inhibition of $5HT_3$ responses, the potency order is: $Zn^{2+} > Cu^{2+} > Cd^{2+}$ with no effect of $Ni^{2+}$ and $Mn^{2+}$, while for $GABA_A$ inhibition it is: $Cd^{2+} > Zn^{2+} >> Ni^{2+} >> Mn^{2+}$. The potentiation of NMDA receptor splice variants by $Zn^{2+}$ is mimicked by $Cd^{2+}$, $Ni^{2+}$, and $Cu^{2+}$ but at lower affinities. Thus modulation of ligand-gated channels is not a general property of divalent cations. There appear to be very specific binding sites for particular divalent cations on different receptors.

$Mg^{2+}$ and $Ca^{2+}$ did not potentiate $I_{ATP}$ at any concentration tested. The channels were clearly sensitive to external $Ca^{2+}$ and $Mg^{2+}$ as lowering the concentration of either cation increased the current amplitude. Conversely, raising the external concentrations reduced $I_{ATP}$ amplitude. In the presence of nominally $Ca^{2+}$-free or $Mg^{2+}$-free external solutions, addition of very low concentrations of either $Ca^{2+}$ or $Mg^{2+}$ inhibited $I_{ATP}$. Thus, these divalent cations have a distinct action on the $P_{2x}$-purinoceptor than those listed above, at least with respect to the potentiation of current amplitude.

In PC12 cells (Nakazawa & Hess, 1993) and nucleus solitarii neurones (Ueno *et al.* 1992b), $Ca^{2+}$ can block its own permeation, as well as that of other permeant cations, through ATP-gated channels, possibly by binding to a high affinity site located within the pore of the channel. In SCG neurones, the sensitivity of ATP-gated channels to $Ca^{2+}$ may reflect a similar mechanism. $Mg^{2+}$ could also bind to this site, or another site in the pore, to reduce current amplitude. Alternatively, $Mg^{2+}$ may act by a distinct mechanism, perhaps as a negative allosteric modulator, causing a reduction in channel open probability. Further experiments would be required to determine the mechanism by which $Mg^{2+}$ and $Ca^{2+}$ reduce $I_{ATP}$ amplitude.

## Does $Zn^{2+}$ bind to ATP?

Because ATP is complexed with divalent cations under physiological conditions, the question arises as to what form of ATP is active at the $P_{2x}$-purinoceptor and whether the effect of $Zn^{2+}$ on $I_{ATP}$ could be explained by binding to the ATP molecule as opposed to the receptor. In regards to the first question, ATP can activate currents in the absence of divalent cations in sensory neurones (Krishtal *et al.* 1988; Bean, 1990b) and rabbit ear artery (Benham & Tsien, 1987b). This suggests that the free anion form of ATP is active. However, the bound form of ATP also appears to be active since currents in SCG cells were recorded in isotonic $Ca^{2+}$ solutions. In rabbit ear artery (Benham & Tsien, 1987b), $I_{ATP}$ can be activated in both isotonic $Ca^{2+}$ and isotonic $Mg^{2+}$ solutions. Therefore, both complexed and uncomplexed ATP is able to activate the $P_{2x}$ receptor though no complete study of the potencies of the different forms of ATP on $P_{2x}$ receptors has been carried out.

$Zn^{2+}$ has a high affinity for ATP ($K_D = 17\ \mu M$) and can certainly bind to ATP, as can other divalent cations which potentiate $I_{ATP}$. The order for binding of divalent cations to ATP is: $Cu^{2+} > Ni^{2+} > Zn^{2+} > Mn^{2+} > Co^{2+} > Mg^{2+} > Ca^{2+} > Ba^{2+}$ (Sillen & Martell, 1964). This order is different than the order of potency for these ions in potentiating $I_{ATP}$, which suggests that $Zn^{2+}$ and other cations produce their effect by interacting with the receptor rather than the ATP molecule

itself. In particular, $Mn^{2+}$ has a similar binding affinity for ATP as $Zn^{2+}$ ( 14 $\mu M$ vs 17 $\mu M$), but it had very little effect on $I_{ATP}$. It has also been reported that the affinity of the phosphate moiety of ATP for $Zn^{2+}$ is, in fact, weaker than for $Mg^{2+}$ and $Ca^{2+}$ (Rimai & Heyde, 1970)    , so that in the presence of physiological concentrations of $Ca^{2+}$ and $Mg^{2+}$, very little $Zn^{2+}$ would be bound to ATP. Given the examples of $Zn^{2+}$ interactions with other receptor-channel complexes (see below), it seems reasonable to propose that $Zn^{2+}$ interacts directly with the $P_{2x}$-purinoceptor to potentiate current amplitude.

## Effects of $Zn^{2+}$ on other ligand-gated channels

While positive modulation of ligand-gated currents by $Zn^{2+}$ has been described previously, the molecular mechanism of this effect varies between the receptors. Low concentrations of $Zn^{2+}$ potentiate kainate and AMPA responses in neurones (Peters et al. 1987; Westbrook & Mayer, 1987; Xie et al. 1993). When these cloned non-NMDA receptors are expressed in oocytes, the apparent affinity for agonists is not altered by $Zn^{2+}$, but the maximum current response is increased (Rassendren et al. 1990). $Zn^{2+}$ also increases the maximum current response of certain splice variants of the NMDA receptor (Hollmann et al. 1993). For these receptors, therefore, $Zn^{2+}$ may be increasing the number of receptors available for binding, altering the permeation pathway through the channels, or changing the maximum open probability of the channels. The ability of the lectin Con A to selectively block the $Zn^{2+}$-induced potentiation of NMDA currents but not ATP currents suggests that different residues are involved in the $Zn^{2+}$ effect.

This is the first report of $Zn^{2+}$ increasing the apparent affinity of a receptor for agonist; however, other molecules have been shown to have this effect. Glycine interacts allosterically with the NMDA receptor to increase channel opening frequency (Johnson & Ascher, 1987). In addition, barbiturates appear to confer their potentiating effect on $I_{GABA}$ by increasing binding of agonist to the $GABA_A$ receptor (Willow & Johnston, 1980; Study & Barker, 1981). It remains to be seen how the molecular

mechanism of $Zn^{2+}$ action on the $P_{2x}$ receptor compares with the effects of divalent cations on other receptors.

Conclusion

In conclusion, $Zn^{2+}$, which is contained in synaptic vesicles in the brain and can be released during neuronal excitation, can potently augment $I_{ATP}$ amplitude. In rat nodose ganglia, $Zn^{2+}$ increases membrane depolarization and action potential firing elicited by ATP (Li et al. 1993), and in SCG neurones, $Zn^{2+}$ increases $Ca^{2+}$ entry through ATP-gated channels (Cloues et al. 1993). The physiological implications of $Zn^{2+}$ enhancement of $I_{ATP}$, therefore, may be quite important. It would be of particular interest to examine modulation of ATP-mediated synaptic events, both in the periphery and in the CNS. As the physiology of ATP as a transmitter becomes better understood, the physiological relevance of $Zn^{2+}$ potentiation will hopefully become clearer as well. In addition, the molecular mechanisms of $Zn^{2+}$ action will be of interest for future studies probing structure-function relationships for this ion channel.

CONTROL 10 $\mu$M Zn$^{2+}$ WASH 30 $\mu$M Zn$^{2+}$



$\begin{array}{c} 100 \\ pA \end{array}$

2 s
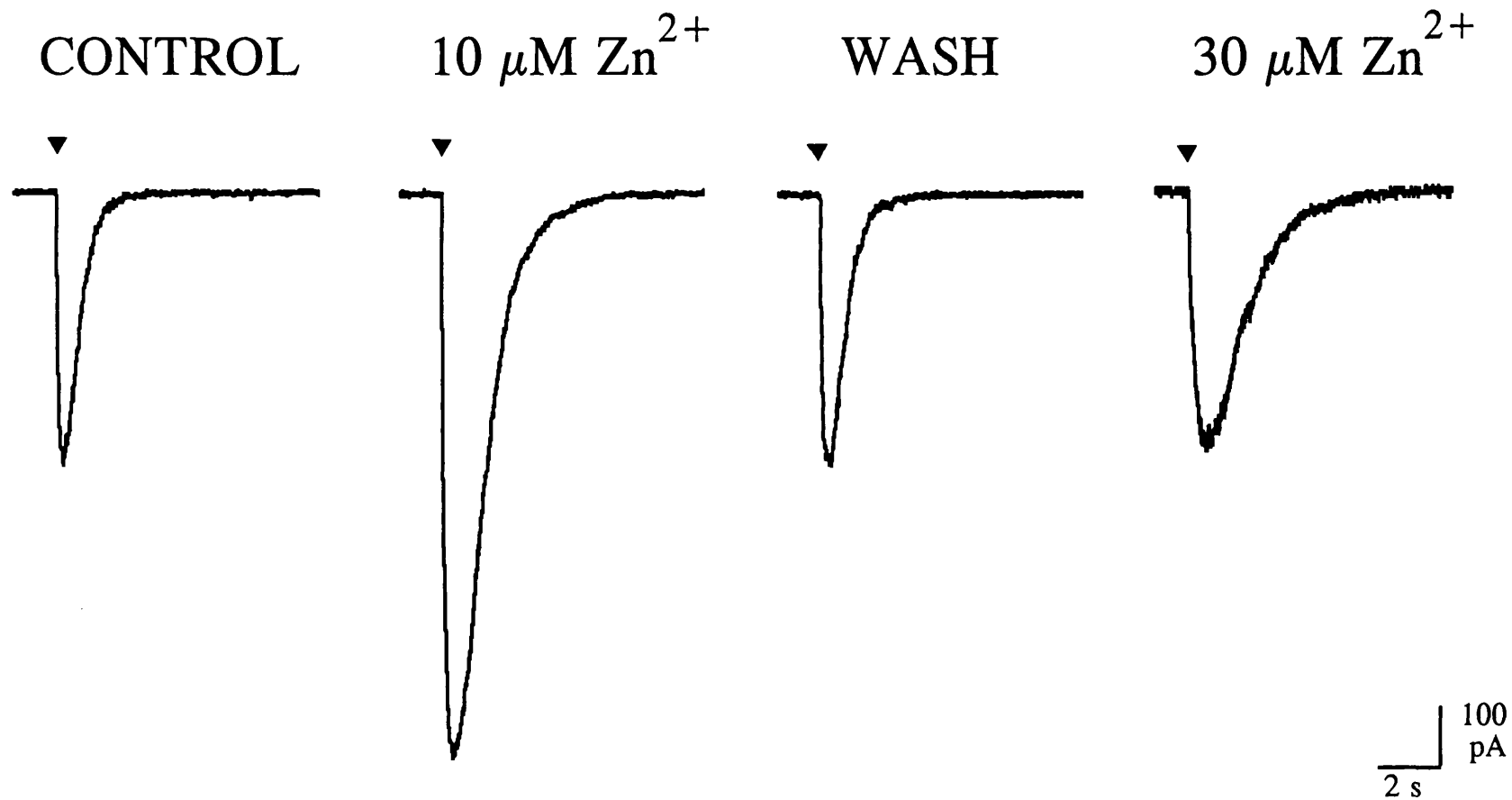
**Figure 11** Effects of two concentrations of extracellular Zn$^{2+}$ on I$_{ATP}$. I$_{ATP}$ was evoked by 20 ms applications of 1 mM ATP (pressure ejection), indicated at the triangles, in either control solution or with 10 $\mu$M or 30 $\mu$M Zn$^{2+}$ included in the bath. Holding potential = -60 mV; 30 s between ATP applications. Zn$^{2+}$ was not included in the puffer pipette.
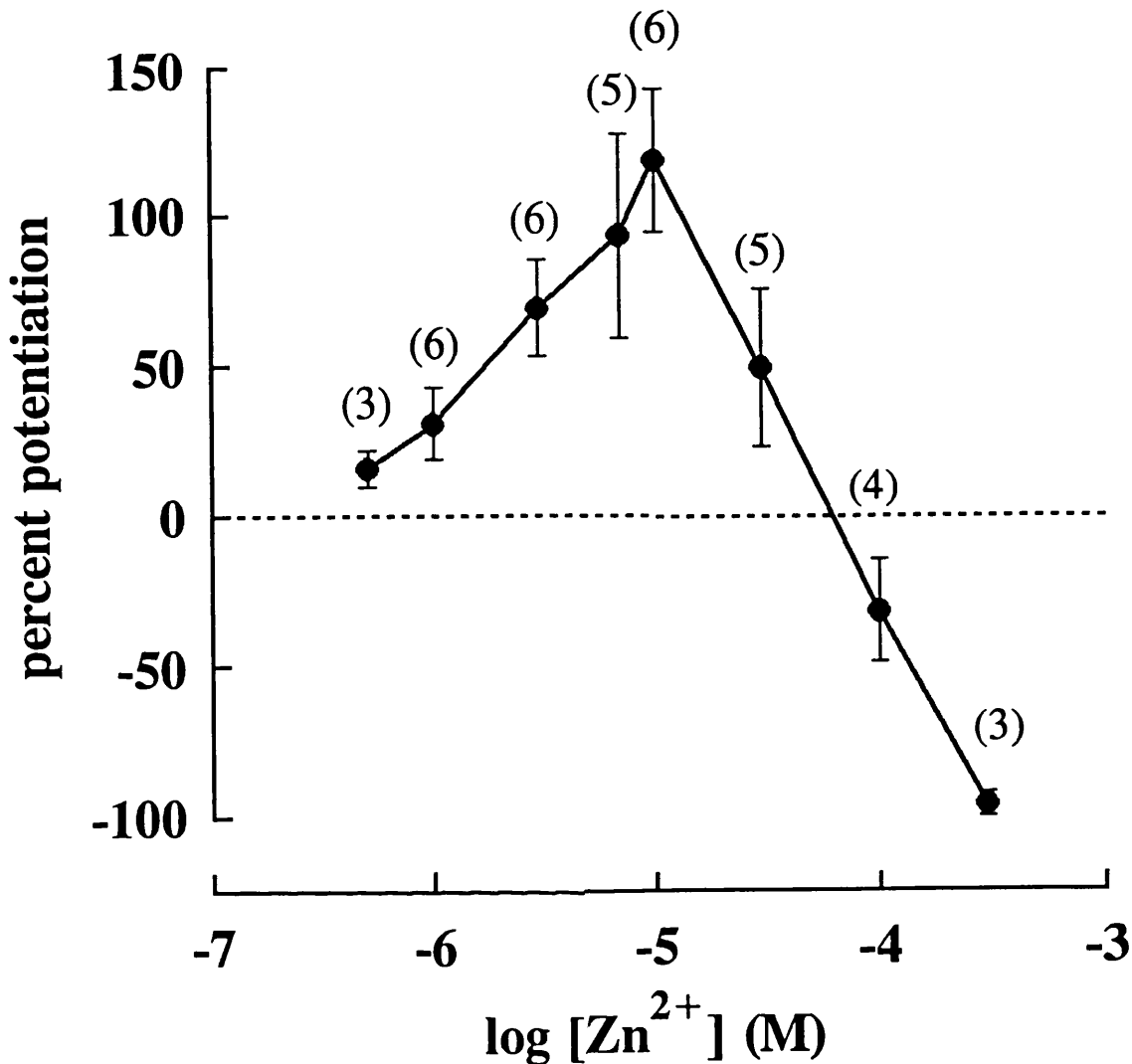
**Figure 12** $Zn^{2+}$ concentration-response curve on $I_{ATP}$ amplitude. The percentage enhancement of $I_{ATP}$ amplitude was plotted as a function of $Zn^{2+}$ concentration (0.5-300 $\mu$M). $I_{ATP}$ was evoked by pressure ejection of 1 mM ATP (20 ms) and $ZnCl_2$ was included in the bath. Holding potential = -60 mV. Currents were evoked 3 times in each solution every 30 seconds, allowing 1 minute for solution changes. With higher concentrations of $Zn^{2+}$ (100-300 $\mu$M), it was necessary to evoke $I_{ATP}$ more times before a stable current amplitude was obtained. The order of $Zn^{2+}$ concentrations for any given cell was randomized. Current rundown was compensated for by measuring the slope of the line of control $I_{ATP}$ taken between exposures to $Zn^{2+}$ and adding this value to the subsequent currents. The rundown was linear and averaged 5.5 ± 1.3 pA/exposure (n=6). Averaged currents were used to calculate the percent change between currents evoked in $Zn^{2+}$ solution relative to the previous control solution. Error bars are SEM (number of cells listed above points).
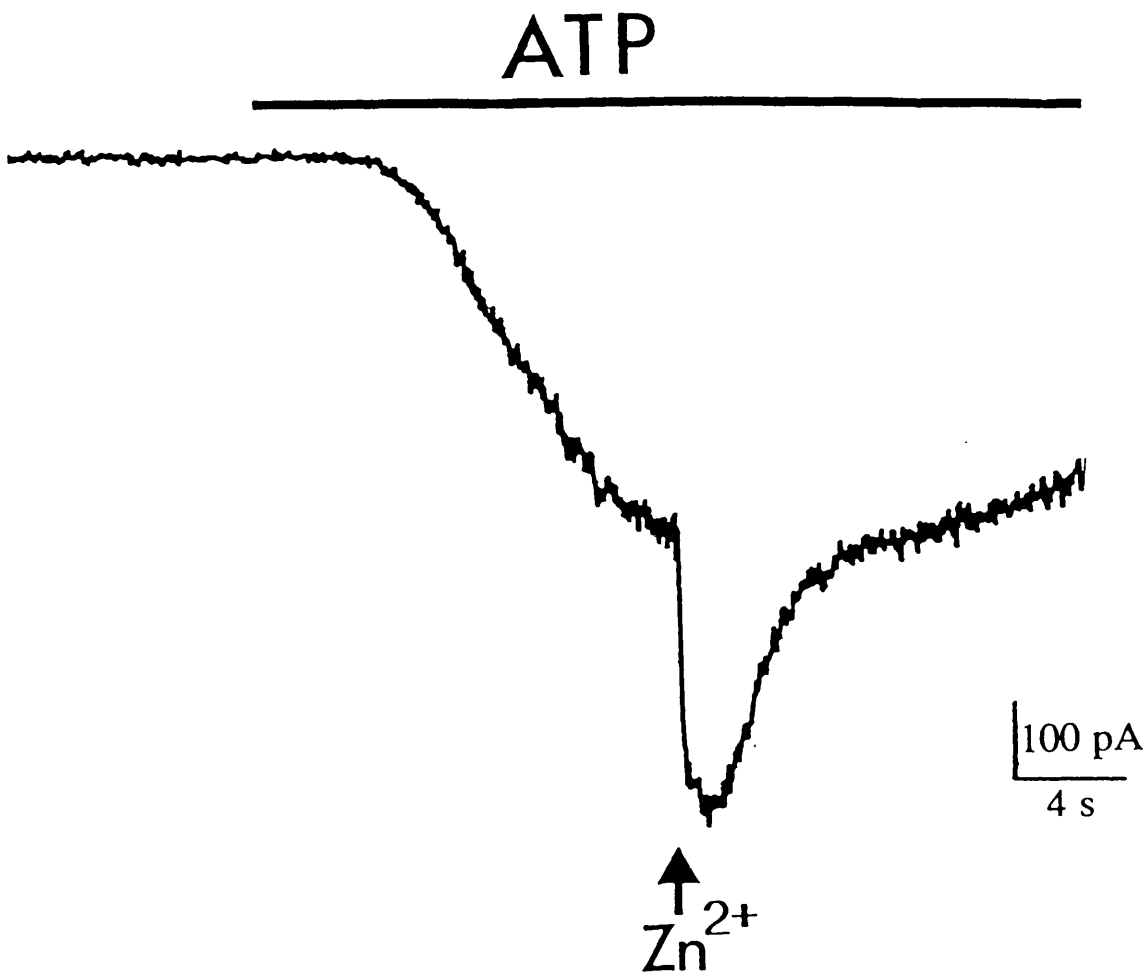
**Figure 13** Fast potentiation of $I_{ATP}$ by $Zn^{2+}$. $I_{ATP}$ evoked by bath application of ATP (100 $\mu$M; indicated by the bar) and subsequent application of $ZnCl_2$. $Zn^{2+}$ (100 $\mu$M) was applied by 500 ms pressure application at the peak of the inward current, indicated by the arrow. Holding potential = -60 mV.

## A



## B



* control = 384 ms
10 $\mu$M Zn$^{2+}$ = 794 ms
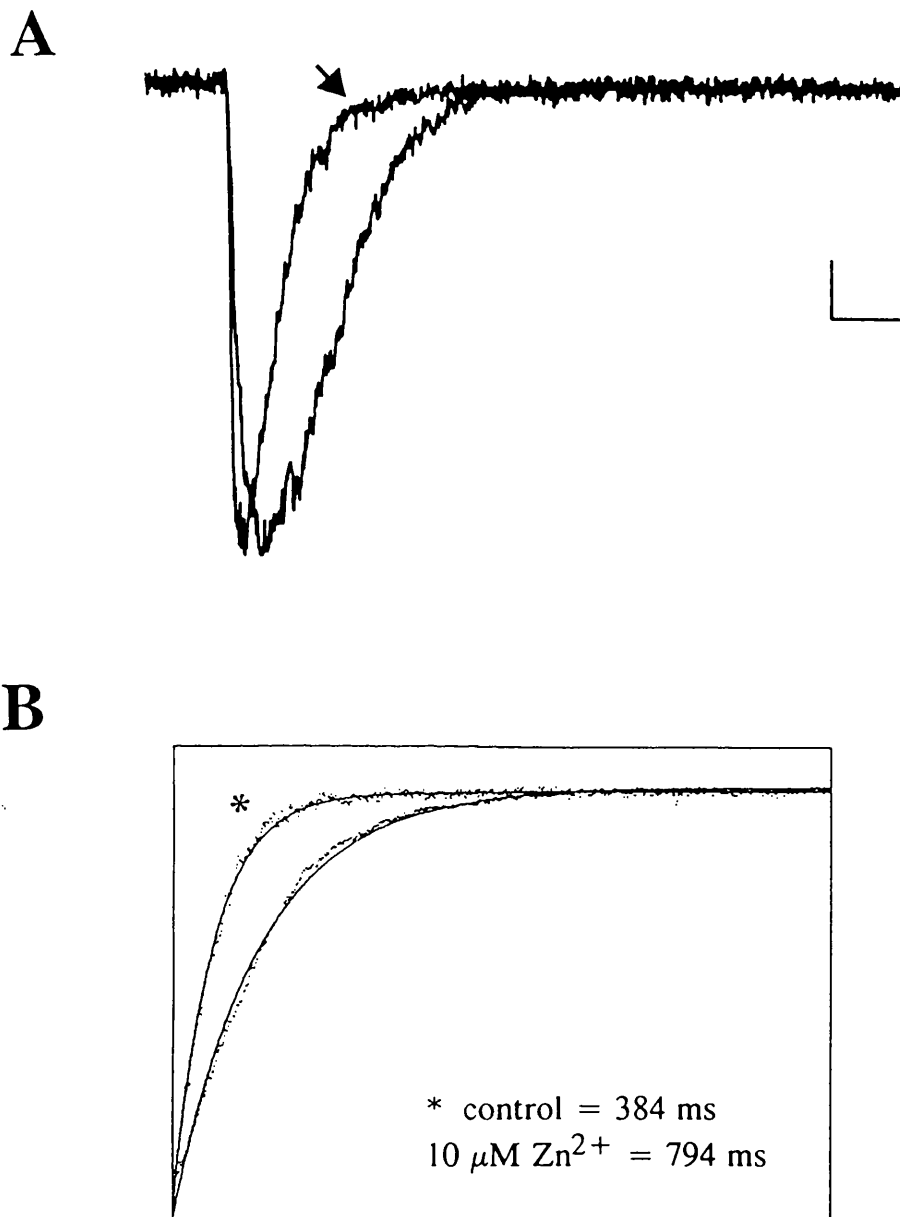
**Figure 14** Effect of 10 $\mu$M Zn$^{2+}$ on I$_{ATP}$ decay kinetics. **A.** Control (arrow) and potentiated (10 $\mu$M Zn$^{2+}$) ATP-evoked currents normalized to illustrate increase in current duration. I$_{ATP}$ was activated by pressure application of 1 mM ATP (50 ms). Scale bar represents 1 second and 30 pA for the control current and 40 pA for the potentiated current. The traces are the average of 3 applications of ATP, evoked once per 30 seconds. **B.** Single exponential fits of the decay of the same current traces shown in A. The traces (averaged) were fitted from approximately 300 ms after the peak of the current to the baseline using a least squares routine. The asterisk indicates the control ATP current.

# Table 1

| conc $Zn^{2+}$ ($\mu M$) | 0 | 0.5 | 1 | 3 | 7 | 10 | 30 |
|---|---|---|---|---|---|---|---|
| tau (ms) | 218 | 227 | 320 | 335 | 496 | 506 | 1315 |

**Table 1** Increase in decay time constant of $I_{ATP}$ by $Zn^{2+}$. The decay of $I_{ATP}$ evoked by 1 mM ATP (pressure ejection) was fitted with a single exponential from 300-400 ms following peak amplitude back to baseline. $I_{ATP}$ was evoked three times in each $Zn^{2+}$ concentration and the traces were averaged for fitting. $Zn^{2+}$ was included in the bath with the order of concentrations randomized.
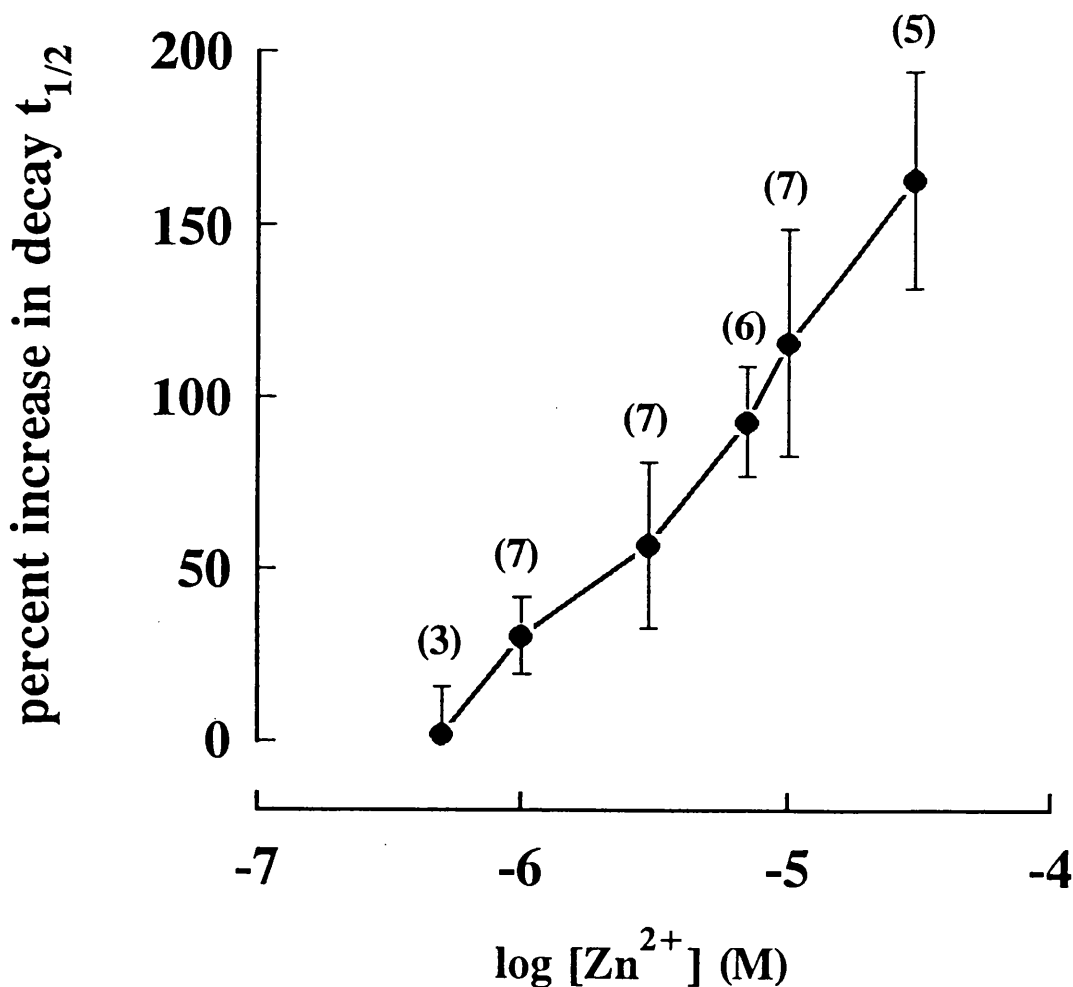
**Figure 15** Dose-response relationship of $Zn^{2+}$ on $I_{ATP}$ decay kinetics. Percentage increase in time from peak current amplitude to one-half recovery of $I_{ATP}$ compared to control current plotted as a function of $Zn^{2+}$ concentration. $ZnCl_2$ was included in the bath. $I_{ATP}$ was evoked 3 times in each solution every 30 seconds by pressure ejection of 1 mM ATP (50 ms) with 1 minute allowed for solution changes. The current traces were averaged. The order of application of different $Zn^{2+}$ concentrations for a given cell was randomized. Error bars are SEM (number of cells listed above points).

# CONTROL

# 10 $\mu$M Zinc
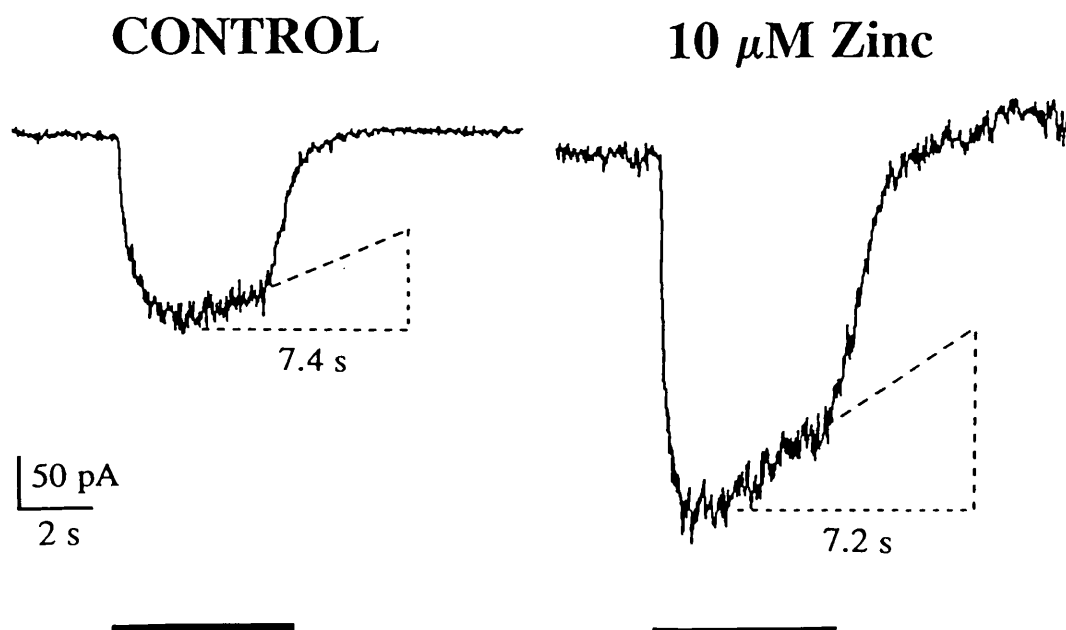


**Figure 16** Effect of $Zn^{2+}$ on desensitization of $I_{ATP}$. Currents evoked by prolonged application of 100 $\mu$M ATP (pressure ejection) in the absence and presence of 10 $\mu$M $Zn^{2+}$. The period of ATP application is indicated by the bars shown below each trace. A two minute wash was allowed between exposures to ATP. The dashed lines indicate the slope of the line of current decay (diagonal), 50% current amplitude (vertical) and the time to 50% current amplitude (horizontal). Holding potential = -60 mV. Currents are digitally filtered at 330 Hz.
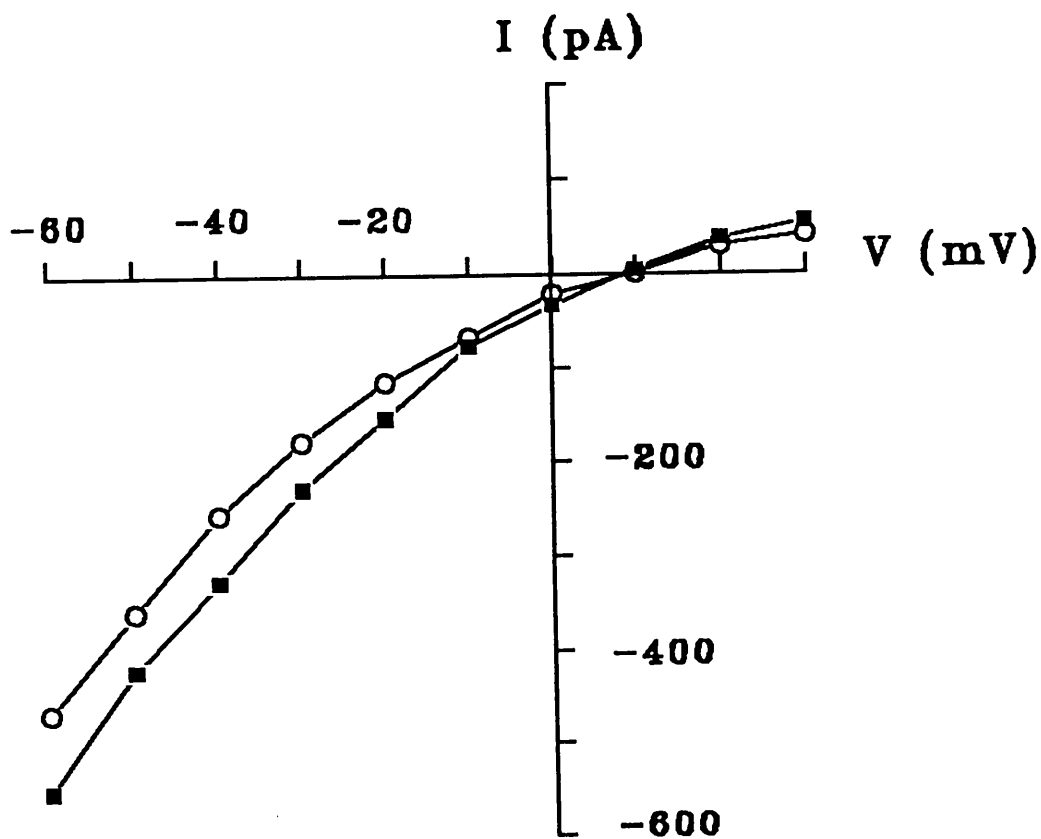
**Figure 17** Current-voltage relation of $I_{ATP}$. $I_{ATP}$ was activated in one cell in the presence (solid squares) and absence (open circles) of 10 $\mu$M $Zn^{2+}$. $I_{ATP}$ was evoked by pressure application of 1 mM ATP (5 s) and the membrane potential jumped for 50 ms every 100 ms over the range -60 mV to +30 mV in 10 mV increments. The extracellular solution nominally $Ca^{2+}$-free and contained the $Na^+$ channel blocker tetrodotoxin (0.5 $\mu$M).

$$0 \ Zn^{2+} \qquad\qquad 10 \ \mu M \ Zn^{2+}$$

10 $\mu$M ATP

50 pA
4 s

60 $\mu$M ATP
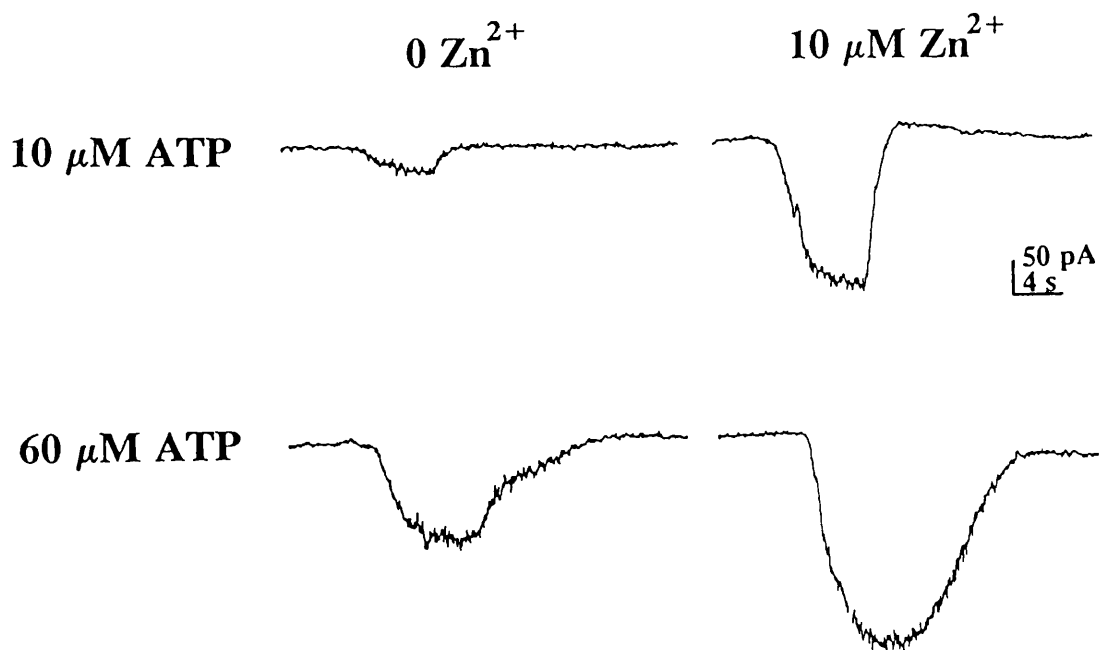
**Figure 18** Effect of $Zn^{2+}$ on $I_{ATP}$ evoked by two concentrations of ATP. Currents activated in two cells by different concentrations of ATP. ATP was applied via the bath for 5 seconds in either 10 $\mu$M $Zn^{2+}$ or nominally $Zn^{2+}$-free solution. The cell was washed 2 minutes between exposures to ATP. Holding potential = -60 mV.
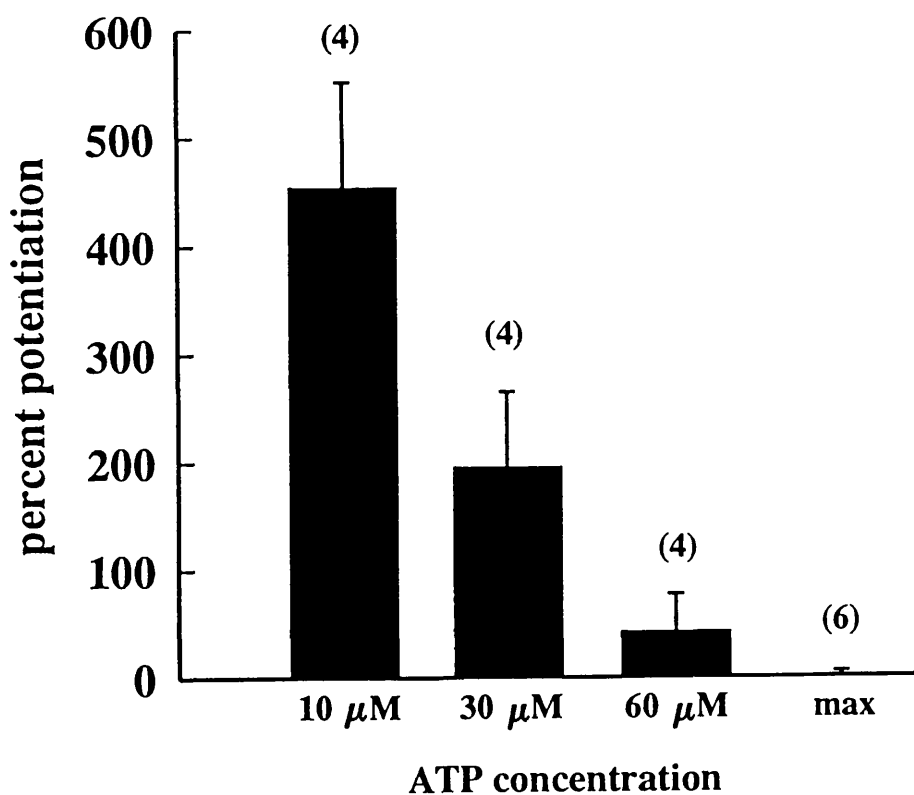
**Figure 19** Dependence of effect of $Zn^{2+}$ on ATP concentration. Percentage potentiation by $Zn^{2+}$ (10 $\mu$M) of $I_{ATP}$ activated by increasing concentrations of ATP. ATP was applied via the bath for 5 seconds allowing a 2 minute wash between exposures. Cells were exposed to one concentration of ATP in the presence and absence of $Zn^{2+}$ and the data were pooled (number of cells indicated above the bars). The maximum was obtained by pressure application of ATP (100 mM) for increasing durations until the current amplitude reached a plateau.
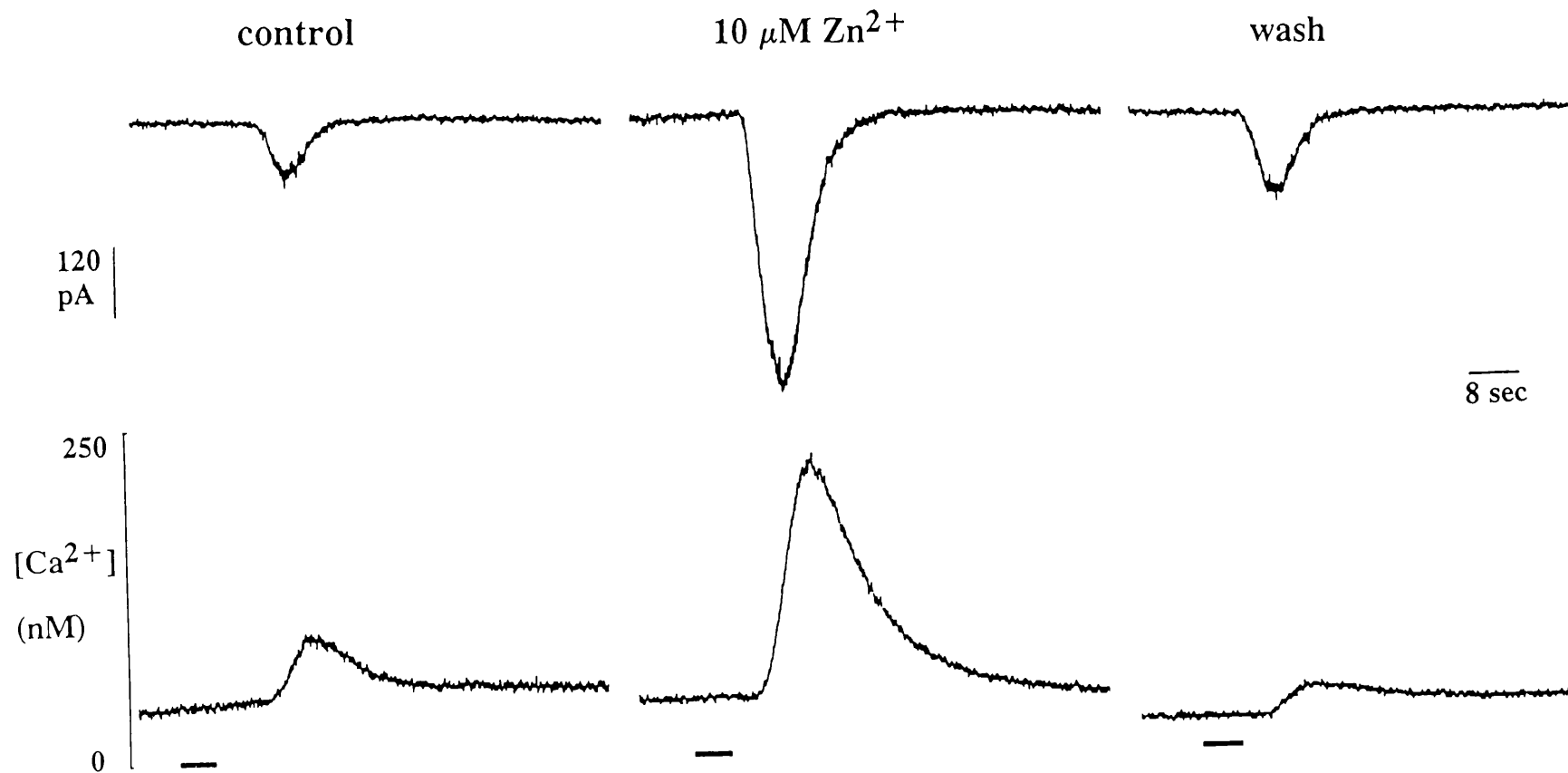
**Figure 20** Effect of $Zn^{2+}$ on ATP-evoked rises in intracellular $Ca^{2+}$. Top traces show ATP-evoked currents and bottom traces show intracellular $Ca^{2+}$ levels measured simultaneously using Indo-1 (included in the patch pipette solution). $I_{ATP}$ was evoked by bath application of ATP (100 $\mu$M, 5 s indicated at the bar) under control conditions and in the presence of 10 $\mu$M $Zn^{2+}$. Holding potential = -60 mV. The cell was washed 2 minutes between exposures to ATP. Traces are digitally filtered at 330 Hz.
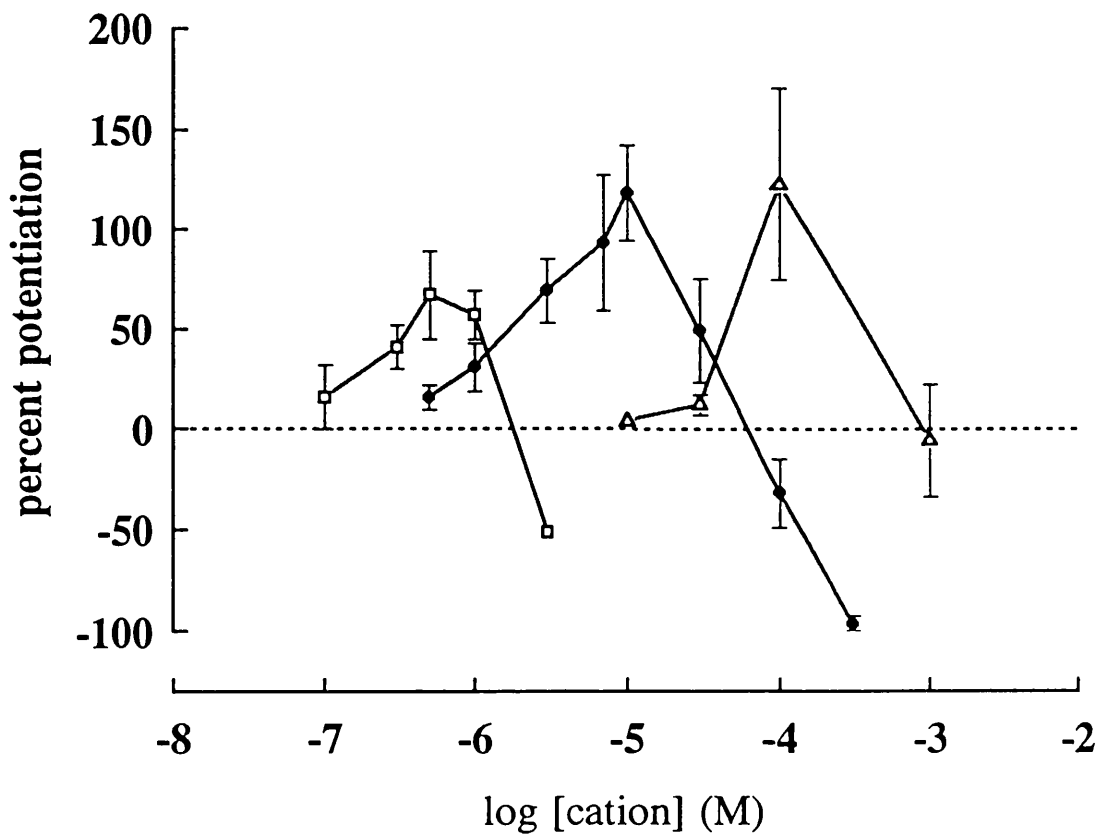
**Figure 21** Dose-response curves for the effect of 3 different divalent cations on $I_{ATP}$ amplitude. Each point represents the mean enhancement of $I_{ATP}$ compared to the previous wash (average of 3 traces) in the presence of different concentrations of $Cu^{2+}$ (open squares); $Zn^{2+}$ (closed circles); and $Ni^{2+}$ (open triangles). Cations (chloride salt) were added via the bath and $I_{ATP}$ was evoked by pressure ejection (1 mM). Points with error bars represent data from at least 3 cells. Points with no error bars represent the mean of 2 cells. Holding potential for all cell = -60 mV. Error bars represent SEM.
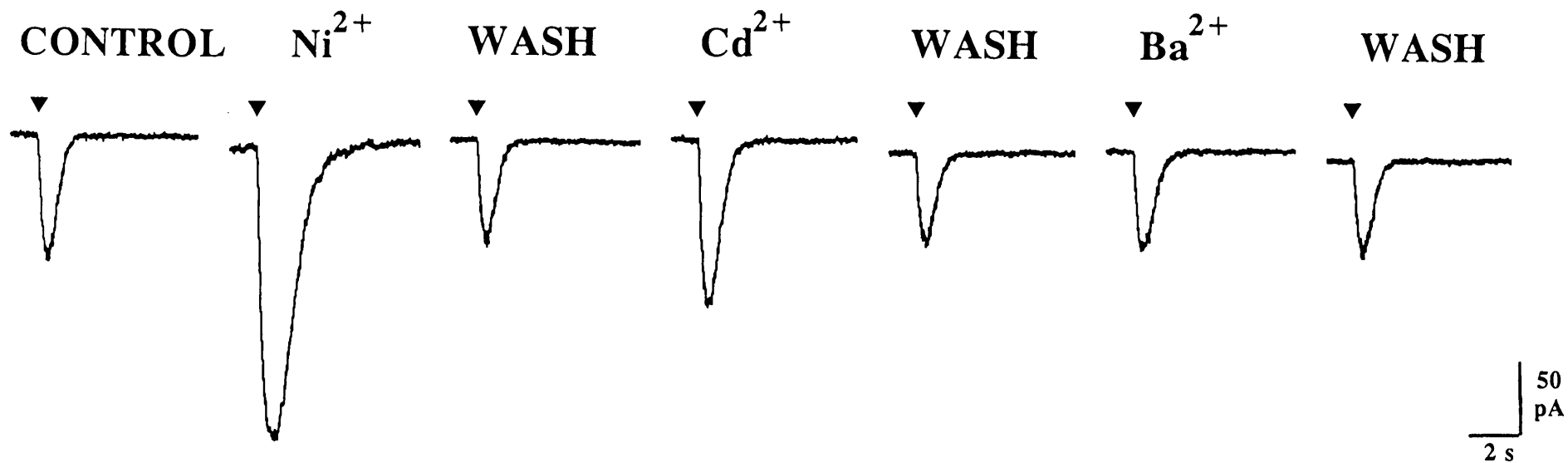
**Figure 22** Effect of different divalent cations on $I_{ATP}$ evoked in one cell. Cations were added as chloride salt to the bath solution (100 $\mu$M for each). $I_{ATP}$ was evoked by pressure application of 1 mM ATP for 50 ms every 30 seconds, indicated at the triangles. Traces represent averages of three ATP applications. The cell was washed 1.5 minutes between sets of ATP applications.
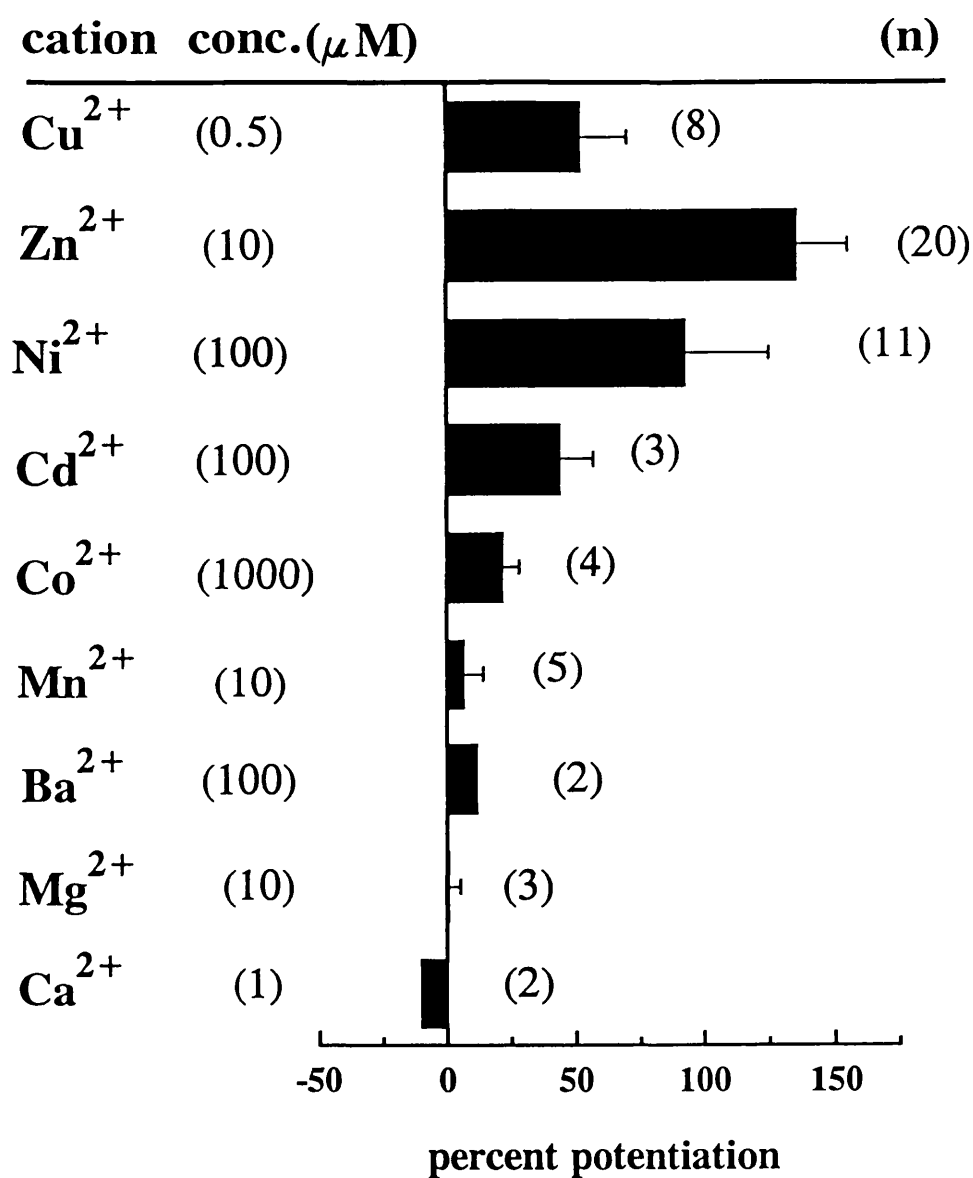
**Figure 23** Percentage potentiation of $I_{ATP}$ by different divalent cations. $I_{ATP}$ was evoked by pressure application (1 mM ATP) and divalent cations were applied as chloride salts via the bath. The concentrations shown are those which maximally potentiated $I_{ATP}$. Error bars are SEM.

## Chapter 5: Single channel currents activated by ATP

## I. Introduction

Whole-cell current responses to exogenously applied ATP have been reported in many different neuronal preparations. There are only a few reports, however, in which single ATP-gated channels have been examined. Thus, little is known about the properties of the channels which mediate fast purinergic transmission in neurones.

From the few reports on ATP-gated channels, there appears to be considerable variation in the properties of the channels between preparations. For example, the unitary current amplitude (recorded at the same potential) ranges from 0.3 pA in sensory neurones (Bean et al. 1990a) to 5 pA in parasympathetic ganglia (Fieber & Adams, 1991). There are also differences in voltage sensitivity, kinetics, and permeability (see Bean & Friel, 1990 for review). This is perhaps not surprising given the variability in whole-cell ATP responses, described in Chapter 4.

The diverse properties of ATP-gated single channels in different neurones may reflect the presence of different $P_{2x}$ receptor subtypes composed of multiple subunits. Subunit heterogeneity has helped explain variation in other fast neurotransmitter responses, and ATP receptors may follow this same pattern. The classification of $P_{2x}$ receptors at the present time is still largely based on pharmacological profile using a limited number of agonists. As these receptors are cloned and their single channel properties are determined, however, the classification scheme is sure to expand.

Single channel analysis can aid in the characterization of native receptors by revealing characteristics of receptor activation that are difficult to assess from whole-cell currents. For example, multiple channel conductances could reveal a non-homologous receptor population which may not be appreciated if the receptors are pharmacologically indistinguishable. This may be particularly important for $P_2$-purinoceptors because of the absence of selective agonists and antagonists. Moreover, the mechanism of inward rectification of $I_{ATP}$ may also be determined at the single channel level, revealing whether it is due to a voltage-dependence of channel open probability or to rectification of current through the channel pore itself. Thus,

examination of single ATP-gated channels can contribute to a mechanistic understanding of the properties of whole-cell ATP-evoked currents.

Of particular interest to this report is the modulation of ATP-gated channel activity by extracellular $Zn^{2+}$. Divalent cations have been reported to affect ligand-gated currents by a variety of mechanisms, including changing apparent binding affinities (Lovinger, 1991), altering channel kinetics (Legendre & Westbrook, 1991; Harrison *et al.*1993b), and affecting the permeability pathway through the channel pore (Christine & Choi, 1990; Ifune & Steinbach, 1991). Single channel analysis can provide important clues of how divalent cations modulate macroscopic currents and, indeed, can often reveal complex mechanisms which are not apparent at the whole-cell level. For example, external $Ca^{2+}$ potentiates nAChR responses in medial habenula neurones (Mulle *et al.*1992). In whole-cell responses, the maximum current amplitude is not potentiated; however, single channel experiments reveal that $Ca^{2+}$ also blocks the permeation pathway through the channels and that after correcting for this phenomenon the maximum current amplitude *is* increased. Thus, the interpretation of the mechanism of $Ca^{2+}$ modulation changes from a possible increase in binding affinity of the receptor to an increase in the maximal probability of channel opening.

The actions of $Zn^{2+}$ on ionic currents are clearly complex. Studies of single NMDA receptor channels reveal that $Zn^{2+}$ can both decrease channel open probability and block conductance through the pore (Christine & Choi, 1990). The frequency of channel opening of $GABA_A$ receptors is also reduced by $Zn^{2+}$ (Smart, 1992). As described in Chapter 4, $Zn^{2+}$ has two actions on macroscopic currents elicited by ATP in rat SCG neurones, potentiating the current at low concentrations and inhibiting the current at high concentrations (Cloues *et al.*1993). Examination of the effect of $Zn^{2+}$ on ATP-gated single channels should contribute to an understanding of the mechanism of $Zn^{2+}$ interaction with $P_{2x}$-purinoceptors.

## II. Results

Recording solution

Excised outside-out patches were used to record unitary currents activated by ATP. Initial experiments were conducted using a caesium acetate-based pipette solution. This solution was reliably used for whole-cell recording of $I_{ATP}$ (Chapter 3). However, channels could not be activated under these recording conditions. In 2/17 patches using this solution, an initial burst of channels was observed in response to ATP application, but the activity could not be recovered with subsequent applications. This suggested that there were channels present in the patch but that they were subject to rapid rundown. Subsequently, nystatin- permeabilized vesicles (outside-out configuration) were used to record ATP channels (27 patches). While this recording configuration maintained channel activity, the baseline noise was too high for purposes of analysis; in addition, the patches were unstable and therefore unsuitable for long experiments.

Gluconate has been used to record ATP-gated channels in rat coeliac ganglia (Silinsky & Gerzanich, 1993). This proved to be successful for SCG neurones as well: using a caesium gluconate-based internal solution, ATP-induced channel activity could now be recorded in outside-out patches for long periods of time (up to 50 minutes) without substantial rundown. Subsequent experiments were thus carried out using excised patches with gluconate as the predominant anion.

ATP-gated channels in outside-out patches

Single ATP-gated channels were recorded in 110 out of 313 patches (including nystatin patches). Sample traces from a patch with channel activity are shown in Figure 24A. Channels were activated by 50 $\mu$M ATP (bath applied), resulting in high channel activity. Most patches contained more than one channel, similar to this patch, as indicated by the multiple opening levels (dotted lines).

The amount of ATP-gated channel activity was dependent on concentration. In 2 patches, 10 $\mu$M ATP (bath applied) resulted in a higher open probability (.047 and .111 for 5 min.) than 3 $\mu$M ATP (.006 and .022, respectively). Channel open probability was estimated as nPo, the product of the number of channels in the patch multiplied by the percent time the channel resided in the open state, determined using the 50% threshold crossing method. The open and closed states were determined from Gaussian distributions fitted to the all-point histogram of the record. In some patches there was spontaneous channel activity in the absence of ATP, but in no case did this resemble the channels evoked by ATP.

The ATP-gated channels were blocked by suramin (Fig 24B)(10-50 $\mu$M, n=5). The effect of suramin on channel activity over the duration of an experiment is shown in Figure 25. This is the same patch as in Figure 24. The patch was exposed to 10 $\mu$M ATP, ATP + 50 $\mu$M suramin, and then again to ATP alone. There was a clear decrease in the open probability of the channels in the presence of suramin. The reversibility of the suramin block is shown when the drug was washed away.

The fine structure of the openings of ATP-gated channels can be seen in Figure 26A. The channels appeared noisy in the open state, demonstrating large fluctuations in current. At least one subconductance state could be identified, denoted O1 in the figure. This was taken to be a subconductance state, as opposed to a separate channel with a different conductance, because the channel frequently opened from the subconductance state to the fully open state and vice versa.

The ATP-gated channels were quite small under these recording conditions. At -80 mV, the usual recording potential, the mean amplitude of the full open state was -0.97 $\pm$ 0.06 pA (n=9) and of the subconductance state was -0.48 $\pm$ 0.04 pA (n=4). Estimates of channel amplitude for the full conductance state were determined by Gaussian fits of amplitude histograms. The subconductance state was relatively infrequent compared to the fully open state and usually could not be resolved in amplitude histograms, even with substantial filtering (250 Hz). The amplitude of the subconductance state was therefore estimated by eye.

## Voltage-dependence

The current-voltage relationship of ATP-activated channels is shown in Figure 26. Part A shows sample traces of channels at three different patch potentials. The sub- and full conductance states are denoted O1 and O2, respectively. Like the whole-cell ATP-evoked currents, the unitary currents decreased in amplitude as the patch potential approached 0 mV. The I/V curve between -120 and

-40 mV for this patch is shown in Figure 26B. The unitary conductance of the full and subconductance states at -80 mV was 11 pS and 6 pS, respectively, assuming a null potential of 0 mV. The full conductance state showed a slight inward rectification in this patch. The mean I/V curve of 8 patches, shown in Figure 27, did not appear to rectify, however. The mean slope conductance for the fully open state, measured between -120 and -40 mV was 19 pS.

The ATP-gated channels showed a strong voltage dependence in their opening probability (Figure 28). Channels were recorded for 15 seconds at each potential in the presence of 5 $\mu$M ATP. The order of holding potentials was randomized for each patch. Open probability was determined from the relative time the channel was in the open state per 15 seconds, based on the 50% threshold crossing method (n=3). No distinction was made for openings to the full and subconductance states as openings to the subconductance state were relatively infrequent. At -120 mV, the channels were approximately 5 times more likely to be open than at -40 mV.

Changes in apparent open probability could result from missed events at potentials close to 0 mV because of the decreased channel amplitude relative to baseline noise. To examine whether this would contribute substantially to the measured change in nPo, channel activity was simulated to produce idealized channel records at two membrane potentials. Current amplitude at -40 mV was -0.3 pA and at -120 mV was -1.6 pA (mean amplitude from experiments in Figure 28). The baseline noise was estimated from the standard deviation of Gaussian fits of the closed state at -40 and -120 mV (0.1 pA and 0.2 pA, respectively) and was digitally filtered to match recorded

signals. The simulation was run for one exponentially distributed open time and two exponentially distributed shut times, with means set at $\tau_o$ = 6 ms, $\tau_{s1}$ = 4 ms, and $\tau_{s2}$ = 200 ms (Figure 29A). These values were obtained from open and shut time distributions of 3 patches in separate experiments (Vm -80 mV, 5 $\mu$M ATP). The number of openings per burst was set at 10 to simulate the "flickery" behaviour of ATP-gated channels (Figure 29B). nPo was determined as the area under the Gaussian curve fitted to the open point histogram and was 0.117 at -40 mV and 0.138 at -120 mV. This is only a 15% reduction in apparent open probability due to missed events and is not enough to account for the large increase in nPo at -120 mV measured experimentally ( >700% increase).

## Comparison to nAChR channels

Single channels activated by the nicotinic receptor agonist DMPP were also recorded in SCG cells (n=4). DMPP (10 $\mu$M) was bath applied to patches which had not responded to ATP. The channels activated by DMPP had a larger slope conductance (27 $\pm$ 4.7, n=3; measured between -120 and -40 mV) in comparison with ATP-gated channels and were not as noisy in their open state (Figure 30). Channels could be recorded at potentials positive to 0 mV, in contrast to ATP-gated channels. In one patch, 100 $\mu$M suramin had no effect on the DMPP-induced channel activity.

## Effect of $Zn^{2+}$ on ATP-gated channel activity

ATP-gated channel activity increased in the presence of low concentrations of $Zn^{2+}$. Figure 31 shows example traces of channel activity in one patch in response to a short (50 ms) application of ATP (pressure ejection). The averaged trace of 10 such records in control and wash solutions is shown below (5 in each). When 5 $\mu$M $Zn^{2+}$ was included in the bath, there was an increased amount of channel activity in the patch in response to the same application of ATP. $Zn^{2+}$ alone did not activate any channels (n=5). The averaged trace of 5 sweeps showed that the potentiating effect of low concentrations of $Zn^{2+}$ on whole-cell ATP currents was mimicked at the single channel

level. Thus, the conditions permitted characterization of the effect of $Zn^{2+}$ on ATP-gated channels.

To better examine the changes in channel activity in the presence of $Zn^{2+}$, experiments were performed using low concentrations of ATP for longer durations. Figure 32 shows the result of one such experiment. In the presence of 5 $\mu$M $Zn^{2+}$, there was an increase in channel open probability compared to control conditions. The increase in channel activity was measured as total charge transfer per 60 seconds. Charge transfer was determined by measuring the area under the curve (Gaussian distributions) of the channel open state amplitude distribution and multiplying this number by the amplitude of each component. For this patch the charge transfer for 1 minute was 49 fC in 5 $\mu$M ATP and 173 fC in ATP + 5 $\mu$M $Zn^{2+}$. In separate experiments over longer durations, the mean charge transfer per 270 seconds was 13 $\pm$ 4 fC in 3 $\mu$M ATP and 46 $\pm$ 16 fC in 3 $\mu$M ATP and 5 $\mu$M $Zn^{2+}$ (n=4). Thus 5 $\mu$M $Zn^{2+}$ increased channel activity by 313 $\pm$ 186% for this concentration of ATP.

The increase in charge transfer in the presence of $Zn^{2+}$ was not due to an increase in unitary current amplitude. Figure 33 shows amplitude histograms of channels in one patch activated by ATP (5 $\mu$M) and ATP + $Zn^{2+}$ (5 $\mu$M), fitted with Gaussian distributions. As can be seen, the unitary current amplitude is the same for both conditions, around -1 pA. For 7 patches, unitary current amplitude at -80 mV was -0.94 $\pm$ 0.08 pA and in the presence of $Zn^{2+}$ (5 $\mu$M) was -0.88 $\pm$ 0.08 pA. The subconductance state was not resolved with sufficient frequency to determine whether there was an effect of $Zn^{2+}$ specifically on this open state. However, openings to the subconductance state could be observed both in ATP and ATP + $Zn^{2+}$.

The increase in charge transfer in the presence of $Zn^{2+}$ appeared to be due to a greater frequency of channel opening. This is illustrated in Figure 34, showing the open time distribution of channels in one patch activated by 3 $\mu$M ATP and 3 $\mu$M ATP + 5 $\mu$M $Zn^{2+}$. There is an increase in the frequency of openings across the entire distribution in the presence of $Zn^{2+}$, consistent with 7 other patches. The data are fitted with two exponentials in this patch, and there is a lengthening of both time

constants with $Zn^{2+}$. However, the effect of $Zn^{2+}$ on the open time constants was not consistent, perhaps due to the noisy behavior of the channels. It was therefore not possible to determine if $Zn^{2+}$ altered the microscopic kinetics of ATP-gated channel opening.

## Effect of $Zn^{2+}$ on burst duration

In addition to causing an increase in the frequency of channel opening, low concentrations of $Zn^{2+}$ caused an apparent increase in the burst duration of ATP-gated channels (Figure 35). To calculate mean burst duration, a critical gap length, $T_{crit}$, was first estimated from shut time histograms for each patch (Figure 36). The histograms were usually fitted with 2 or 3 exponentials with time constants that were well separated. The shortest exponential ($tau_{c1}$) did not vary consistently with ATP concentration (Table 2); this was taken as the mean shut time within bursts. For 3 $\mu$M ATP mean $tau_{c1}$ = 3.7 $\pm$ 0.6 ms (n=5) and for 5 $\mu$M ATP mean $tau_{c1}$ = 3.6 $\pm$ 1.0 ms (n=3).

To estimate burst duration, $T_{crit}$ was calculated as 5 times the mean shut time ($tau_{c1}$) for each record, and closures shorter than $T_{crit}$ were omitted. The accuracy of this was checked by increasing the length of the excluded closures. The mean burst duration did not change with $T_{crit}$ up to 7 times the mean shut time, as would be expected from the clear separation of short and long closures. The mean burst durations for three patches in ATP alone and ATP with $Zn^{2+}$ are shown in Table 3. The ratio of the mean burst duration in ATP + $Zn^{2+}$ to the mean burst duration in ATP alone was 2.08 $\pm$ 0.33 (n=3). Thus, 5 $\mu$M $Zn^{2+}$ approximately doubled the channel burst duration.

## High concentrations of $Zn^{2+}$

In three patches, ATP-gated channels were recorded in the presence of high concentrations of $Zn^{2+}$ (100 $\mu$M). Under these conditions, the channels were open almost continuously (Figure 37). During the course of the application, however, the

channel openings became much less distinct and the unitary conductance decreased. The unitary current after 30 seconds exposure to 100 $\mu$M $Zn^{2+}$ was 0.41 $\pm$ 0.13 pA (n=3), compared to 0.74 $\pm$ 0.05 pA under control conditions.

## III. Discussion

This chapter describes the single channel currents underlying $I_{ATP}$. There is a good correlation between the whole-cell data and the single channel data with regard to concentration dependent activation of the channels by ATP and block by suramin. In addition, the channels are sensitive to changes in extracellular $Zn^{2+}$ concentration, showing an increase in activity with low concentrations and a reduced unitary conductance with higher concentrations. The ability to record ATP-gated channels in excised outside-out patches is consistent with activation of a $P_{2x}$-, ligand-gated receptor-channel complex. In addition, modulation of the channels by $Zn^{2+}$ in a manner consistent with whole-cell currents supports the idea that $Zn^{2+}$ acts at an extracellular site and does not require diffusible intracellular messengers.

Recording solution

ATP-gated channels could be successfully recorded in excised outside-out patches using caesium gluconate as the internal solution. The fact that channels could not be recorded using an acetate-based pipette solution suggests that acetate has a detrimental effect that gluconate does not have. Single ATP-gated channels have also been recorded using chloride as the internal anion (Nakazawa & Hess, 1993; Nakazawa & Inoue, 1993), suggesting that it may be a negative effect of acetate on the channels, as opposed to a positive effect of gluconate, that permits channel activity in gluconate solution. It is interesting, however, that ATP-evoked currents in whole-cell conditions were not obviously affected by using acetate intracellularly.

Kinetic Behaviour

ATP-gated channels showed large fluctuations in current amplitude in their open state. The unresolved rapid kinetic behaviour of the channels did not permit detailed kinetic analysis of channel open times. In most cases, it was impossible to distinguish between closings to the subconductance state and full closures, and openings to the

subconductance state and full openings. Lowering the concentration of agonist reduced channel opening frequency but did not eliminate the open channel noise.

The "flickery" behaviour of ATP-gated channels observed in this study is characteristic of ATP-gated channels in several preparations, including PC12 cells (Nakazawa & Hess, 1993) and sensory neurones (Krishtal et al. 1988; Bean et al. 1990a), though the amount of flicker varies between different cell types. In parasympathetic neurones the openings are fairly clean with apparently no subconductance states (Fieber & Adams, 1991). Channels recorded from coeliac ganglion cells also appear to have less open channel noise than SCG neurones (Silinsky & Gerzanich, 1993), even though they are both sympathetic ganglia. In frog sensory neurones, by comparison, the channel kinetics are so rapid that the unitary conductance cannot be resolved (Bean et al. 1990a).

The causes of the current fluctuations are unknown. Open channel block by non-permeant ions can increase channel noise (Yellen, 1984; Ascher & Nowak, 1988); however, in PC12 cells (Nakazawa & Hess, 1993) and sensory neurones (Krishtal et al. 1988; Bean et al. 1990a), the flickery behaviour of ATP-gated channels remains even in the absence of divalent cations. The current fluctuations may be due to rapid transitions between conducting states of the channel, possibly induced by thermal oscillations (Lauger, 1983). That these fluctuations are so much greater for ATP-gated channels than for other ligand-gated ion channels may reflect differences in 3-dimensional structure.

## Unitary Conductance

The unitary conductance of the ATP-gated channels in SCG neurones was 11 pS at -80 mV. The channels are roughly the same size as ATP-gated channels in PC12 cells (Nakazawa & Hess, 1993) and rat sensory neurones (Krishtal et al. 1988), where the unitary conductances are 15 pS and 17 pS, respectively. There is great variation in the single channel properties of ATP-gated channels in different preparations. In parasympathetic cardiac ganglia, the unitary conductance is 60 pS, and the channels

show very little noise in the open state (Fieber & Adams, 1991). In contrast, ATP

channels in frog sensory ganglia are so flickery that the fully open state is unresolved

and a conductance is impossible to define (Bean *et al.* 1990a); noise analysis gave an

estimated channel conductance of 0.13 pS. In sympathetic cells from guinea-pig coeliac

ganglion, unitary channel conductance is 37 pS (at -90 mV; Silinsky & Gerzanich,

1993). In rat SCG neurones, the unitary current amplitude at -80 mV is 1.3 pA

(Nakazawa & Inoue, 1993), in accord with this report.

The unitary channel amplitude can be used to estimate the number of channels in

a cell. The mean whole-cell current amplitude activated by 100 $\mu$M ATP (maximum

current amplitude) was -422 pA at -60 mV (see Chapter 3). The mean unitary current

amplitude at this potential was -.65 pA, which would correspond to 650 channels per

cell. This would be a lower limit, as this assumes that all of the channels are open

during current activation (open probability = 1). The average area of an SCG neurone

is 5500 $\mu m^2$ (see Chapter 2), predicting approximately 1 channel per 8 $\mu m^2$. Assuming

a patch area of around 1 $\mu m^2$ (Sakmann & Neher, 1983), one would expect to record a

channel in approximately 1 out of 8 patches. The fact that ATP-gated channels were

observed in approximately 1 in 3 patches suggests that the open probability of the

channels is much lower than 1 and that there are, in fact, many more channels in the

cell. In addition, the channels may be clustered and/or concentrated on the cell soma.

Voltage-dependence

ATP-gated channels in rat SCG showed a strong voltage-dependence in their

opening probability. At negative potentials the channels were much more likely to be

open than at more positive potentials. The effect of this phenomenon would contribute

substantially to the inward rectification of whole-cell ATP-evoked currents. The mean

whole-cell conductance of $I_{ATP}$ was 3 times greater at -120 mV (7.7 $\pm$ 1.5 nS; n=8)

than at -40 mV (2.7 $\pm$ 0.5 nS; n=11). Since the mean channel I/V was linear, it can

be assumed that the single channel conductance is the same at all potentials. This

increase in whole-cell conductance must be accounted for by the increase in channel

open probability. At -120 mV channel nPo was 5 times greater than at -40 mV, which is larger than expected from the whole-cell conductance (3x). The increase between -40 mV and -100 mV in nPo (2.3x) and whole-cell conductance (2.2x) is in better agreement. Thus, the decrease in channel open probability at depolarized potentials can completely account for the rectification of whole-cell ATP-evoked currents.

Not surprisingly, given the variation of other properties of ATP-gated channels in various cell types, there are multiple causes of $I_{ATP}$ rectification. In frog sensory neurones, there is no evidence of voltage-dependence of channel opening, and the rectification appears to be an instantaneous property of ion permeation (Bean *et al.*1990a). In contrast, ATP-gated channels in parasympathetic ganglia have a linear current-voltage relationship (Fieber & Adams, 1991). The rectification in these cells is, therefore, determined entirely by the voltage-dependence of the channels. This appears to be the case for SCG neurones as well.

## Comparison to nicotinic AChR channels

ATP-gated channels were compared to channels activated by the nicotinic agonist DMPP in the same cells. The nAChR channels have quite different characteristics from the ATP-gated channels in that they have a larger unitary conductance and much cleaner openings. The channels could also be recorded at positive holding potentials, as described previously (Mathie *et al.*1990). Suramin did not affect the DMPP-activated channels. In no case were "ATP-like" channels activated by DMPP. Likewise, nAChR channels were not evoked by application of ATP. In addition, the patches in which nAChR channels were activated had not contained ATP-gated channels. Thus, ATP and DMPP appear to activate distinct channels in rat SCG neurones.

In skeletal muscle, ATP activates nAChR receptor channels (Igusa, 1988; Lu & Smith, 1991). Channels activated by the two agonists have the same unitary conductance and channel kinetics. It has been proposed, therefore, that nAChR receptors have a binding site for ATP which increases the frequency of opening of the

channels. A similar mechanism has been proposed for ATP responses in PC12 cells (Nakazawa *et al.* 1991) and sympathetic neurones (Gabella, 1985). In both cell types, the whole-cell properties of $I_{ATP}$ and $I_{ACh}$ are quite distinct, but the two currents are non-additive, indicating a common receptor pool or some other mode of interaction. Single channel studies, however, indicate that ACh and ATP activate distinct channels (Nakazawa & Inoue, 1993; Silinsky & Gerzanich, 1993; this report), even in the same patch. This would suggest that there are two distinct receptor-ionophore complexes and not one channel activated by both ligands. This does not preclude some level of interaction between the two receptors, however.

## Effect of $Zn^{2+}$ on channel activity

The potentiating effect of low concentrations of $Zn^{2+}$ on $I_{ATP}$ observed under whole-cell conditions were mimicked in single channel recordings. There was an increase in charge transfer in the presence of $Zn^{2+}$ which was due to an increase in channel opening frequency and not to a change in unitary current amplitude. $Zn^{2+}$ does not appear to activate ATP-gated channels itself, as no channel activity was seen when $Zn^{2+}$ was applied in the absence of ATP.

In addition to increasing the frequency of channel opening, $Zn^{2+}$ increased the mean burst duration of ATP-gated channels. This is the expected channel behaviour if the affinity of the receptor for the agonist had increased (Adams, 1974; Colquhoun, 1975; Neher & Sakmann, 1975). The increase in burst duration also fits well with the effect of $Zn^{2+}$ on whole-cell currents (Chapter 4), in which $Zn^{2+}$ increased the time course of current decay. Increased burst duration would contribute to both the lengthening of the decay time constant and the potentiation of current amplitude.

## Channel block

With high concentrations of $Zn^{2+}$ (100 $\mu$M), the unitary channel conductance was decreased, but the ATP channel burst duration was increased. $Zn^{2+}$ was therefore not decreasing channel open time nor was it chelating available ATP (a possibility

because of the high affinity of $Zn^{2+}$ for ATP). Thus, high concentrations of extracellular $Zn^{2+}$ can reduce $I_{ATP}$ amplitude by channel block, similar to the effects of $Zn^{2+}$ on NMDA channels (Christine & Choi, 1990).

Conclusion

The channels activated by ATP in rat SCG neurones are similar to ATP-gated channels in rat sensory neurones (Krishtal *et al.* 1988) and PC12 cells (Nakazawa & Hess, 1993) in their unitary conductance, kinetic behaviour, and voltage-dependence. They differ markedly from ATP-gated channels in other neuronal preparations, however. As discussed earlier, this may reflect expression of distinct receptor subtypes, but confirmation of this will have to await cloning of the $P_{2x}$ receptor and studies of receptor structure and composition.

The actions of low concentrations of $Zn^{2+}$ on channel activity correlate well with the whole-cell data (Chapter 4). The increase in both channel opening frequency and burst duration are consistent with $Zn^{2+}$ increasing the affinity of the $P_{2x}$ receptor for ATP. At higher concentrations, $Zn^{2+}$ blocks conductance through the channel pore. The possible physiological relevance of $Zn^{2+}$ action will be addressed in the main discussion (Chapter 6).

**A** ATP

**B** ATP + Suramin

*

*

1 pA

100ms
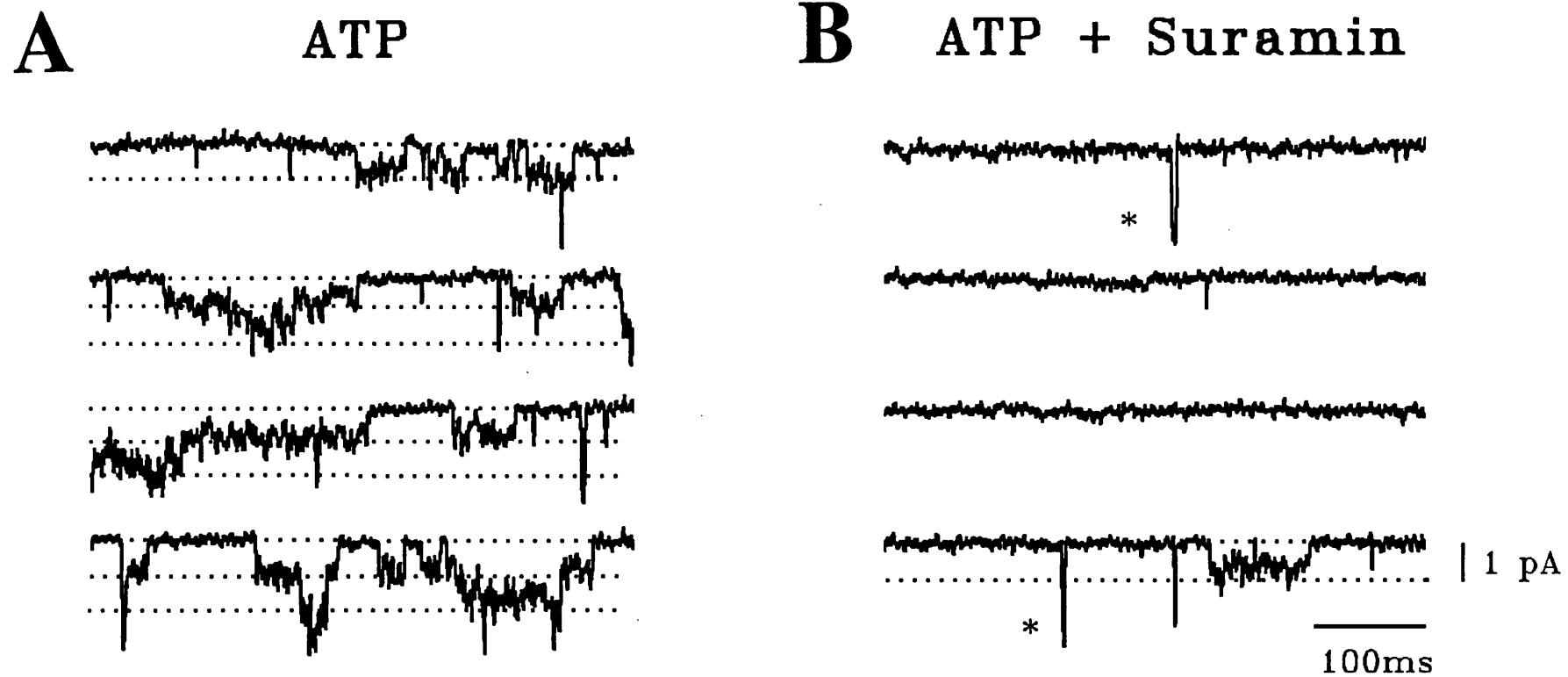
Figure 24 ATP-evoked single channel currents and block by suramin. **A.** Continuous sweeps of single channel currents recorded in an excised outside-out patch. 50 $\mu$M ATP was applied via the bath. **B.** Block of ATP-gated channel activity by 50 $\mu$M suramin in the same patch. ATP and suramin were applied via the bath following a 2 minute wash after the initial ATP application. There was one burst of ATP channels (bottom trace) in the presence of suramin. Spontaneous activity of another, larger channel can also be seen (*). Filtering = 500 Hz (-3dB Bessel); sampling = 2.5 KHz.
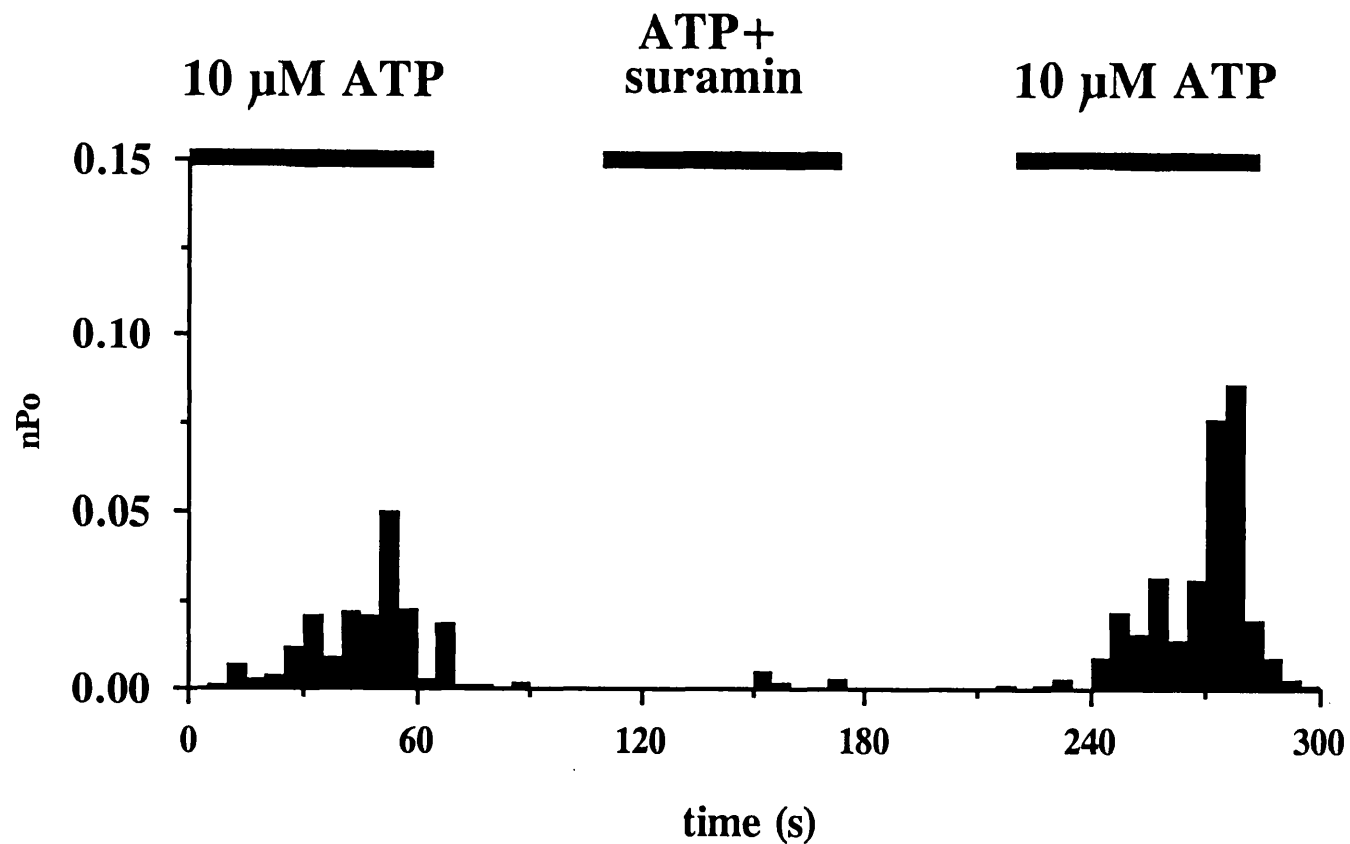
**Figure 25** Stability plot showing relative open time (nPo) measured for 5 second bins. The patch was exposed to 10 μM ATP, 10 μM ATP + 50 μM suramin, and then again to 10 μM ATP. nPo is the number of channels present in the patch multiplied by the fraction of time each channel spends in the open state over 5 second intervals. The fraction of time spent in the open state was determined by the 50% threshold crossing method.

## A

-40 mV

-80 mV

— ▽ O1

— ● O2

-120 mV

▽

← ●

1
pA

150 ms

## B

Vm (mV)

-150    -100    -50    0
0

O1

O2

-1

current (pA)

-2
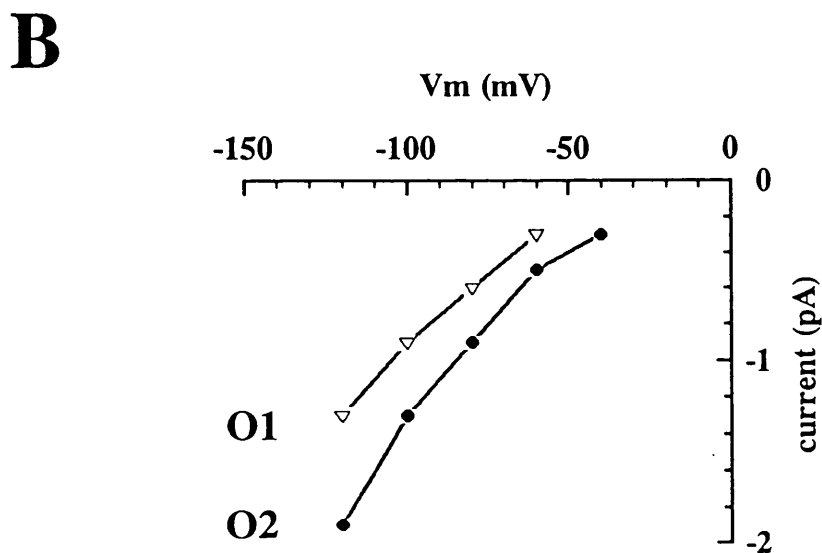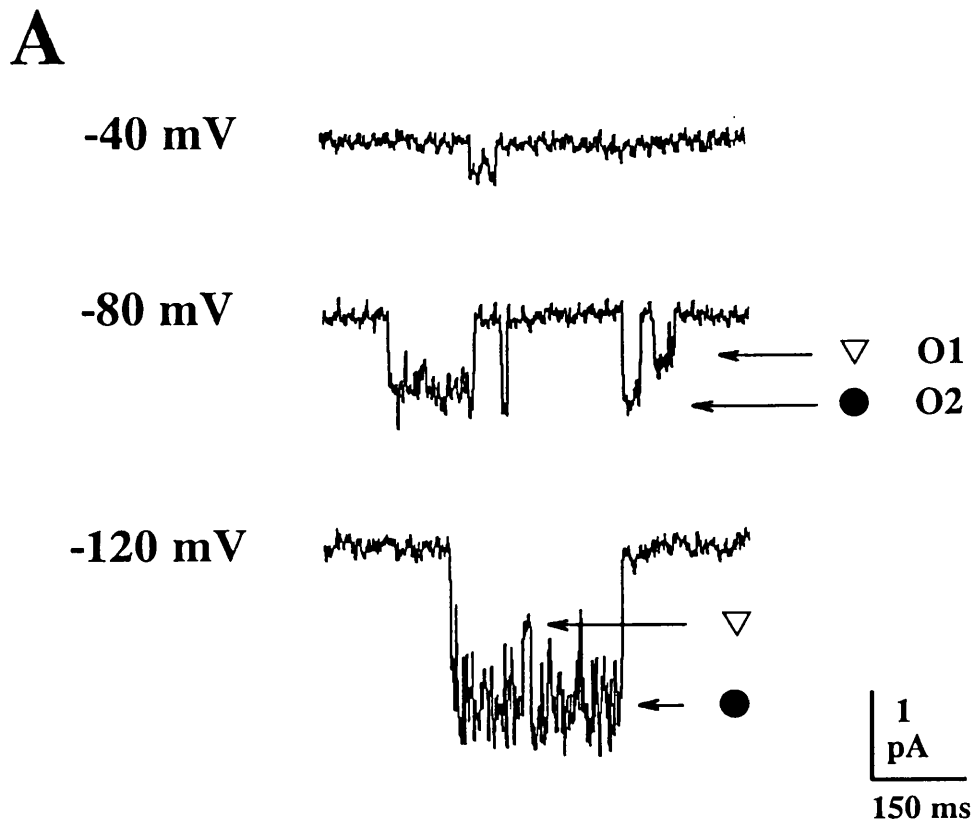
**Figure 26** Current-voltage relationship of ATP-gated channels. A. Selected traces of channel openings at three different patch potentials. Channels were activated by 5 $\mu$M ATP, bath applied. The subconductance state is denoted O1 (open triangle) and the full conductance state is denoted O2 (closed circle). Filtering = 250 Hz; sampling = 1 KHz. B. Current voltage relationship for the patch shown in part A. The patch was held at different patch potentials for 15 seconds and the current amplitude determined from Gaussian fits of the amplitude histogram. Amplitudes for the subconductance state were estimated by eye.
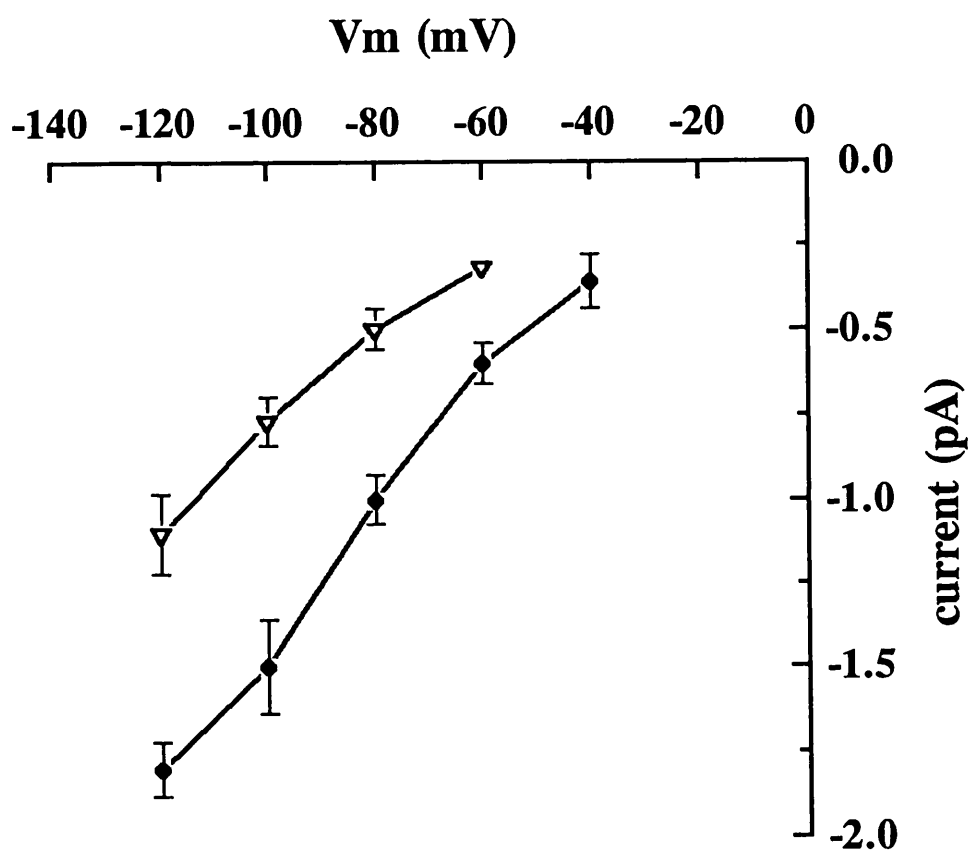
**Figure 27** Mean current-voltage relationship for ATP-gated channels. The mean amplitudes and SEM are plotted for the two open states for 8 patches (at least 3 cells for each value). The subconductance state is denoted with the open triangle and the full conductance state with the closed circle. ATP (3-10 $\mu$M) was applied via the bath. Current values were determined from Gaussian fits to the amplitude histogram for the full conductance state; for the subconductance state the amplitude was estimated by eye.
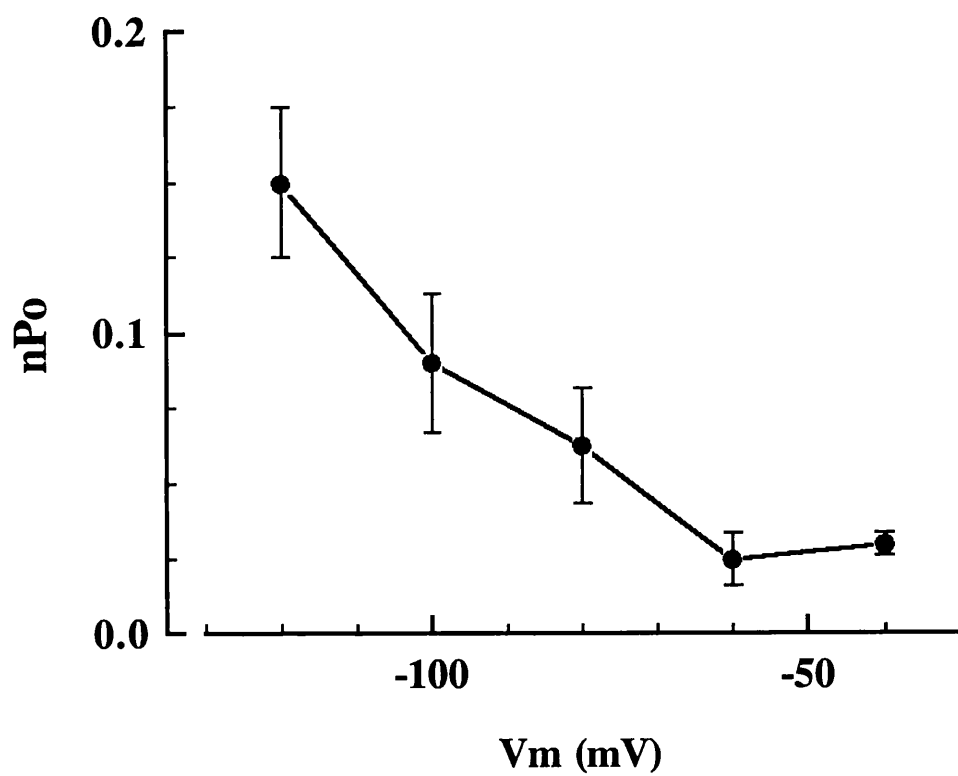
**Figure 28** Voltage-dependence of ATP-gated channels. Mean open probability (nPo) is plotted at different potentials for three patches exposed to 5 $\mu$M ATP (bath applied). The patches were held for 15 seconds at each potential (randomized).

**A**

$t_{S1}$    $t_{S2}$

C

O

$t_O$

i

**B**

.5pA

25.ms
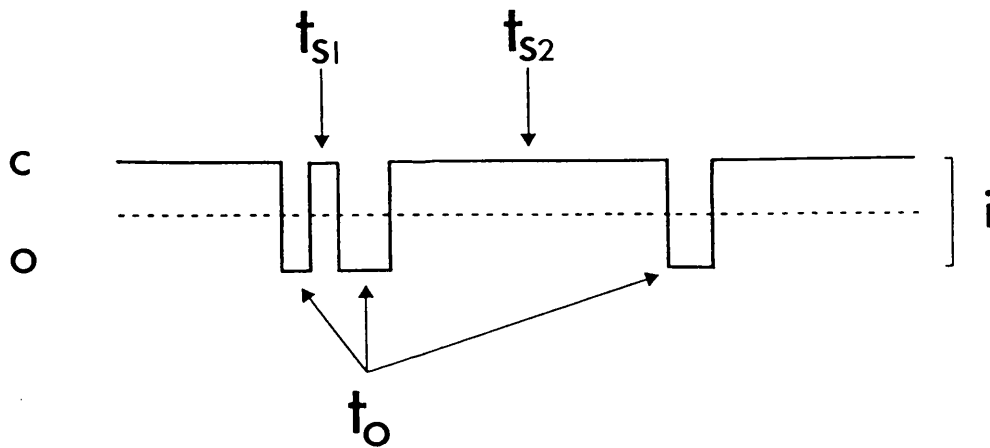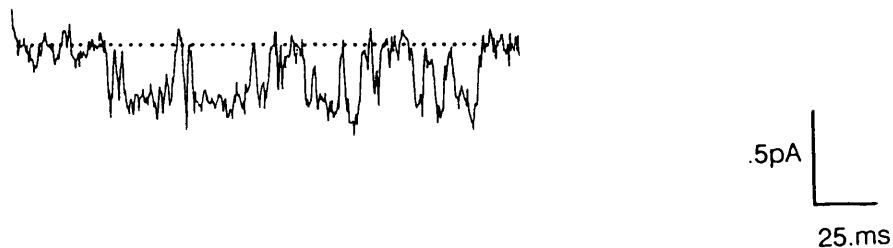
**Figure 29** Simulation of ATP-gated channel activity. A. Schematic representation of ATP-gated channel activity. The mean values of channel open ($t_o$) and shut ($t_{s1}$ and $t_{s2}$) are equal to $\tau_o = 6$ ms, $\tau_{s1} = 4$ ms, and $\tau_{s2} = 200$ ms, respectively. These values were the mean from three experiments examining channel kinetics. Channel amplitude (i) was -0.3 pA for -40 mV simulation and -1.6 pA for -120 mV simulation. Dashed line represents threshold for event detection, set at 50% channel amplitude. B. Sample trace of simulated channel activity for -40 mV holding potential.

A

-40 mV

-80 mV

-120 mV

2
pA

100 ms

B

I (pA)

3

2

1

-150    -100    -50         50    100    Vm (mV)

-1

-2

-3
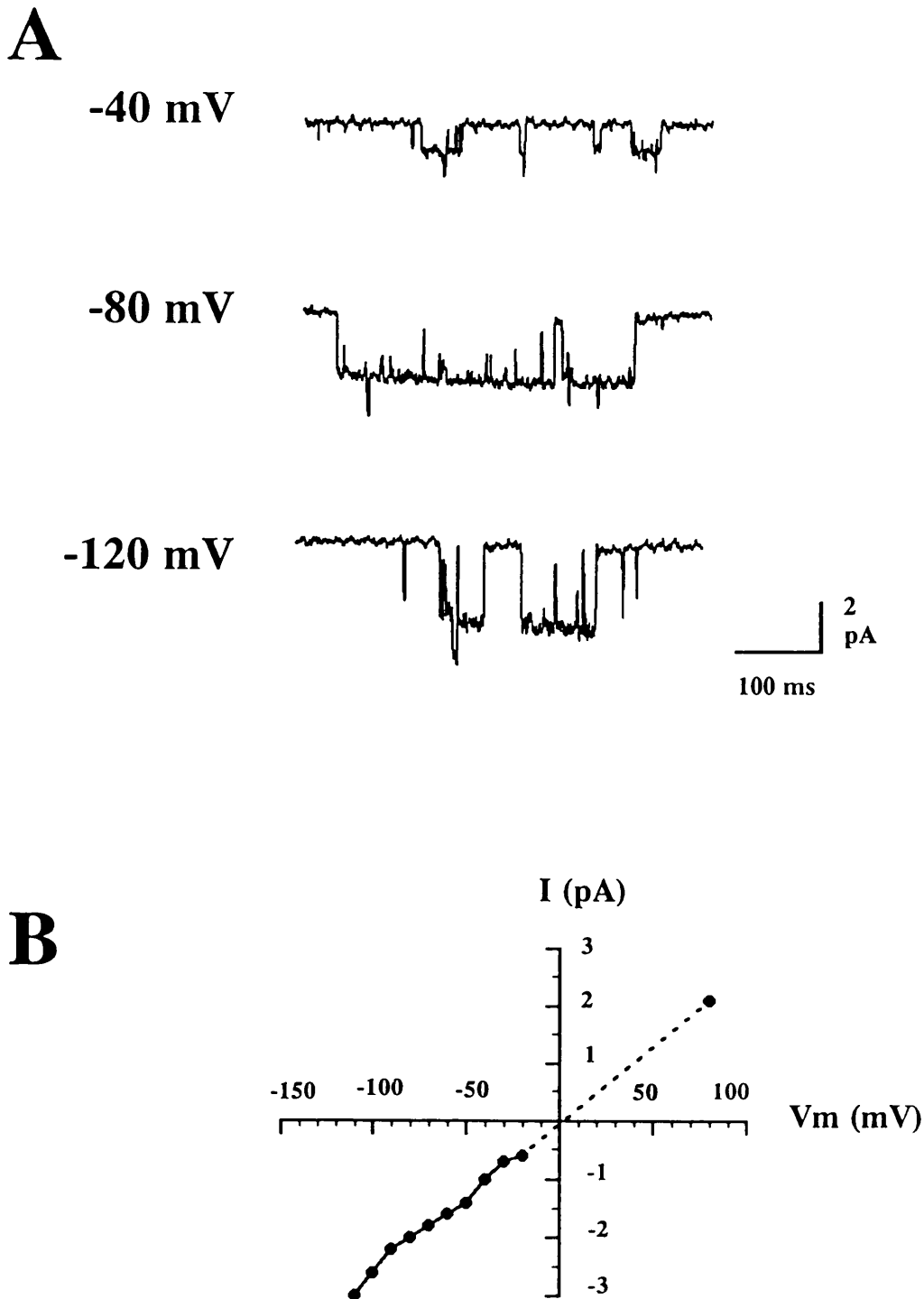
**Figure 30** Nicotinic AChR channels in SCG neurones. A. Selected traces of channels activated by DMPP in a nystatin outside-out patch at three different potentials. DMPP (10 $\mu$M) was applied via the bath. Filtering = 1 KHz; sampling = 5 KHz. B. Current-voltage relationship for DMPP-gated channel activity in the same patch as in A. The patch was held at each potential for 15 seconds and the current amplitude estimated by Gaussian fits to the amplitude histogram.

**Control/ Wash**               **5 $\mu$M Zn$^{2+}$**

ATP                             ATP               1
                                                  pA

**Averaged Currents**

                                                  0.5
                                                  pA

                                                  100 ms
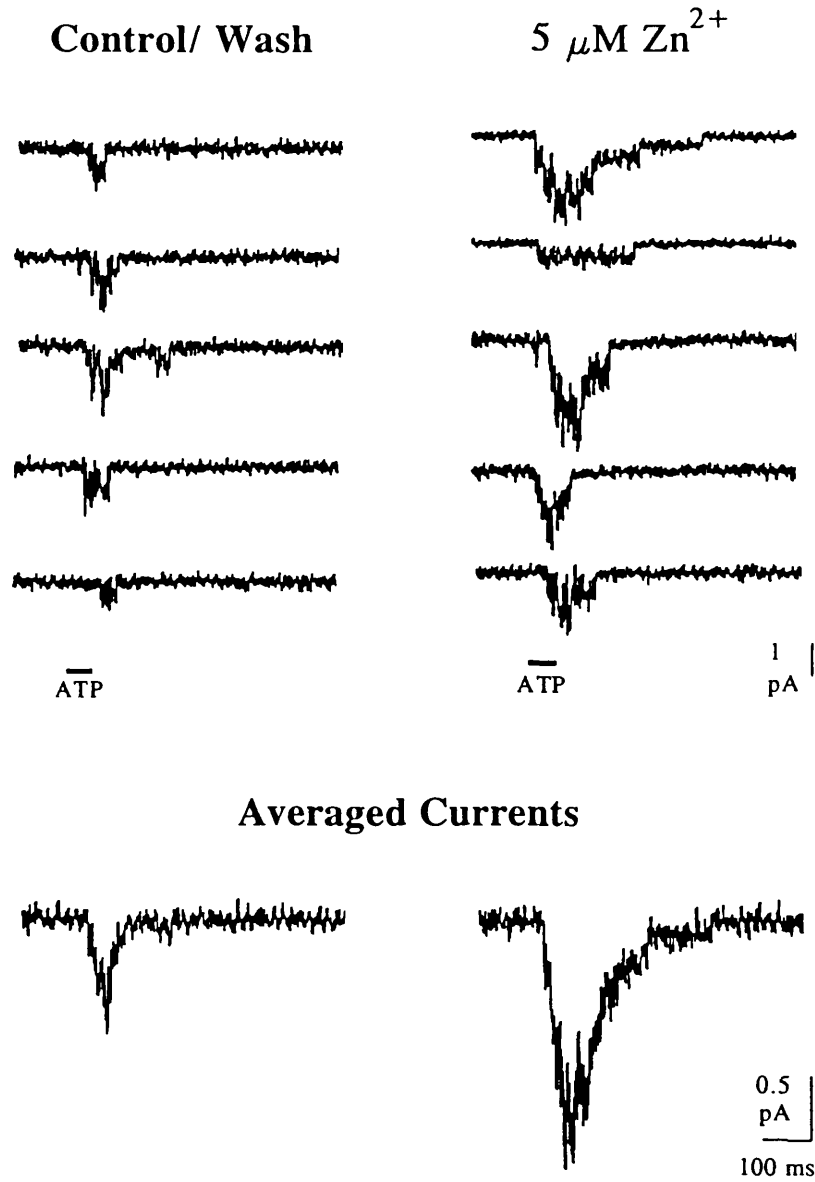
**Figure 31** Effect of Zn$^{2+}$ on ATP-gated channel activity. Single channels activated by a 50 ms application of ATP (50 $\mu$M, pressure ejection). Left hand panel shows 3 consecutive sweeps in control conditions and 2 sweeps in wash. Right hand panel shows 5 consecutive sweeps of ATP-gated channels activated in the presence of 5 $\mu$M Zn$^{2+}$. The average of 10 sweeps of control and wash (5 of each) and 5 sweeps in 5 $\mu$M Zn$^{2+}$ are shown below. Filtering = 1 KHz; sampling = 5 KHz. Patch potential = -80 mV.
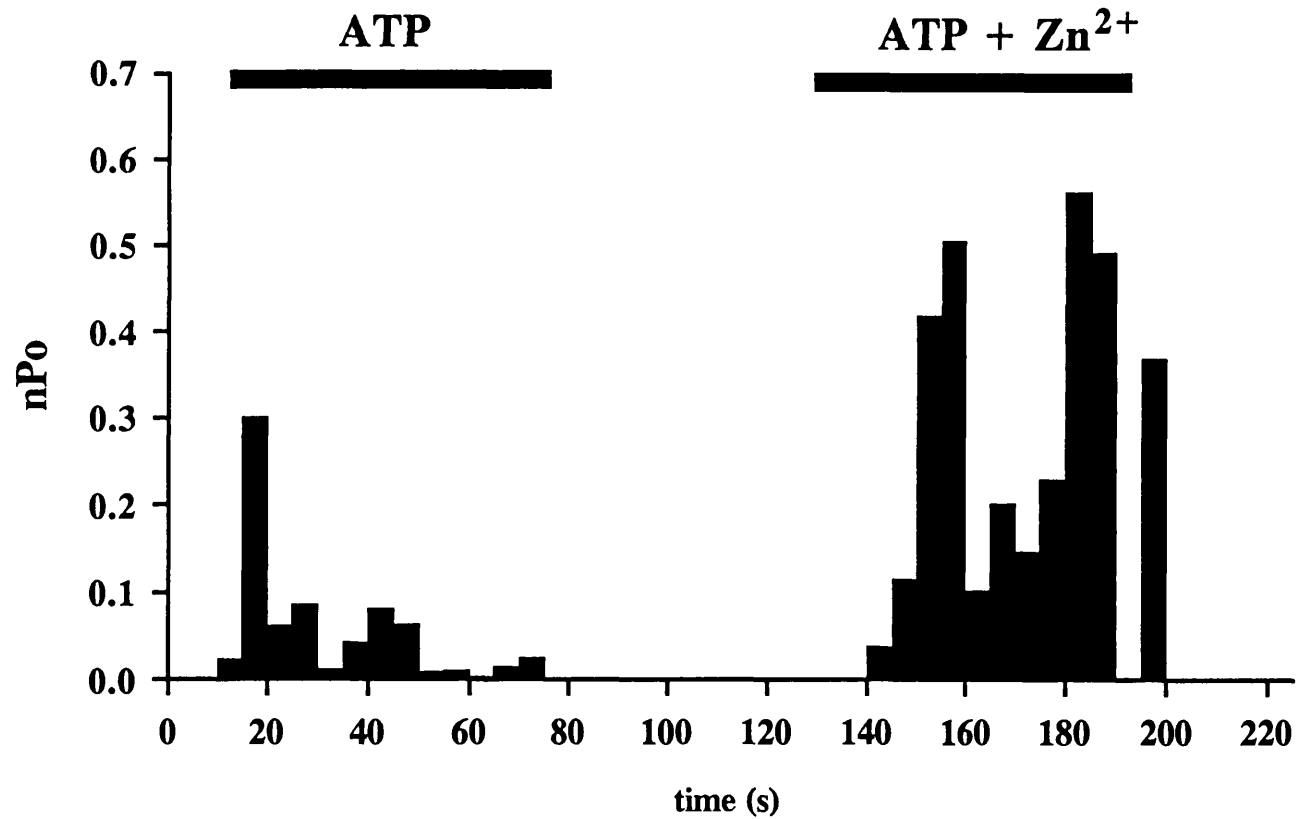
**Figure 32** Effect of $Zn^{2+}$ on ATP-gated channel activity: stability plot. Stability plot for a nystatin outside-out patch in the presence of 5 $\mu$M ATP and 5 $\mu$M ATP + 5 $\mu$M $Zn^{2+}$ (bath applied). nPo is graphed for 5 second bins and was determined as described previously. Patch potential = -80 mV.
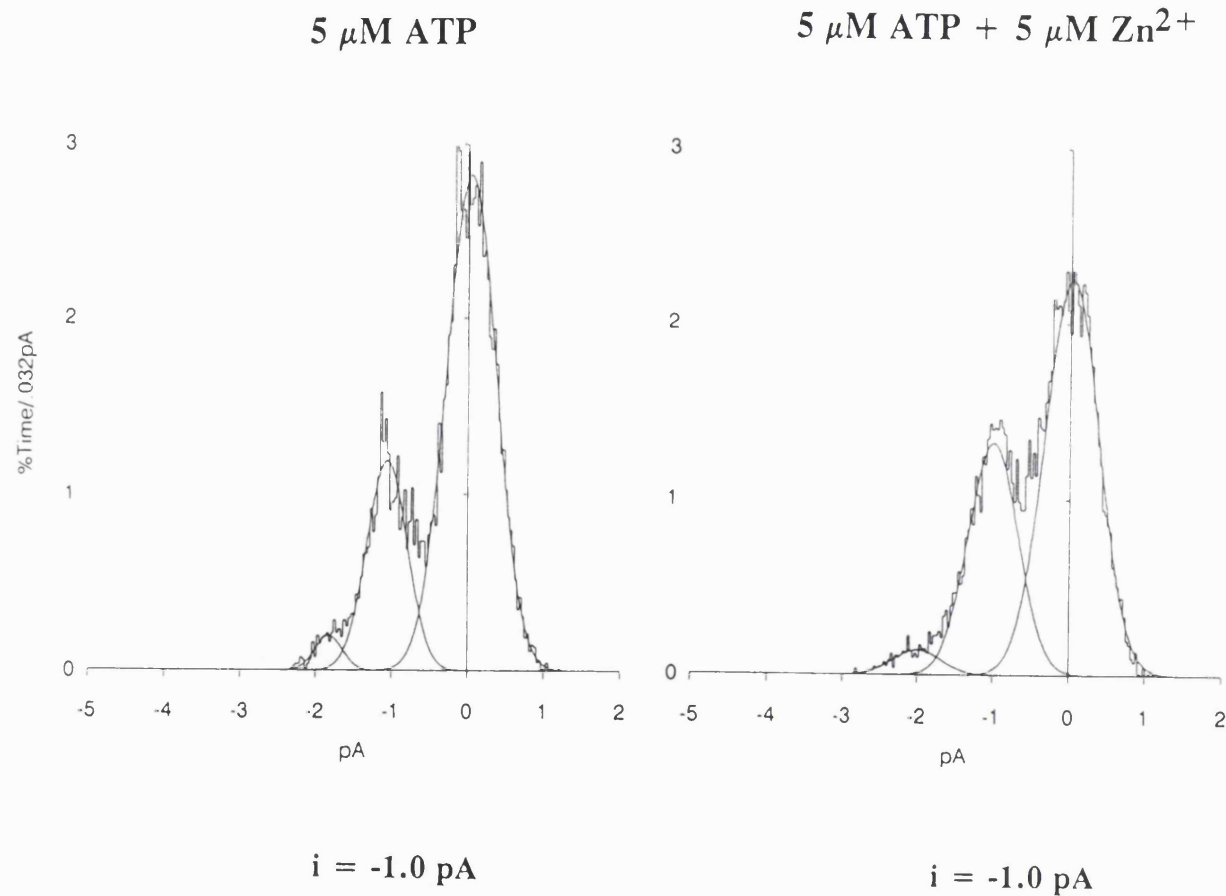
**Figure 33** Amplitude histograms for a nystatin outside-out patch exposed to 5 $\mu$M ATP (bath applied) and then 5 $\mu$M ATP + 5 $\mu$M Zn$^{2+}$. The histogram represents 10 seconds of channel activity, filtered at 250 Hz. ATP and ATP + Zn$^{2+}$ were applied for 30 seconds with a 1 minute wash between exposures. Patch potential = -80 mV. The histogram was fit by 3 Gaussian curves representing the closed state and the open states of two channels.
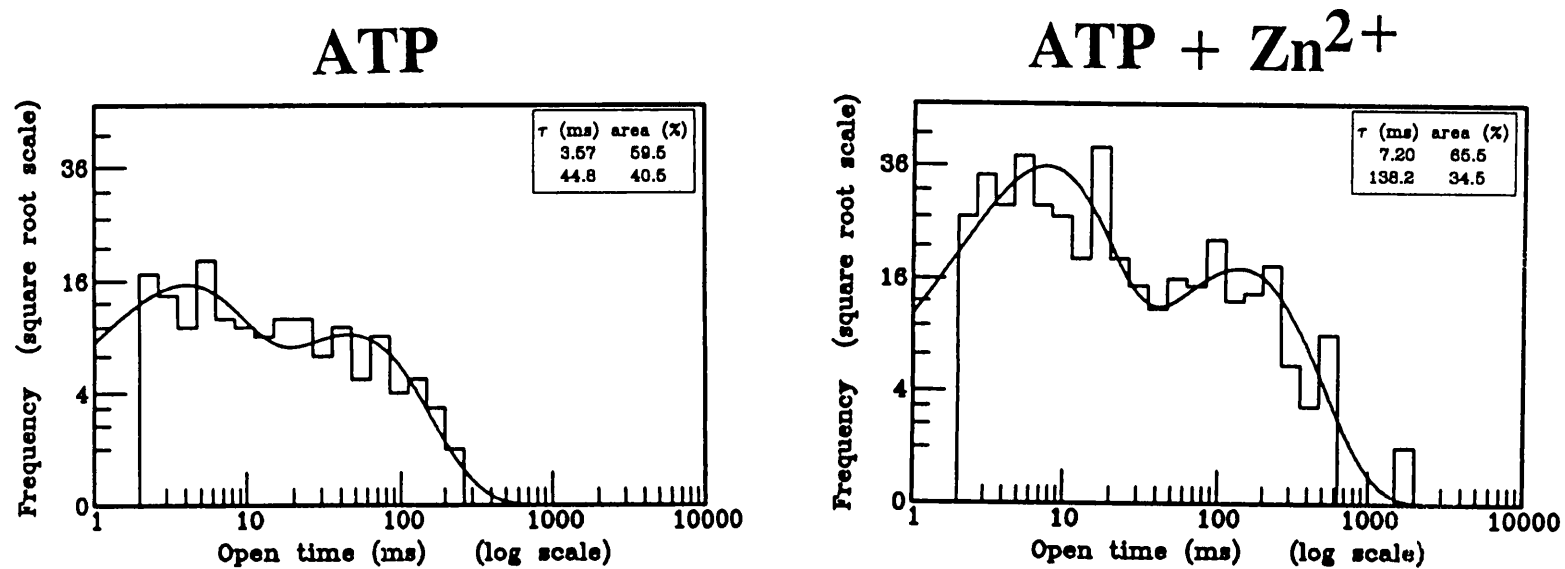
**Figure 34** Increase in channel opening frequency in the presence of $Zn^{2+}$. Open time histograms were plotted for channels recorded in an excised outside-out patch. The channels were activated by bath applied ATP (3 $\mu$M) then ATP and $Zn^{2+}$ (5 $\mu$M) for 5 minutes in each solution. The patch was washed 3 minutes between exposures. Holding potential = -80 mV; filtering = 750 Hz; sampling = 3.3 KHz. Open time distributions (8 bins/decade) were fitted using a maximum likelihood fitting routine between 2-15000 ms by the sum of two exponentials (inset shows mean taus).

# 3 μM ATP

# 3 μM ATP + 5 μM Zn$^{2+}$



3 pA

1 S
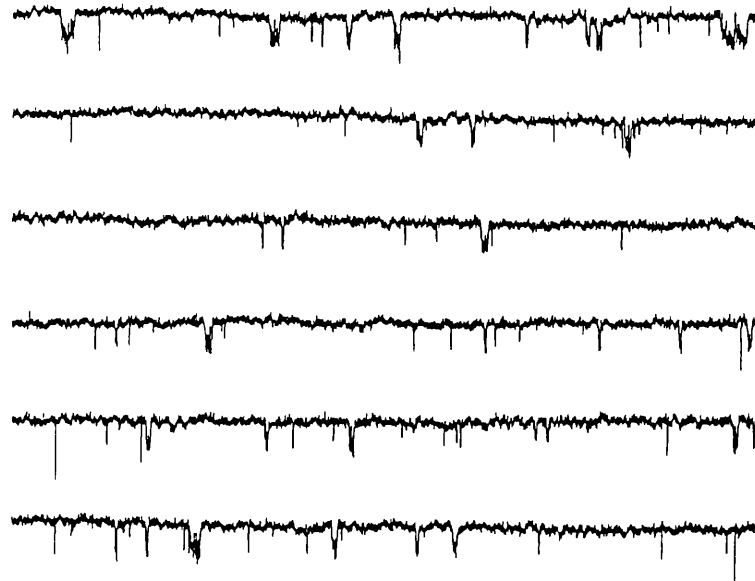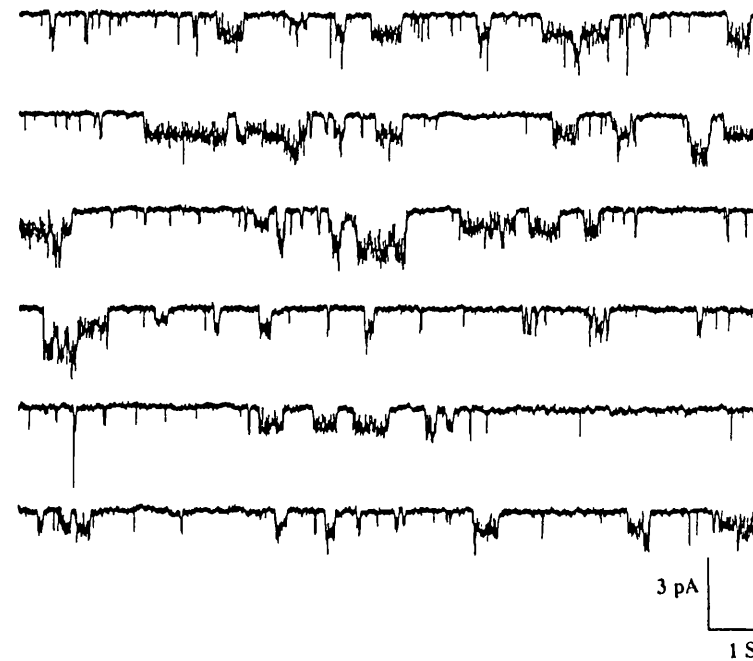
**Figure 35** Increase in channel burst duration by Zn$^{2+}$. Single channel currents were recorded in an excised outside-out patch and are plotted on a long time scale to illustrate bursting activity. Traces in the left hand panel represent 60 seconds of recording with 3 μM ATP (bath applied). Traces in the right hand panel show 60 seconds with 3 μM ATP + 5 μM Zn$^{2+}$. Patch potential = -80 mV. Filtering = 250 Hz; sampling = 1 KHz. There were at least two channels in this patch.

107

3 μM ATP

Frequency (square root scale)

64

36

16

4

0

| τ (ms) | area (%) |
|--------|----------|
| 2.07 | 49.3 |
| 127.7 | 16.4 |
| 1556. | 34.2 |

Shut time (ms)   (log scale)

1   10   100   1000   10000   100000

3 μM ATP + 5 μM Zn2+

Frequency (square root scale)

64

36

16

4

0

| τ (ms) | area (%) |
|--------|----------|
| 1.80 | 52.1 |
| 27.2 | 12.6 |
| 766.6 | 35.3 |

Shut time (ms)   (log scale)

1   10   100   1000   10000   100000
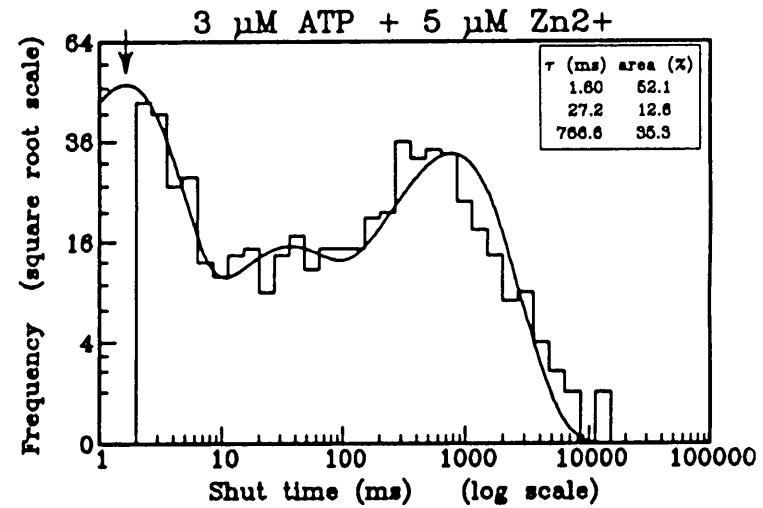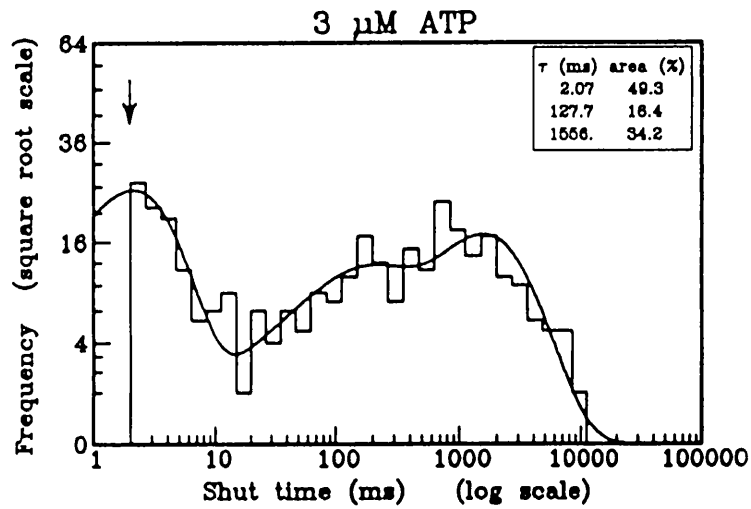
**Figure 36** Channel shut time distributions for one patch exposed to 3 μM ATP (5 min., bath applied) and 3 μM ATP + 5 μM $Zn^{2+}$ (5 min.). The patch was washed for 4 minutes between applications. Patch potential = -80 mV. Filtering = 750 Hz; sampling = 3.3 KHz. Distributions (8 bins/decade) were fitted by the sum of 3 exponentials (inset shows mean taus). The arrow indicates the shut time used to calculate $T_{crit}$ for analysis of burst duration.

# Table 2

| cell | [ATP]($\mu$M) | tau 1 | tau 2 (ms) |
|------|---------------|-------|------------|
| 1 | 3 | 6.0 | 8123 |
|   | 5 | 2.7 | 5646 |
| 2 | 3 | 2.9 | 1813 |
|   | 5 | 5.5 | 978 |
| 3 | 3 | 3.8 | 4428 |
|   | 5 | 2.7 | 1847 |

**Table 2** Components for shut time distributions of ATP-gated channels. The shut time distributions of three patches were fitted by the sum of two exponentials, tau 1 and tau 2. Tau 2 decreased with increasing concentrations of ATP while the tau 1 did not change consistently. Tau 1 was thus taken to be channel closures within a burst. The patches were exposed to each concentration of ATP for 5 minutes with a 3 minute was between exposures. The data was analyzed as described in the methods. Filtering = 750 Hz; sampling = 3.3 KHz. Holding potential for all patches = -80 mV.

# Table 3

| | 3 $\mu$M ATP | | ATP + 5 $\mu$M Zn$^{2+}$ | | |
|---|---|---|---|---|---|
| cell | T$_{crit}$ | burst | T$_{crit}$ | burst | (ms) |
| 1 | 10 | 35 | 8 | 92 | |
| 2 | 19 | 59 | 28 | 88 | |
| 3 | 9 | 54 | 21 | 114 | |

**Table 3** Mean burst durations of ATP-gated channels. The mean burst duration was calculated from idealized records by omitting closures shorter than T$_{crit}$. T$_{crit}$ was determined as five times the shortest closed time (tau 1) for each patch. Channels were activated by 3 $\mu$M ATP and ATP + 5 $\mu$M Zn2+ applied via the bath for 5 minutes with a 3 minute was between exposures. Filtering = 750 Hz; sampling = 3.3 KHz. Holding potential for all patches = -80 mV.
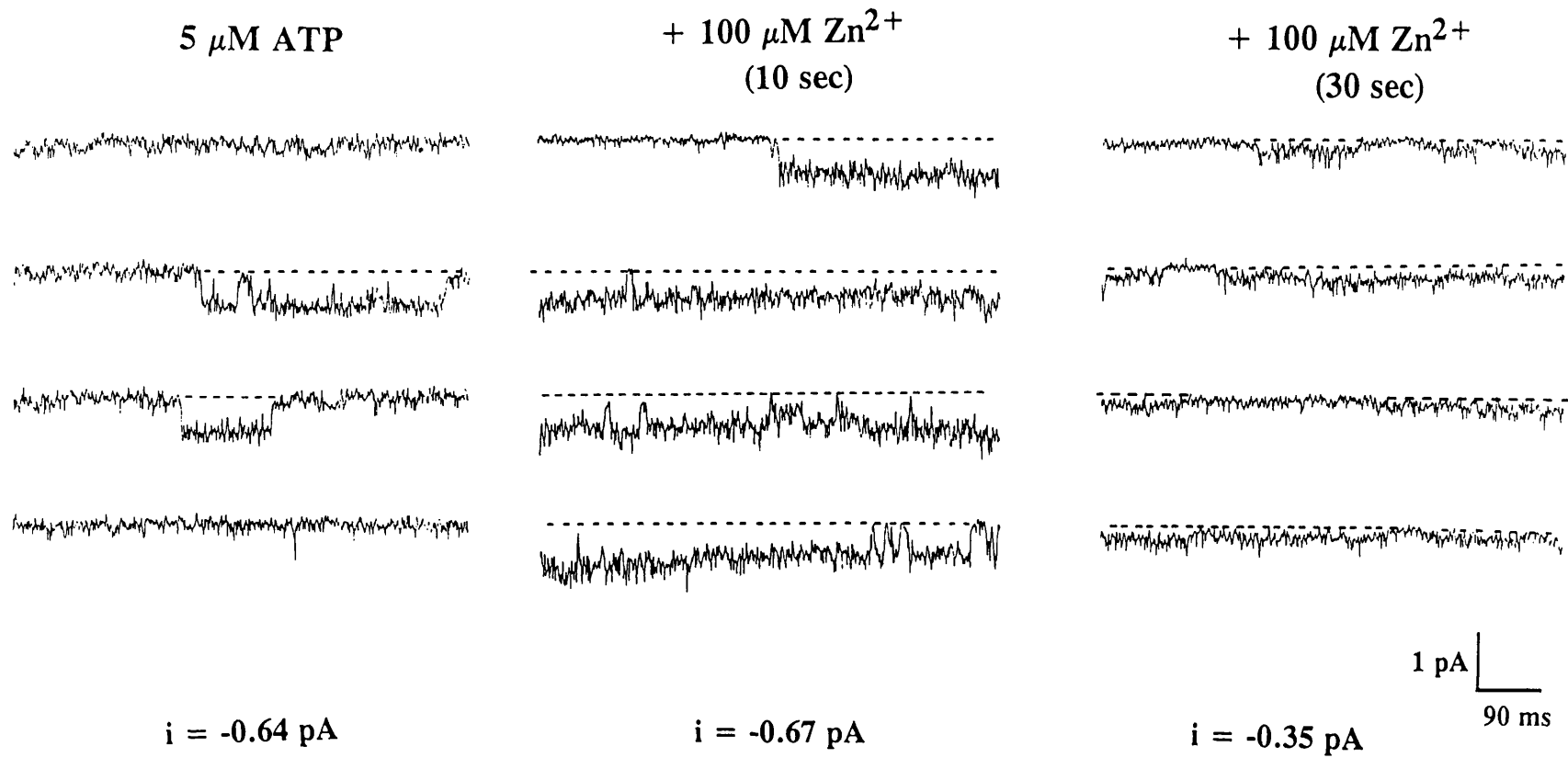
**Figure 37** Effect of high concentrations of $Zn^{2+}$ on ATP-gated channel activity. Traces from an outside-out patch exposed to 5 $\mu$M ATP and 5 $\mu$M ATP + 100 $\mu$M $Zn^{2+}$ after 10 seconds and after 30 seconds. The patch was exposed to ATP for 30 seconds, washed in control solution for 1 minute, and then exposed to ATP + $Zn^{2+}$ for 40 seconds. Filtering = 750 Hz; sampling = 3.3 KHz. Patch potential = -80 mV.

**Chapter 6:  Discussion**

The main findings of the experiments presented in this thesis are:

1) ATP activates a $P_{2x}$-purinoceptor in cultured rat SCG neurones, opening non-selective cation channels and causing a rise in intracellular $Ca^{2+}$.

2) $I_{ATP}$ is potently modulated by changes in extracellular $Zn^{2+}$ concentration. Low concentrations potentiate and high concentrations inhibit the current amplitude.

3) Single ATP-gated channels can be recorded in excised outside-out patches. The frequency of channel opening and the channel burst duration are increased in the presence of low concentrations of $Zn^{2+}$.

4) Both the whole-cell and single channel data are consistent with $Zn^{2+}$ acting to increase the apparent affinity of the $P_{2x}$-purinoceptor to ATP.

## Physiological significance of ATP

The transmitter role of ATP in sympathetic and sensory innervation of smooth muscles is well established (Burnstock, 1972; Hoyle, 1992). In addition, ATP mediates fast synaptic transmission in the medial habenula of the central nervous system (Edwards *et al.* 1992). However, the physiological function of ATP in the superior cervical ganglion is less clear. ATP is co-released with ACh (Morris & Gibbins, 1992), the primary transmitter of nerves innervating the SCG (see Skok, 1983 for review). ATP may therefore mediate a component of transmission to the SCG. This component must necessarily be very subtle, however, as studies have shown that evoked synaptic currents are completely abolished by nicotinic ACh receptor blockers (Chiappinelli & Dryer, 1984).

Another possible role of ATP is as a mediator of transmission within the ganglion. There is anatomical evidence for dendro-dendritic and dendro-somatic synapses in adult rat sympathetic ganglia (Kondo *et al.* 1980), and it has been suggested that activity in one ganglion cell could influence adjacent cells via these connections.

The functional role of these synapses and the nature of their transmitter remain to be studied.

ATP may also be important in development. In the rat, synapse formation takes place during the first three weeks after birth (Smolen & Raisman, 1980). During this time, there is substantial reorganization and elimination of numerous synaptic connections (Lichtman & Purves, 1980). There are also many axosomatic connections during this period which later disappear (Smolen & Raisman, 1980). ATP may participate in this process during development, becoming redundant at older stages. The high permeability of the ATP-activated channels to $Ca^{2+}$ could be particularly important during this time. There is evidence from neuromuscular synapses that ATP can act as a positive trophic factor during development, causing an increase in spontaneous transmitter release (Fu & Poo, 1991). This effect is dependent on $Ca^{2+}$ entry. ATP may similarly contribute to synaptic development in the non-mature SCG.

In addition to the above mentioned post-synaptic mechanisms, ATP may act presynaptically on the SCG neurones which release ATP. ATP is contained in synaptic vesicles in the rat SCG (Richards & Prada, 1977), and is released with NA (Potter *et al.* 1983; Wolinsky & Patterson, 1985; McCaman & McAfee, 1986). In addition to purinoceptors located on target cells, ATP could bind to presynaptic autoreceptors on sympathetic nerve endings. The channels are highly permeable to $Ca^{2+}$, so that binding of ATP would enhance transmitter release. Indeed, ATP has been demonstrated to induce catecholamine release in PC12 cells (Nakazawa & Inoue, 1992; Rhoads *et al.* 1993). This presynaptic action of ATP is dependent on $P_{2x}$ receptors being localized at the terminals. While this may be the case for SCG neurones, it is not true for sympathetic nerves innervating the vas deferens. In these terminals it was recently demonstrated that ATP, acting presynaptically via a G protein-linked purinoceptor, decreases transmitter release from sympathetic nerve terminals (von Kûgelgen *et al.* 1993). In other preparations as well, ATP has an inhibitory effect on transmitter release (Shinozuka *et al.* 1988). Indeed, most presynaptic modulation is

mediated by G protein-linked receptors while fast transmission is reserved for the receptor-channel complexes.

Finally, it is possible that $P_{2x}$ receptors expressed on SCG neurones do not participate in synaptic transmission at all but are expressed for other purposes. For example, ATP is released during injury, both from damaged neurones and from degranulation of platelets (Gordon, 1986). ATP, acting via purinoceptors on peripheral neurones, could thus serve as a general signalling molecule of tissue damage.

## Modulation of $I_{ATP}$ by extracellular $Zn^{2+}$

The concentration of free $Zn^{2+}$ in blood plasma is reportedly quite low (0.2 nM; Magneson et al. 1987) and below the threshold necessary to increase $I_{ATP}$. Under certain conditions, however, the concentration of $Zn^{2+}$ can rise to levels which would modulate $I_{ATP}$. As discussed in Chapter 4, $Zn^{2+}$ is sequestered in synaptic vesicles in some brain areas and can be released during cell excitability (Crawford & Connor, 1972; Assaf & Chung, 1984; Howell et al. 1984). It has been estimated that concentrations in the extracellular space could reach 300 $\mu M$ during periods of high stimulation (Assaf & Chung, 1984). This concentration would inhibit $I_{ATP}$; however, during low levels of cell activity the concentration of released $Zn^{2+}$ may be within the range to potentiate $I_{ATP}$. It will be interesting to see whether $P_{2x}$ receptors localized in high $Zn^{2+}$-containing areas are modulated by extracellular $Zn^{2+}$.

There is no evidence for vesicular $Zn^{2+}$ in the peripheral nervous system (Frederickson, 1974; Vallee & Falchuk, 1993). However, mast cells, which are found in many tissues including the SCG (Gabella, 1985), release $Zn^{2+}$ during degranulation (Kerp, 1963; Angyal & Archer, 1968). This could serve as a potential source of $Zn^{2+}$ to modulate $I_{ATP}$ in SCG cells. In addition, blood serum and cerebrospinal fluid levels of $Zn^{2+}$ change during stress (Flynn et al. 1971) and in certain disease states (Palm & Hallmans, 1982a; Palm & Hallmans, 1982b; Mody & Miller, 1985). It seems likely that under particular circumstances, $Zn^{2+}$ could influence ionic currents like $I_{ATP}$ in peripheral neurones.

## Future directions

In addition to addressing the many questions on ATP physiology, future work will likely examine $P_{2x}$ receptors at a molecular level. The cloning of the $P_{2x}$-purinoceptor will be of particular importance in the study of ATP transmission. At the present time, due to the lack of highly selective antagonists and agonists, the distribution of $P_{2x}$ receptors in the central nervous system is not known, with the exception of regions where electrophysiological responses have been assessed. Access to molecular probes will allow determination of areas where synaptic transmission may be purinergic and indicate how widespread this phenomenon is.

Characterization of $I_{ATP}$, its underlying single channels, and its modulation by extracellular $Zn^{2+}$ may contribute to structure-function studies of this channel. The receptor-ionophore has several unusual properties, including high open channel noise and voltage dependence, which will be interesting to study at the molecular level. The $Zn^{2+}$ binding site may prove to be especially useful if it is localized to particular subunits or developmentally regulated, like the $Zn^{2+}$ binding site of the $GABA_A$ receptor (Draguhn *et al.* 1990; Smart *et al.* 1991). Comparison to $Zn^{2+}$ binding domains of other ion channels may also contribute to knowledge of the structural makeup of this protein.

**<u>References</u>**

ABBRACCHIO, M.P. & BURNSTOCK, G. (1993). Purinoceptors: are there families of $P_{2x}$ and $P_{2y}$ purinoceptors? *Journal of Pharmacology and Expermental Therapeutics* (submitted).

ABERER, W., STITZEL, R., WINKLER, H. & HUBER, E. (1979). Accumulation of [$^3$H]ATP in small dense core vesicles of superfused vasa deferentia. *Journal of Neurochemistry* **33**, 797-801.

ADAMS, P.R. (1974). Kinetics of agonist conductance changes during hyperpolarization at frog endplates. *British Journal of Pharmacology* **53**, 308-310.

ADAMS, P.R. (1977). Voltage jump analysis of procaine action at frog endplate. *Journal of Physiology* **268**, 291-318.

AKASU, T., HIRAI, K. & KOKETSU, K. (1983a). Modulatory actions of ATP on membrane potentials of bullfrog sympathetic ganglion cells. *Brain Research* **258**, 313-317.

AKASU, T., HIRAI, K. & KOKETSU, K. (1983b). Modulatory actions of ATP on nicotinic transmission in bullfrog sympathetic ganglia. In *Physiology and Pharmacology of Adenosine Derivatives*, eds. DALY, J.W., KURODA, Y. & PHILLIS, J.W., pp. 165-171. New York: Raven Press.

AKASU, T. & KOKETSU, K. (1985). Effect of adenosine triphosphate on the sensitivity of the nicotinic acetylcholine-receptor in the bullfrog sympathetic ganglion cell. *Br.J.Pharmacol* **84**, 525-531.

ALLCORN, R.J., CUNNANE, T.C. & KIRKPATRICK, K. (1986). Actions of $\alpha,\beta$-methylene ATP and 6-hydroxydopamine on sympathetic neurotransmission in the vas deferens of the guinea-pig, rat and mouse: support for co-transmission. *British Journal of Pharmacology* **89**, 647-659.

ALLEN, T.G.J. & BURNSTOCK, G. (1990). The actions of adenosine 5'-triphosphate on guinea-pig intracardiac neurones in culture. *Br.J.Pharmacol* **100**, 269-276.

ANGYAL, A.M. & ARCHER, G.T. (1968). The zinc content of rat mast cells. *Australian Journal of Experimental Biology and Medical Sciences* **46**, 119-121.

ASCHER, P. & NOWAK, L. (1988). The role of divalent cations in the N-methyl-D-aspartate responses of mouse central neurones in culture. *Journal of Physiology* **399**, 247-266.

ASSAF, S.Y. & CHUNG, S. (1984). Release of endogenous $Zn^{2+}$ from brain tissue during activity. *Nature* **308**, 734-736.

BABA, A., ETOH, S. & IWATA, H. (1991). Inhibition of NMDA-induced protein kinase C translocation by a $Zn^{2+}$ chelator: implication of intracellular $Zn^{2+}$. *Brain Research* **557**, 103-108.

BARKER, J.L. & RANSOM, B.R. (1978). Pentobarbitone pharmacology of mammalian central neurones grown in tissue culture. *Journal of Physiology* **280**, 355-372.

BARRY, P.H. & LYNCH,J.W. (1991). Liquid junction potentials and small cell effects in patch-clamp analysis. *The Journal of Membrane Biology* **121**, 101-117.

BEAN, B.P. & FRIEL, D.D. (1990). ATP-activated channels in excitable cells. In *Ion Channels*, ed. NARAHASHI, T., pp. 169-203. New York: Plenum Press.

BEAN, B.P., WILLIAMS, C.A. & CEELEN, P.W. (1990a). ATP-activated channels in rat and bullfrog sensory neurons: current-voltage relation and single-channel behavior. *Journal of Neuroscience* 10, 11-19.

BEAN, B.P. (1990b). ATP-activated channels in rat and bullfrog sensory neurons: concentration dependence and kinetics. *Journal of Neuroscience* 10, 1-10.

BENHAM, C.D., BOLTON, T.B., BYRNE, N.G. & LARGE, W.A. (1987a). Action of externally applied adenosine triphosphate on single smooth muscle cells dispersed from rabbit ear artery. *Journal of Physiology* 387, 473-488.

BENHAM, C.D. & TSIEN, R.W. (1987b). A novel receptor-operated $Ca^{2+}$-permeable channel activated by ATP in smooth muscle. *Nature* 328, 275-278.

BENNET, D.W. & DRURY, A.N. (1931). Further observations relating to the physiological activity of adenine compounds. *Journal of Physiology* 72, 288-320.

BETZ, H. (1990). Ligand-gated ion channels in the brain: the amino acid receptor superfamily. *Neuron* 5, 383-392.

BURNSTOCK, G., CAMPBELL, G., BENNET, M. & HOLMAN, M.E. (1963). Inhibition of the smooth muscle of the taenia coli. *Nature* 200, 581-582.

BURNSTOCK, G., CAMPBELL, G., BENNET, M. & HOLMAN, M.E. (1964). Innervation of the guinea-pig taenia coli: are there intrinsic inhibitory nerves which are distinct from sympathetic nerves? *International Journal of Neuropharmacology* **3**, 163-166.

BURNSTOCK, G., CAMPBELL, G., SATCHELL, D. & SMYTHE, A. (1970). Evidence that adenosine triphosphate or a related nucleotide is the transmitter substance released by non-adrenergic inhibitory nerves in the gut. *British Journal of Pharmacology* **40**, 668-688.

BURNSTOCK, G. (1971). Neural Nomenclature. *Nature* **229**, 282-283.

BURNSTOCK, G. (1972). Purinergic nerves. *Pharmacological Reviews* **24**, 509-581.

BURNSTOCK, G. (1978a). A basis for distinguishing two types of purinergic receptor. In *Cell Membrane Receptors for Drugs and Hormones: A Multidisciplinary Approach*, eds. BOLIS, L. & STRAUB, R.W., pp. 107-118. New York: Raven Press.

BURNSTOCK, G., COCKS, T., KASAKOV, L. & WONG, H.K. (1978b). Direct evidence for ATP release from non-adrenergic, non-cholinergic ("purinergic") nerves in the guinea-pig taenia coli and bladder. *European Journal of Pharmacology* **49**, 145-149.

BURNSTOCK, G. & KENNEDY, C. (1985). Is there a basis for distinguishing two types of $P_2$-purinoceptor? *General Pharmacology* **16**, 433-440.

BURNSTOCK, G. & WARLAND, J.J.I. (1987). $P_2$-purinoceptors of two subtypes in the rabbit mesenteric artery: reactive blue 2 selectively inhibits responses mediated via the $P_{2y}$- but not the $P_{2x}$-purinoceptor. *British Journal of Pharmacology* **90**, 383-391.

BUSSELBERG, D., MICHAEL, D., EVANS, M.L., CARPENTER, D.O. & HAAS, H.L. (1992). Zinc ($Zn^{2+}$) blocks voltage gated calcium channels in cultured rat dorsal root ganglion cells. *Brain Research* **593**, 77-81.

CELENTANO, J.J., GYENES, M., GIBBS, T.T. & FARB, D.H. (1991). Negative modulation of the gamma-aminobutyric acid response by extracellular zinc. *Molecular Pharmacology* **40**, 766-773.

CHARTON, G., ROVIRA, C., BEN-ARI, Y. & LEVIEL, V. (1985). Spontaneous and evoked release of endogenous $Zn^{2+}$ in the hippocampal mossy fiber zone of the rat in situ. *Experimental Brain Research* **58**, 202-205.

CHIAPPINELLI, V.A. & DRYER, S.E. (1984). Nicotinic transmission in sympathetic ganglia: blockade by the snake venom neurotoxin kappa-bungarotoxin. *Neuroscience Letters* **50**, 239-244.

CHOI, D.W., YOKOYAMA, M. & KOH, J. (1988). Zinc neurotoxicity in cortical cell culture. *Neuroscience* **24**, 67-79.

CHRISTINE, C.W. & CHOI, D.W. (1990). Effect of zinc on NMDA receptor-mediated channel currents in cortical neurons. *Journal of Neuroscience* **10**, 108-116.

CLEMENTI, E., SCHEER, H., RAICHMAN, M. & MELDOLESI, J. (1992). ATP-induced $Ca^{2+}$ influx is regulated via a pertussis toxin sensitive mechanism in a PC12 cell clone. *Biochemical and Biophysical Research Commununications* **188**, 1184-1190.

CLOUES, R., JONES, S. & BROWN, D.A. (1993). $Zn^{2+}$ potentiates ATP-activated currents in rat sympathetic neurons. *Pflugers Archive* **424**, 152-158.

COLQUHOUN, D. (1975). Conductance of channels opened by acetylcholine-like drugs in muscle end-plate. *Nature* **253**, 204-206.

COLQUHOUN, D. & SHERIDAN, R.E. (1981). The modes of action of gallamine. *Proceedings of the Royal Society, London* **211**, 181-203.

CRAWFORD, I.L. & CONNOR, J.D. (1972). Zinc in maturing rat brain: hippocampal concentration and localization. *Journal of Neurochemistry* **19**, 1451-1458.

CUNNANE, T.C. & STJARNE, L. (1984). Transmitter secretion from individual varicosities of guinea-pig and mouse vas deferens: highly intermittent and monoquantal. *Neuroscience* **13**, 1-20.

CUSACK, N.J., HICKMAN, M.E. & BORN, G.V.R. (1979). Effects of D- and L-enantiomers of adenosine, AMP and ADP and their 2-chloro- and 2-azido- analogues on human platelets. *Proceedings of the Royal Society, London* **206**, 139-144.

DAVIDSON, J.S., WAKEFIELD, I.K., SOHNIUS, U., VAN DER MERWE, A.P. & MILLAR, R.P. (1990). A novel extracellular nucleotide receptor coupled phosphoinositidase-C in pituitary cells. *Endocrinology* **126**, 80-87.

DAY, T.A., SIBBALD, J.R. & KHANNA, S. (1993). ATP mediates an excitatory noradrenergic neuron input to supraoptic vasopressin cells. *Brain Research* **607**, 341-344.

DEL CASTILLO, J. & KATZ, B. (1957). Interaction at end-plate receptors between different choline derivatives. *Proceedings of the Royal Society, London* **B146**, 369-381.

DRAGUHN, A., VERDORN, T.A., EWERT, M., SEEBURG, P.H. & SAKMANN, B. (1990). Functional and molecular distinction between recombinant rat $GABA_A$ receptor subtypes by $Zn^{2+}$. *Neuron* **5**, 781-788.

DRURY, A.N. & SZENT-GYORGYI, A. (1929). The physiological activity of adenine compounds with especial reference to their action upon the mammalian heart. *Journal of Physiology* **68**, 213-237.

DUBYAK, G.R. & EL-MOATASSIM, C. (1993). Signal transduction via $P_2$-purinergic receptors for extracellular ATP and other nucleotides. *American Journal of Physiology* **265**, C577-C606.

DUNN, P.M. & BLAKELEY, A.G.H. (1988). Suramin: a reversible $P_2$-purinoceptor antagonist in the mouse vas deferens. *Br.J.Pharmacol* **93**, 243-245.

DVERGSTEN, C.L., FOSMIRE, G.J., OLLERICH, D.A. & SANDSTEAD, H.H. (1983). Alterations in the postnatal development of the cerebellar cortex due to zinc deficiency. I. Impaired acquisition of granule cells. *Brain Research* **271**, 217-226.

EDWARDS, F.A., GIBB, A.J. & COLQUHOUN, D. (1992). ATP receptor-mediated synaptic currents in the central nervous system. *Nature* **359**, 144-147.

EDWARDS, F.A. & GIBB, A.J. (1993). ATP-a fast neurotransmitter. *FEBS Letters* **325**, 86-89.

EVANS, R.J., DERKACH, V. & SURPRENANT, A. (1992). ATP mediates fast synaptic transmission in mammalian neurons. *Nature* **357**, 503-505.

FEDAN, J.S., HOGABOOM, G.K., O'DONNELL, J.P., COLBY, J. & WESTFALL, D.P. (1981). Contribution by purines to the neurogenic response of the vas deferens of the guinea pig. *European Journal of Pharmacology* **69**, 41-53.

FIEBER, L.A. & ADAMS, D.J. (1991). Adenosine triphosphate-evoked currents in cultured neurones dissociated from rat parasympathetic cardiac ganglia. *Journal of Physiology* **434**, 239-256.

FLYNN, A., PORIES, W.J., STRAIN, W.H. & HILL, O.A.JR. (1971). Mineral element correlation with adenohypophyseal-adrenal cortex function and stress. *Science* **173**, 1035-1036.

FREDERICKSON, C.J. (1974). Neurobiology of zinc and zinc-containing neurons. *International Review of Neurobiology* **31**, 145-238.

FRENCH, A.M. & SCOTT, N.C. (1983). Evidence to support the hypothesis that ATP is a co-transmitter in rat vas deferens. *Experientia* **39**, 264-265.

FRIEDMAN, B. & PRICE, J.L. (1984). Fiber systems in the olfactory bulb and cortex: a study in adult and developing rats, using the Timm method with the light and electron microscope. *Journal of Comparative Neurology* **223**, 88-109.

FRIEL, D.D. & BEAN, B.P. (1988). Two ATP-activated conductances in bullfrog atrial cells. *Journal of General Physiology* **91**, 1-27.

FRIEL, D.D. (1988). An ATP-sensitive conductance in single smooth muscle cells from the rat vas deferens. *Journal of Physiology* **401**, 361-380.

FU, W. & POO, M. (1991). ATP potentiates spontaneous transmitter release at developing neuromuscular synapses. *Neuron* **6**, 837-843.

FURSHPAN, E.J., POTTER, D.D. & MATSUMOTO, S.G. (1986). Synaptic functions in rat sympathetic neurons in microcultures. III. A purinergic effect on cardiac myocytes. *Journal of Neuroscience* **6**, 1099-1107.

GABELLA, G. (1985). Autonomic nervous system. In *The Rat Nervous System: Hindbrain and Spinal Cord*, ed. PAXINOS, G., pp. 325-353. London: Academic Press.

GARRITSEN, A., ZHANG, Y. & COOPER, D.M.F. (1992). Purinergic receptor regulation of signal transduction in NCB-20 cells. *Molecular Pharmacology* **41**, 743-749.

GORDON, J.L. (1986). Extracellular ATP: effects, sources and fate. *Biochem.J.* **233**, 309-319.

GRYNKIEWICZ, G., POENIE, M. & TSIEN, R.Y. (1985). A new generation of $Ca^{2+}$ indicators with greatly improved fluorescence properties. *The Journal of Biological Chemistry* **260**, 3440-3450.

HAMILL, O.P., MARTY, A., NEHER, E., SAKMANN, B. & SIGWORTH, F.J. (1981). Improved patch-clamp techniques for high-resolution current recording from cells and cell-free membrane patches. *Pflugers Archive* **391**, 85-100.

HARMS, L., FINTA, E.P., TSCHOPL, M. & ILLES, P. (1992). Depolarization of rat locus coeruleus neurons by adenosine 5'-triphosphate. *Neuroscience* **48**, 941-952.

HARRISON, N.L., RADKE, H.K., TALUKDER, G. & FFRENCH-MULLEN, J.M.H. (1993a). Zinc modulates transient outward current gating in hippocampal neurons. *Receptors and Channels* **1**, 153-163.

HARRISON, N.L., RADKE, H.K., TAMKUN, M.M. & LOVINGER, D.M. (1993b). Modulation of gating of cloned rat and human $K^+$ channels by micromolar $Zn^{2+}$. *Molecular Pharmacology* **43**, 482-486.

HENNING, R.H., DUIN, M., DEN HERTOG, A. & NELEMANS, A. (1993). Activation of the phospholipase C pathway by ATP is mediated exclusively through nucleotide type $P_2$-purinoceptors in C2C12 myotubes. *British Journal of Pharmacology* **110**, 747-752.

HESSE, G.W. (1979). Chronic zinc deficiency alters neuronal function of hippocampal mossy fibers. *Science* **205**, 1105-1007.

HIGASHI, H. & NISHI, S. (1982). Effect of barbiturates on the GABA receptor of cat primary afferent neurones. *Journal of Physiology* **332**, 299-314.

HIRANO, Y., OKAJIMA, F., TOMURA, H., MAJID, M.A., TAKEUCHI, T. & KONDO, Y. (1991). Change of intracellular calcium of neural cells induced by extracellular ATP. *FEBS Letters* **284**, 235-237.

HOLLMANN, M., BOULTER, J., MARON, C., BEASLEY, L., SULLIVAN, J., PECHT, G. & HEINEMANN, S. (1993). Zinc potentiates agonist-induced currents at certain splice variants of the NMDA receptor. *Neuron* **10**, 943-954.

HOLTON, F.A. & HOLTON, P. (1953). The possibility that ATP is a transmitter at sensory nerve endings. *Journal of Physiology* **119**, 50P-51P.

HOLTON, F.A. & HOLTON, P. (1954). The capillary dilator substances in dry powders of spinal roots; a possible role of adenosine triphosphate in chemical transmission from nerve endings. *Journal of Physiology* **126**, 124-140.

HOLTON, P. (1959). The liberation of adenosine triphosphate on antidromic stimulation of sensory nerves. *Journal of Physiology* **145**, 494-504.

HORN, R. & MARTY, A. (1988). Muscarinic activation of ionic currents measured by a new whole-cell recording method. *The Journal of General Physiology* **92**, 145-159.

HORNORE, E., MARTIN, C., MIRONNEAU, C. & MIRONNEAU, J. (1989). An ATP-sensitive conductance in cultured smooth muscle cells from pregnant rat myometrium. *American Journal of Physiology* **257**, C297-C305.

HOWELL, G.A., WELCH, M.G. & FREDERICKSON, C.J. (1984). Stimulation-induced uptake and release of zinc in hippocampal slices. *Nature* **308**, 736-738.

HOYLE, C.H.V. (1992). Transmission: purines. In *Autonomic Neuroeffector Mechanisms*, eds. BURNSTOCK, G. & HOYLE, C.H.V., pp. 367-407. Reading: Harwood.

HOYLE, C.V.H., KNIGHT, G.E. & BURNSTOCK, G. (1990). Suramin antagonizes responses to $P_2$-purinoceptor agonists and purinergic nerve stimumlation in the guinea-pig urinary bladder and taenia coil. *Br.J.Pharmacol* **99**, 617-621.

HUME, R.I. & THOMAS, S.A. (1988). Multiple actions of adenosine 5'-triphosphate on chick skeletal muscle. *Journal of Physiology* **406**, 503-524.

HURLEY, L.S. & SHRADER, R.E. (1972). Congenital malformations of the nervous system in zinc-deficient rats. *International Review of Neurobiology Supplement* **1**, 7-51.

IFUNE, C.K. & STEINBACH, J.H. (1991). Voltage-dependent block by magnesium of neuronal nicotinic acetylcholine receptor channels in rat phaeochromocytoma cells. *Journal of Physiology* **443**, 683-701.

IGUSA, Y. (1988). Adenosine 5'-triphosphate activates acetylcholine receptor channels in cultured Xenopus myotomal muscle cells. *Journal of Physiology* **405**, 169-185.

ITOH, M. & EBADI, M. (1982). The selective inhibition of hippocampal glutamic acid decarboxylase in zinc-induced epileptic seizures. *Neurochemical Research* **7**, 1287-1298.

JAHR, C.E. & JESSEL, T.M. (1983). ATP excites a subpopulation of rat dorsal horn neurones. *Nature* **304**, 730-733.

JOHNSON, J.W. & ASCHER, P. (1987). Glycine potentiates the NMDA response in cultured mouse brain neurons. *Nature* **325**, 529-531.

KASAKOV, L. & BURNSTOCK, G. (1983). The use of the slowly degradable analog, $\alpha,\beta$-methylene ATP, to produce desensitisation of the $P_2$-purinoceptor: effect on non-adrenergic, non-cholinergic responses of the guinea-pig urinary bladder. *European Journal of Pharmacology* **86**, 291-294.

KERP, V.L. (1963). Bedeutung von zink fur die histaminspeicherung in mastzellen. *International Archives of Allergy* **22**, 112-123.[*]

KILIC, G., MORAN, O. & CHERUBINI, E. (1993). Currents activated by GABA and their modulation by $Zn^{2+}$ in cerebellar granule cells in culture. *European Journal of Neuroscience* **5**, 65-72.

KIRKPATRICK, K. & BURNSTOCK, G. (1987). Sympathetic nerve-mediated release of ATP from the guinea-pig vas deferens is unaffected by reserpine. *European Journal of Pharmacology* **138**, 207-214.

KITANAKA, J., HASHIMOTO, H., GOTOH, M., MAYUMI, T. & BABA, A. (1992). Mechanism of extracellular ATP-stimulated phosphoinositide hydrolysis in rat glioma C6 cells. *Journal of Pharmacology and Experimental Therapeutics* **263**, 1248-1252.

KOLB, H.A. & WAKELAM, M.J.O. (1983). Transmitter-like action of ATP on patched membranes of cultured myoblasts and myotubes. *Nature* **303**, 621-623.

KONDO, H., DUN, N.J. & PAPPAS, G.D. (1980). A light and electron microscopic study of the rat superior cervical ganglion cells by intracellular HRP-labeling. *Brain Research* **197**, 193-199.

KRISHTAL, O.A., MARCHENKO, S.M. & PIDOPLICHKO, V.I. (1983). Receptor for ATP in the membrane of mammalian sensory neurones. *Brain Research* 41-45.

KRISHTAL, O.A., MARCHENKO, S.M. & OBUKHOV, A.G. (1988). Cationic channels activated by extracellular ATP in rat sensory neurons. *Neuroscience* **27**, 995-1000.

LAUGER, P. (1983). Conformational transitions of ionic channels. In *Single-channel Recording*, eds. SAKMANN, B. & NEHER, E., pp. 177-189. New York: Plenum Press.

LEGENDRE, P. & WESTBROOK, G.L. (1991). Noncompetitive inhibition of gamma-aminobutyric acid channels by zinc. *Molecular Pharmacology* **39**, 267-274.

LEVITAN, E.S. & KRAMER, R.H. (1990). Neuropeptide modulation of single calcium and potassium channels detected with a new patch clamp configuration. *Nature* **348**, 545-547.

LI, C., PEOPLES, R.W., LI, Z. & WEIGHT, F.F. (1993). $Zn^{2+}$ potentiates excitatory action of ATP on mammalian neurons. *Proceedings of the National Academy of Science* **90**, 8264-8267.

LICHTMAN, J.W. & PURVES, D. (1980). The elimination of redundant preganglionic innervation to hamster sympathetic ganglion cells in early post-natal life. *Journal of Physiology* **301**, 213-228.

LIN, M., HUME, R.I. & NUTTALL, A.L. (1993). Voltage-dependent block by neomycin of the ATP-induced whole cell current of guinea-pig outer hair cells. *Journal of Neurophysiology* **70**, 1593-1605.

LOVINGER, D.M. (1991). Inhibition of 5-HT$_3$ receptor-mediated ion current by divalent metal cations in NCB-20 neuroblastoma cells. *Journal of Neurophysiology* **66**, 1329-1337.

LU, Z. & SMITH, D.O. (1991). Adenosine 5'-triphosphate increases acetylcholine channel opening frequency in rat skeletal muscle. *Journal of Physiology* **436**, 45-56.

LUSTIG, K.D., SHIAU, A.K., BRAKE, A.J. & JULIUS, D. (1993). Expression cloning of an ATP receptor from mouse neuroblastoma cells. *Proceedings of the National Academy of Science* **90**, 5113-5117.

MACDONALD, R.L. & BARKER, J.L. (1979). Anticonvulsant and anesthetic barbiturates: different postynaptic actions in cultured mammalian neurons. *Neurology* **29**, 432-447.

MAGNESON, G.R., PUVATHINGAL, J.M. & RAY, W.J.JR. (1987). The concentrations of free $Mg^{2+}$ and free $Zn^{2+}$ in equine blood plasma. *The Journal of Biological Chemistry* **262**, 11140-11148.

MAGOSKI, N.S. & WALZ, W. (1992). Ionic dependence of a $P_2$-purinoceptor mediated depolarization of cultured astrocytes. *Journal of Neuroscience Research* **32**, 530-538.

MARRION, N.V., SMART, T.G. & BROWN, D.A. (1987). Membrane currents in adult rat superior cervical ganglia in dissociated tissue culture. *Neuroscience Letters* **77**, 55-60.

MATHIE, A., COLQUHOUN, D. & CULL-CANDY, S.G. (1990). Rectification of currents activated by nicotinic acetylcholine receptors in rat sympathetic ganglion neurones. *Journal of Physiology* **427**, 625-655.

McCAMAN, M.W. & McAFEE, D.A. (1986). Effects of synaptic activity on the metabolism and release of purines in the rat superior cervical ganglion. *Cellular and Molecular Neurobiology* **6**, 349-360.

MELDRUM, L.A. & BURNSTOCK, G. (1983). Evidence that ATP acts as a co-transmitter with noradrenaline in sympathetic nerves supplying the guinea-pig vas deferens. *European Journal of Pharmacology* **92**, 161-163.

MILEDI, R., PARKER, I. & WOODWARD, R.M. (1989). Membrane currents elicited by divalent cations in Xenopus oocytes. *Journal of Physiology* **417**, 173-195.

MODY, I. & MILLER, J.J. (1985). Levels of hippocampal calcium and zinc following kindling-induced epilepsy. *Canadian Journal of Physiological Pharmacology* **63**, 159-161.

MONOD, J., WYMAN, J. & CHANGEUX, J-P. (1965). On the nature of allosteric transitions: a plausible model. *Journal of Molecular Biology* **12**, 88-118.

MORITA, K., KATAYAMA, Y., KOKETSU, K. & AKASU, T. (1984). Actions of ATP on the soma of bullfrog primary afferent neurons and its modulating action on the GABA-induced response. *Brain Research* **293**, 360-363.

MORRIS, J.L. & GIBBINS, I.L. (1992). Co-transmission and neuromodulation. In *Autonomic Neuroeffector Mechanisms*, eds. BURNSTOCK, G. & HOYLE, C.H.V., pp. 33-120. Chur: Harwood Academic Publishers.

MOZRZYMAS, J.W. & RUZZIER, F. (1992). ATP activates junctional and extrajunctional acetylcholine receptor channels in isolated adult rat muscle fibres. *Neuroscience Letters* **139**, 217-220.

MULLE, C., LENA, C. & CHANGEUX, J-P. (1992). Potentiation of nicotinic receptor response by external calcium in rat central neurons. *Neuron* **8**, 937-945.

NAGY, A.K., SHUSTER, T.A. & DELGADO-ESCUETA, A.V. (1986). Ecto-ATPase of mammalian synaptosomes: identification and enzymic characterization. *Journal of Neurochemistry* **47**, 976-986.

NAKAZAWA, K., FUJIMORI, K., TAKANAKA, A. & INOUE, K. (1990). An ATP-activated conductance in pheochromocytoma cells and its suppression by extracellular calcium. *Journal of Physiology* **428**, 257-272.

NAKAZAWA, K., FUJIMORI, K., TAKANAKA, A. & INOUE, K. (1991). Comparison of adenosine triphosphate- and nicotine-activated inward currents in rat phaeochromocytoma cells. *Journal of Physiology* **434**, 647-660.

NAKAZAWA, K. & HESS, P. (1993). Block by calcium of ATP-activated channels in pheochromocytoma cells. *Journal of General Physiology* **101**, 377-392.

NAKAZAWA, K. & INOUE, K. (1992). Roles of $Ca^{2+}$ influx through ATP-activated channels in catecholamine release from pheochromocytoma PC12 cells. *Journal of Neurophysiology* **68**, 2026-2032.

NAKAZAWA, K. & INOUE, K. (1993). ATP- and acetylcholine-activated channels co-existing in cell-free membrane patches from rat sympathetic neuron. *Neuroscience Letters* **161**, 97-100.

NEHER, E. (1992). Correction for liquid junction potentials in patch clamp experiments. *Methods in Enzymology* **207**, 123-131.

NEHER, E. & SAKMANN, B. (1975). Voltage-dependence of drug-induced conductance in frog neuromuscular junction. *Proceedings of the National Academy of Science* **72**, 2140-2144.

NEHER, E. & STEINBACH, J.H. (1978). Local anaesthetics transiently block currents through single acetylcholine-receptor channels. *Journal of Physiology* **277**, 153-176.

NICOLL, R.A., ECCLES, J.C., OSHIMA, T. & RUBIA, F. (1975). Prolongation of hippocampal inhibitory postynaptic potentials by barbiturates. *Nature* **258**, 625-627.

NOWAK, L., BREGESTOVSKI, P., ASCHER, P., HERBERT, A. & PROCHIANTZ, A. (1984). Magnesium gates glutamate-activated channels in mouse central neurones. *Nature* **307**, 462-465.

O'CONNOR, S.E., DAINTY, I.A. & LEFF, P. (1991). Further subclassification of ATP receptors based on agonist studies. *Trends in Pharmacological Sciences* **12**, 137-141.

PALM, R. & HALLMANS, G. (1982a). Zinc and copper in multiple sclerosis. *Journal of Neurology, Neurosurgery and Psychiatry* **45**, 691-698.

PALM, R. & HALLMANS, G. (1982b). Zinc concentrations in the cerebrospinal fluid of normal adults and patients with neurological diseases. *Journal of Neurology, Neurosurgery and Psychiatry* **45**, 685-690.

PETERS, S., KOH, J. & CHOI, D.W. (1987). Zinc selectively blocks the action of N-methyl-D-aspartate on cortical neurons. *Science* **236**, 589-593.

POTTER, D.D., FURSHPAN, E.J. & LANDIS, S.C. (1983). Transmitter status in cultured rat sympathetic neurons: plasticity and multiple function. *Federation Proceedings* **42**, 1626-1632.

RANSOM, B.R. & BARKER, J.L. (1976). Pentobarbital selectively enhances GABA-mediated post-synaptic inhibition in tissue cultured mouse spinal neurons. *Brain Research* **114**, 530-535.

RASSENDREN, F.A., LORY, P., PIN, J.P. & NARGEOT, J. (1990). Zinc has opposite effects on NMDA and non-NMDA receptors expressed in Xenopus oocytes. *Neuron* **4**, 733-740.

REDDINGTON, M. & LEE, K.S. (1991). Adenosine receptor subtypes: classification and distribution. In *Adenosine in the Nervous System*, ed. STONE, T., pp. 77-102. London: Academic Press.

RHOADS, A.R., PARUI, R., VU, N-D., CADOGAN, R. & WAGNER, P.D. (1993). ATP-induced secretion in PC12 cells and photoaffinity labeling of receptors. *Journal of Neurochemistry* **61**, 1657-1666.

RICHARDS, J.G. & PRADA, M.D. (1977). Uranaffin reaction: a new cytochemical technique for the localization of adenine nucleotides in organelles storing biogenic amines. *The Journal of Histochemistry and Cytochemistry* **25**, 1322-1336.

ROBBINS, J., TROUSLARRD, J., MARSH, S.J. & BROWN, D.A. (1992). Kinetic and pharmacological properties of the m-current in rodent neuroblastoma x glioma hybrid cells. *Journal of Physiology* **451**, 159-185.

SAKMANN, B. & NEHER, E. (1983). Geometric parameters of pipettes and membrane patches. In *Single-channel Recording*, eds. SAKMANN, B. & NEHER, E., pp. 37-51. New York: Plenum Press.

SALT, T.E. & HILL, R.G. (1983). Excitation of single sensory neurones in the rat caudal trigeminal nucleus by iontophoretically applied adenosine 5'-triphosphate. *Neuroscience Letters* **35**, 53-57.

SHEN, K.-Z. & NORTH, R.A. (1993). Excitation of rat locus coeruleus neurons by adenosine 5'-triphosphate: ionic mechanism and receptor characterization. *Journal of Neuroscience* **13**, 894-899.

SHINOZUKA, K., BJUR, R.A. & WESTFALL, D.P. (1988). Characterization of prejunctional purinoceptors on adrenergic nerves of the rat caudal artery. *Naunyn-Schmiedeberg's Archives of Pharmacology* **338**, 221-227.

SILINSKY, E.M. & GERZANICH, V. (1993). On the excitatory effects of ATP and its role as a neurotransmitter in coeliac neurons of the guinea-pig. *Journal of Physiology* **464**, 197-212.

SILINSKY, E.M. & GINSBORG, B.L. (1983). Inhibition of acetylcholine release from preganglionic frog nerves by ATP but not adenosine. *Nature* **305**, 327-328.

SILINSKY, E.M. & HUBBARD, J.I. (1973). Release of ATP from rat motor nerve terminals. *Nature* **243**, 404-405.

SILLEN, L.G. & MARTELL, A.E. (1964). *Stability Constants of Metal-ion Complexes*. London: The Chemical Society.

SIM, J.A. & CHERUBINI, E. (1990). Submicromolar concentrations of zinc irreversibly reduce a calcium-dependent potassium current in rat hippocampal neurons in vitro. *Neuroscience* **36**, 623-629.

SKOK, V.I. (1983). Fast synaptic transmission in autonomic ganglia. In *Autonomic Ganglia*, ed. ELFVIN, L.G., pp. 265-279. New York: John Wiley & Sons,Ltd.

SMART, T.G. & CONSTANTI, A. (1981). A novel effect of zinc on the lobster muscle GABA receptor. *Proceedings of the Royal Society, London* **215**, 327-341.

SMART, T.G., MOSS, S.J., XIE, X. & HUGANIR, R.L. (1991). GABA$_A$ receptors are differentially sensitive to zinc: dependence on subunit composition. *British Journal of Pharmacology* **103**, 1837-1839.

SMART, T.G. (1992). A novel modulatory binding site for zinc on the GABA$_A$ receptor complex in cultured rat neurones. *Journal of Physiology* **447**, 587-625.

SMART, T.G. & CONSTANTI, A. (1991). Differential effect of zinc on the vertebrate GABA$_A$-receptor complex. *British Journal of Pharmacology* **99**, 643-654.

SMOLEN, A. & RAISMAN, G. (1980). Synapse formation in the rat superior cervical ganglion during normal development and after neonatal deafferentation. *Brain Research* **181**, 315-323.

SNEDDON, P. & BURNSTOCK, G. (1984). Inhibition of excitatory junction potentials in guinea-pig vas deferens by α,ß-methylene-ATP: further evidence for ATP and noradrenaline as cotransmitters. *European Journal of Pharmacology* **100**, 85-90.

SNEDDON, P. & WESTFALL, D.P. (1984). Pharmacological evidence that adenosine triphosphate and noradrenaline are co-transmitters in the guinea-pig vas deferens. *Journal of Physiology* **347**, 561-580.

STARKE, K., GOTHERT, M. & KILBINGER, H. (1989). Modulation of neurotransmitter release by presynaptic autoreceptors. *Physiological Reviews* **69**, 864-970.

STJARNE, L. & ASTRAND, P. (1984). Discrete events measure single quanta of adenosine 5'-triphosphate secreted from sympathetic nerves of guinea-pig and mouse vas deferens. *Neuroscience* **13**, 21-28.

STUDY, R.E. & BARKER, J.L. (1981). Diazepam and (-)-pentobarbital: fluctuation analysis reveals different mechanisms for potentiation of gamma-aminobutyric acid responses in cultured central neurons. *Proceedings of the National Academy of Science* **78**, 7180-7184.

SU, C., BEVAN, J.A. & BURNSTOCK, G. (1971). [$^3$H]Adenosine triphosphate: release during stimulation of enteric nerves. *Science* **173**, 336-338.

TAGLIALATELA, M., DREWE, J.A. & BROWN, A.M. (1993). Barium blockade of a clonal potassium channel and its regulation by a critical pore residue. *Molecular Pharmacology* **44**, 180-190.

THOMAS, S.A. & HUME, R.I. (1990). Permeation of both cations and anions through a single class of ATP-activated ion channels in developing chick skeletal muscle. *Journal of General Physiology* **95**, 569-590.

TOKIMASA, T. & AKASU, T. (1990). ATP regulates muscarine-sensitive potassium current in dissociated bull-frog primary afferent neurones. *Journal of Physiology* **426**, 241-264.

TOLKOVSKY, A.M. & SUIDAN, H.S. (1987). Adenosine 5'-triphosphate synthesis and metabolism localized in neurites of cultured sympathetic neurons. *Neuroscience* **23**, 1133-1142.

TROUSLARD, J., MARSH, S.J. & BROWN, D.A. (1993). Calcium entry through nicotinic receptor channels and calcium channels in cultured rat superior cervical ganglion cells. *Journal of Physiology* **468**, 53-71.

UENO, S., ISHIBASHI, H. & AKAIKE, N. (1992a). Perforated-patch method reveals extracellular ATP-induced $K^+$ conductance in dissociated rat nucleus solitarii neurons. *Brain Research* **597**, 176-179.

UENO, S., HARATA, N., INOUE, K. & AKAIKE, N. (1992b). ATP-gated current in dissociated rat nucleus solitarii neurons. *Journal of Neurophysiology* **68**, 778-785.

VALLEE, B.L. & FALCHUK, K.H. (1993). The biochemical basis of zinc physiology. *Physiological Reviews* **73**, 79-118.

VON KUGELGEN, I., SCHOFFEL, E. & STARKE, K. (1989). Inhibition by nucleotides acting at presynaptic $P_2$-receptors of sympathetic neuro-effector transmission in the mouse isolated vas deferens. *Naunyn-Schmiedeberg's Archives of Pharmacology* **340**, 522-532.

VON KÜGELGEN, I., KURZ, K. & STARKE, K. (1993). Axon terminal $P_2$-purinoceptors in feedback control of sympathetic transmitter release. *Neuroscience* **56**, 263-267.

WALZ, W., ILSCHNER, S., OHLEMEYER, C., BANATI, R. & KETTENMANN, H. (1993). Extracellular ATP activates a cation conductance and a $K^+$ conductance in cultured microglial cells from mouse brain. *Journal of Neuroscience* **13**, 4403-4411.

WEBB, T.E., SIMON, J., KRISHEK, B.J., BATESON, A.N., SMART, T.G., KING, B.F., BURNSTOCK, G. & BARNARD, E.A. (1993). Cloning and functional expression of a brain G-protein-coupled ATP receptor. *FEBS Letters* **324**, 219-225.

WESTBROOK, G.L. & MAYER, M.L. (1987). Micromolar concentrations of $Zn^{2+}$ antagonize NMDA and GABA responses of hippocampal neurons. *Nature* **328**, 640-643.

WIERASZKO, A. & SEYFRIED, T.N. (1989). ATP-induced synaptic potentiation in hippocampal slices. *Brain Research* **491**, 356-359.

WIERASZKO, A., GOLDSMITH, G. & SEYFRIED, T.N. (1989a). Stimulation-dependent release of adenosine triphosphate from hippocampal slices. *Brain Research* **485**, 244-250.

WIERASZKO, A. & SEYFRIED, T.N. (1989b). Increased amount of extracellular ATP in stimulated hippocampal slices of seizure prone mice. *Neuroscience Letters* **106**, 287-293.

WILLOW, M. & JOHNSTON, A.R. (1981). Pentobarbitone slows the dissociation of GABA from rat brain synaptosomal binding sites. *Neuroscience Letters* **23**, 71-74.

WILLOW, M. & JOHNSTON, G.A.R. (1980). Enhancement of GABA binding by pentobarbitone. *Neuroscience Letters* **18**, 323-327.

WOLINSKY, J.E. & PATTERSON, H.P. (1985). Potassium-stimulated purine release by cultured sympathetic neurons. *Journal of Neuroscience* **5**, 1680-1687.

WRIGHT, D.M. (1984). Zinc: effect and interaction with other cations in the cortex of the rat. *Brain Research* **311**, 343-347.

XIE, X., GERBER, U., GAHWILER, B.H. & SMART, T.G. (1993). Interaction of zinc with ionotropic and metabotropic glutamate receptors in rat hippocampal slices. *Neuroscience Letters* **159**, 46-50.

YELLEN, G. (1984). Ionic permeation and blockade in $Ca^{2+}$-activated $K^+$ channels of bovine chromaffin cells. *Journal of General Physiology* **84**, 157-186.

YOKOYAMA, M., KOH, J. & CHOI, D.W. (1986). Brief exposure to zinc is toxic to cortical neurons. *Neuroscience Letters* **71**, 351-355.

ZALEWSKI, P.D., FORBES, I.J., GIANNAKIS, C., COWLED, P.A. & BETTS, W.H. (1990). Synergy between zinc and phorbol ester in translocation of protein kinase C to cytoskeleton. *FEBS Letters* **273**, 131-134.

RIMAI, L. & HEYDE, M.E. (1970). An investigation by raman spectroscopy of the base-proton dissociation of ATP in aqueous solution and the interactions of ATP with $Zn^{++}$ and $Mn^{++}$. *Biochem Biophys Res Commun* **41**, 313-320.

# IUPS GLASGOW 1993    1 - 6 August 1993    Abstract form

For Office Use Only

Signing Author's
Participant ID#: _____

Boxes 13,14,15: **TYPE or WRITE IN BLOCK CAPITALS.**
Boxes 16a,16b: **TYPE ONLY**
You may submit only **ONE** Abstract.

**Mailing Address of Signing Author:**

[13]

Title _Ms._ Last Name _Cloues_ Initials _R_

Department _Pharmacology_

Institute _University College London_

Address _____

City _____ County/State/Province _____

Postal/Zip Code _____ Country _____

Tel. Nos: Office [____] _____ Fax [____] _____

**Symposia and Workshops:**
See list of Symposia/Workshops in the Scientific Programme. Indicate below [as a code; eg 15] your first

[14]

& second choice of Symposia/Workshops or write in **Other** to help programming and printing of your abstract.

1st Choice Code._____ 2nd Choice Code._____ or Other _____

[15]

Most abstracts will be Poster presentations however some may be selected for oral presentation
Indicate if you are **UNWILLING** to present your material orally by placing a cross here. ☐

[16a]

ZINC POTENTIATES ATP-ACTIVATED CURRENTS IN CULTURED RAT SYMPATHETIC NEURONES
CLOUES, R., JONES, S. AND BROWN, D.A.
Department of Pharmacology, University College London, London, UK

[16b]

It has recently been shown that ATP can act as a fast excitatory transmitter at
neuro-neuronal synapses in both the central and the peripheral nervous systems.
We have examined the ATP-activated inward current ($I_{ATP}$) in cultured rat
superior cervical ganglion neurones and its modulation by extracellular $Zn^{2+}$.
ATP activated a non-specific cation conductance and caused a transient rise in
intracellular $Ca^{2+}$. Activation of the current and the underlying single channels
by ATP was reversibly blocked by the $P_2$-purinoceptor antagonist, suramin. Low
concentrations of extracellular $Zn^{2+}$ rapidly and reversibly potentiated both
$I_{ATP}$ and the intracellular $Ca^{2+}$ rise. Higher concentrations of $Zn^{2+}$ reduced and
prolonged the current, consistent with open-channel block. The potentiation by
$Zn^{2+}$ was dependent on the concentration of agonist; $Zn^{2+}$ increased the sensitivit
of activation without potentiating the maximum response. These results are
consistent with two sites of action for $Zn^{2+}$: a positively acting allosteric
site which enhances current amplitude and a site, possibly within the pore, which
blocks conductance through the channel.

Signing Author's Signature _Robin Cloues_

2

SOCIETY FOR NEUROSCIENCE
# 1993 ABSTRACT FORM

Read all instructions before typing abstract.
See *Call for Abstracts* and reverse of this sheet.
Complete abstract and all boxes
at left and below before making copy
(please type or print in black ink).

## First (Presenting) Author

Provide full name (no initials), address, and phone numbers *of first author on abstract. You may present (first author) only one abstract.* (Please type or print in black ink.)

Robin Kimberly Cloues

Department of Pharmacology

University College London

Gower Street    London    WC1E 6BT

U.K.    Fax: ( 071 380 7298

Office: (071 387 7050 x327 Home: ( 081 348 1793

SMALLEST RECOMMENDED TYPE SIZE: 10 POINT

SAMPLE:
1993 Annual Meeting
Washington, D.C.
November 7–12, 1993

POSTMARK DEADLINE:

MONDAY, MAY 3, 1993

An asterisk must be placed after the sponsor's (signing member) name on the abstract.

## Presentation Preference

Check one: ☑ poster ☐ slide

## Themes and Topics

See list of themes and topics, pp. 17–18. Indicate below a first and second choice appropriate for programming and publishing your paper.

1st theme title: Excitable Membranes
_____ theme letter: C

1st topic title: ion channels: mod-ulation _____ topic number: 43

2nd theme title: Excitable Membranes
_____ theme letter: C

2nd topic title: postsynaptic mechanisms _____ topic number: 34

## Special Requests (e.g., projection/ video requirements)

**MODULATION OF SINGLE ATP-GATED CHANNEL ACTIVITY BY EXTRACELLULAR ZINC IONS IN RAT SYMPATHETIC NEURONS. R. Cloues* and D.A. Brown.** Department of Pharmacology, University College London, London WC1E 6BT, U.K.

Adenosine 5'-triphosphate (ATP) is a neurotransmitter in both the central and peripheral nervous systems. We examined ATP-activated currents and their modulation by extracellular zinc ($Zn^{2+}$) in cultured rat superior cervical ganglion cells. In whole-cell recordings, ATP activated a non-specific cation current with a null potential near 0 mV. The current was carried in part by $Ca^{2+}$ and was blocked by the $P_2$-purinoceptor antagonist, suramin. Low concentrations of $Zn^{2+}$ (0.5–10$\mu$M) strongly potentiated the current amplitude. The effect of $Zn^{2+}$ was dependent on the concentration of agonist: $Zn^{2+}$ lowered the threshold of activation without increasing the maximum response. The ATP-induced rise in intracellular $Ca^{2+}$, measured using Indo-1 fluorescence, was also enhanced by $Zn^{2+}$. Single channels activated by ATP were recorded using outside-out, nystatin-perforated vesicles. The channels were small (1.2 pA at -80 mV) and showed considerable flicker in the open state. $Zn^{2+}$ significantly increased the ATP-evoked channel open probability without affecting the unitary current amplitude. Thus, changes in the concentration of extracellular $Zn^{2+}$ may modulate activation of the receptor by ATP, thereby affecting ATP-mediated $Ca^{2+}$ entry into the cell. Supported by the Wellcome Trust.

## KEY WORDS: (see instructions p. 4)

1. purinergic
2. potentiation
3. calcium
4. patch clamp

# Zn²⁺ potentiates ATP-activated currents in rat sympathetic neurons

Robin Cloues, Susan Jones, David A. Brown

Department of Pharmacology, University College London, Gower Street, London WC1E 6BT, UK

**Abstract.** The ATP-activated inward current ($I_{ATP}$) in cultured rat superior cervical ganglion neurons and its modulation by extracellular $Zn^{2+}$ were examined. ATP activated a non-specific cation conductance and caused a transient rise in intracellular $Ca^{2+}$. The current response was specifically activated by ATP and was blocked by the $P_2$-purinoceptor antagonist, suramin. Low concentrations of extracellular $Zn^{2+}$ rapidly and reversibly potentiated both $I_{ATP}$ and the intracellular $Ca^{2+}$ rise. The potentiation by 10 µM $Zn^{2+}$ was dependent on the concentration of agonist; $Zn^{2+}$ increased the sensitivity of activation without potentiating the maximum response. Higher concentrations of $Zn^{2+}$ reduced and prolonged the current, consistent with open-channel block. We hypothesize that there exist two sites of action for $Zn^{2+}$: a positively acting allosteric site that enhances current amplitude and a site, possibly within the pore, that blocks conductance through the channel.

**Key words:** Adenosine triphosphate – Zinc – $P_2$-purinoceptor – Allosteric site

## Introduction

Adenosine 5′-triphosphate (ATP) is a well-established mediator of sympathetic transmission to various smooth muscle tissues [6, 22]. In some neurons extracellularly applied ATP can activate a cation conductance [4, 25], but it was uncertain whether ATP was actually utilized as a transmitter under physiological conditions. It was recently shown, however, that ATP can act as a fast excitatory transmitter at neuro-neuronal synapses in both the central nervous system [14] and the peripheral nervous system [15]. The examination of ATP-activated currents ($I_{ATP}$) in neurons and the identification of factors that modulate these currents will therefore be of interest.

*Correspondence to:* R. Cloues

One potential modulator of ionic conductances is the divalent transition metal zinc ($Zn^{2+}$). $Zn^{2+}$ is critical for normal development of the nervous system [13, 23], and elevated concentrations can alter neuronal activity [24, 39]. In the brain, $Zn^{2+}$ is found concentrated in axon terminals of the cortex, olfactory bulb, and hippocampus [11, 17]. This endogenous $Zn^{2+}$ can be released into the extracellular space during excitatory stimulation [2, 21], where it may influence synaptic transmission.

$Zn^{2+}$ has previously been reported to modify ionic currents gated by excitatory and inhibitory amino acids [9, 27, 32, 33, 36, 38]. In the present paper we report that $Zn^{2+}$ strongly enhances the cation current gated by ATP in rat superior cervical ganglion (SCG) neurons.

## Materials and methods

*Cell culture.* Superior cervical ganglion (SCG) neurons were cultured from 17-day Sprague-Dawley rats as previously described [30]. Cells were used after 1–4 days in culture. For intracellular $Ca^{2+}$ measurements, cells were plated onto glass coverslips.

*Electrophysiological recordings.* The whole-cell recording configuration of the tight-seal patch-clamp technique [19] was used to record currents in voltage-clamp (Axopatch-1D, Axon Instruments, California, USA). Cells were superfused by gravity (12 ml/min) with a bicarbonate-buffered Krebs' solution of the following composition (mM): NaCl 120, KCl 3, $MgCl_2$ 1.2, $NaHCO_3$ 22.6, $CaCl_2$ 2.5, D-glucose 11.1, 4-(2-hydroxyethyl)-1-piperazineethane-sulphonic acid (HEPES) 5, at room temperature. The pH was maintained at 7.4 by constantly gassing with 95% $O_2$/5% $CO_2$.

Patch electrodes were filled with a solution of the following composition (mM): potassium acetate 102.4, KCl 15.6, HEPES 40, $MgCl_2$ 1, NaOH 12, [ethylenebis(oxonitrilo)]tetraacetic acid (EGTA) 1, $CaCl_2$ 0.420 (buffered with EGTA = 100 nM), pH 7.2. Adenosine 5′-triphosphate (ATP) was applied to the cells via the bath or by pressure ejection (70–100 kPa) through a second pipette placed 5–50 µm from the cell. Data were recorded and analysed on a Ness PC-486 computer using the pClamp acquisition and analysis programs, Clampex, Clampan and Clampfit (Axon Instruments).

The ATP current amplitude was measured from the baseline holding current to the peak of the response. In some experiments, current run-down was compensated for by measuring the slope of

the line of control $I_{ATP}$ taken between exposures to $Zn^{2+}$ and adding this value to the subsequent currents. During voltage ramps, tetrodotoxin (0.5 μM) was included in the bath solution.

*Intracellular $Ca^{2+}$ measurements.* Intracellular $Ca^{2+}$ was estimated using Indo-1 fluorescence by dual-wavelength emission. The $Ca^{2+}$-sensitive dye (200 μM) was included in the patch pipette solution and the 407/488-nm emission ratio ($R$) was recorded. The pipette solution contained (mM) caesium acetate 108, CsCl 30, HEPES 10, $MgCl_2$ 1, and BAPTA 0.1. $Ca^{2+}$ concentrations were determined using the equation $[Ca^{2+}] = K_d(F_o/F_s)(R-R_{min})/(R_{max}-R)$ [18] where $R_{min} = 0.38$, $R_{max} = 4$ and $K_d(F_o/F_s) = 1400$ nM [34]. For $Ca^{2+}$-free experiments, $CaCl_2$ was omitted from the extracellular solution and $MgCl_2$ (5 mM) was added to compensate for surface charge effects.

*Chemicals.* Standard laboratory chemicals used for making solutions were purchased from BDH Limited (Poole, Dorset, UK, Analar grade). Suramin was purchased from Bayer UK Limited (Newbury, Berkshire, UK). Adenosine 5'-triphosphate and other nucleotides and nucleosides were purchased from Sigma (Dorset, UK). Indo-1 pentasodium salt was purchased from Calbiochem (Nottingham, UK).

## Results

### Effect of ATP on SCG cells

Figure 1 A (top trace) shows the voltage response of an SCG neuron to a short application of ATP. ATP caused a rapid depolarization of the cell membrane potential with a corresponding decrease in membrane resistance. In some cells the depolarization was large enough to initiate action potentials. Figure 1 A (bottom trace) shows the current underlying the ATP-induced depolarization. ATP evoked an inward current ($I_{ATP}$) accompanied by an increase in conductance. Inward currents were recorded in response to ATP in all cells tested, though the current amplitude varied between cells [mean current at $V_m$ −60 mV: 145 ± 15 pA (SEM); $n = 39$].

The current response in SCG cells declined during prolonged exposure to ATP (Fig. 1 B). The decline in amplitude in the presence of agonist was accompanied by a decrease in conductance and was relatively slow (half-time 11.5 ± 0.9 s; $n = 7$). In addition to this slow waning, ATP currents tended to run down with repeated applications of ATP, particularly with long exposures. For this reason ATP applications were kept to a short duration (< 100 ms) for most experiments.

The concentration/response relationship for $I_{ATP}$ is shown in Fig. 2 A. Responses were normalised by reference to the average of an initial and final response to 100 μM ATP for a given cell. 100 μM ATP was taken to be maximum as higher concentrations did not substantially increase current amplitude but did result in greater current rundown. The threshold for activation of $I_{ATP}$ under these conditions was 10 μM. The $EC_{50}$ value was estimated to be 45 μM (curve fit by eye).

Figure 2 B shows the current/voltage relationship for $I_{ATP}$ in one cell. The current amplitude increased as the potential was held more negative and decreased closer to 0 mV. The current/voltage curve showed strong inward
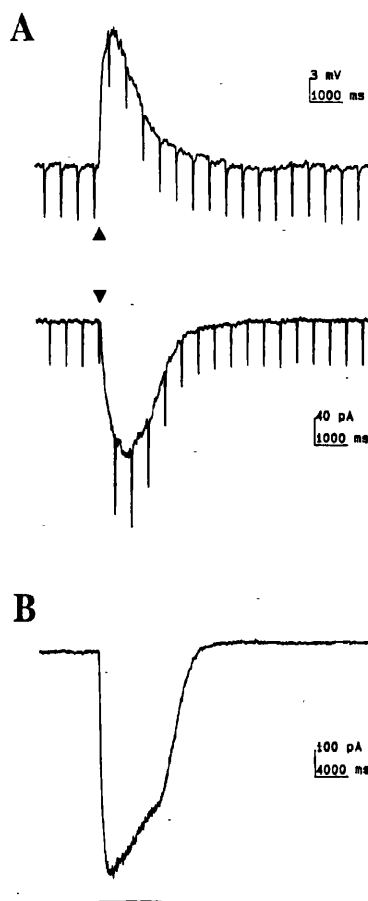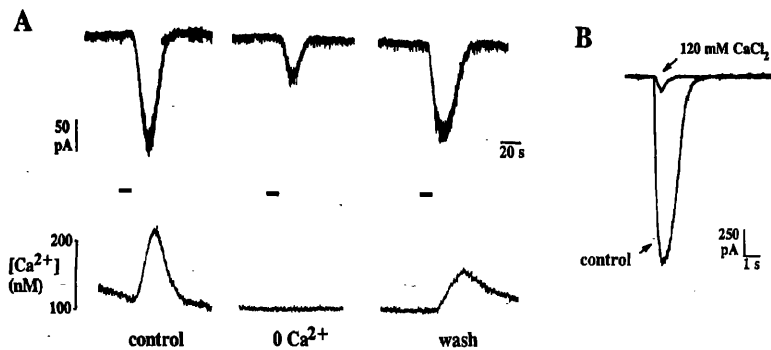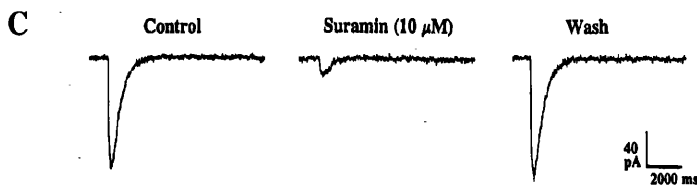


**Fig. 1 A,B.** ATP-evoked responses in rat superior cervical ganglion neurons. A Membrane voltage response recorded in current clamp (*top trace*) and underlying current response recorded in voltage clamp (*bottom trace*) to 1 mM ATP (pressure ejection, 50 ms). Downward deflections represent responses to −10 pA/−15 mV pulses (15 ms) to monitor changes in conductance. Membrane potential for both traces: −60 mV. Current trace has been filtered (100 Hz) to eliminate capacity transients. B Voltage-clamp record of response to prolonged application of 1 mM ATP (pressure ejection, 5 s). Holding potential: −60 mV

rectification; no outward currents were detected at holding potentials positive to 0 mV. The null potential in these experiments was −7 ± 4 mV ($n = 6$). This null potential does not correspond to the equilibrium potential of any individual cation present in the intra- and extracellular solutions, indicating that $I_{ATP}$ is carried through non-selective cation channels. Both the rectification and the null potential are comparable to $I_{ATP}$ currents reported in rat sensory neurons [3, 26], rat nucleus solitarii neurons [37], guinea-pig intracardiac neurons [1], and PC12 cells [31].

$I_{ATP}$ was reversibly antagonized by the $P_2$-purinoceptor antagonist suramin (Fig. 2 C). Suramin at 10−50 μM blocked the response to ATP ($n = 6$) while the $P_1$-purinoceptor antagonist theophylline (100 μM; $n = 3$) had no effect on the current. The nicotinic antagonist mecamylamine likewise did not affect $I_{ATP}$ at concentrations up to 100 μM ($n = 3$). No inward current was evoked by 100 μM adenosine ($n = 3$), ADP ($n = 4$), AMP ($n = 4$) or UTP ($n = 1$) at a holding potential of −60 mV. $I_{ATP}$ was activated by the poorly hydrolysable ATP analogue, ATP[γS] (100 μM; $n = 3$), indicating that the response

**A**



**B**
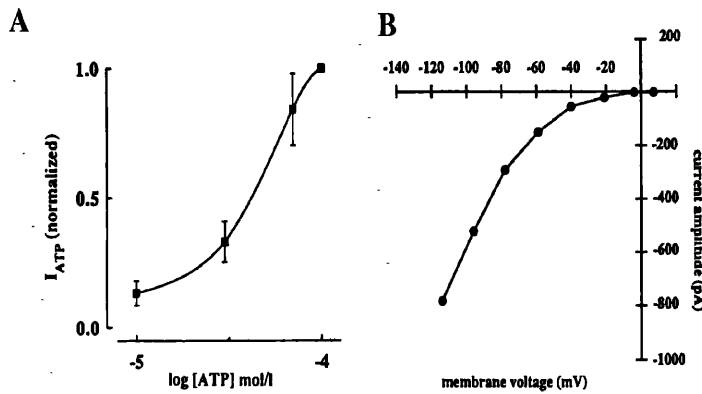


Fig. 2. A Concentration/effect curve for the ATP-activated current fit by eye. Responses were normalised to the average of an initial and final response to 100 μM ATP (bath application). Error bars are SEM ($n = 4$ for each point). B Peak current amplitude in response to 1 mM ATP (pressure ejection, 20 ms) in one cell plotted with respect to holding potential. Holding potentials were adjusted for series resistance error. C The $P_2$-purinoceptor antagonist suramin (10 μM) reversibly blocked the current response to 1 mM ATP (pressure ejection, 20 ms). Current traces are an average of three responses

**C**

Control    Suramin (10 μM)    Wash



40 pA

2000 ms

**A**



50 pA

200 [Ca²⁺] (nM) 100

20 s

control    0 Ca²⁺    wash

**B**



120 mM CaCl₂

control

250 pA 1 s

Fig. 3. A ATP causes a rise in intracellular $Ca^{2+}$. $I_{ATP}$ (top traces) was evoked by bath application of 100 μM ATP (12 s exposure at the bar) and intracellular $Ca^{2+}$ levels monitored (bottom traces). In the absence of external $Ca^{2+}$ (middle column), no rise in $Ca^{2+}$ was observed. Holding potential was −60 mV. B Comparison of currents evoked by 1 mM ATP (500 ms, pressure ejection) in control solution and with $Ca^{2+}$ as the only external cation (120 mM CaCl₂, 3.2 mM HEPES, 3.6 mM glucose). Holding potential was −90 mV

to ATP was not due to a breakdown product or to a phosphorylation reaction. The ATP-derivative, adenosine 5′-[α,β-methylene]-triphosphate (100 μM) evoked a small inward current in some cells (3/6 cells) but did not antagonize the response to ATP (up to 1 mM; $n = 2$). These results are qualitatively consistent with ATP activating a $P_2$-purinoceptor, which is thought to gate a nonspecific cation channel directly [7, 12] (see [4, 22] for review).

### Effect of ATP on intracellular [Ca²⁺]

The effect of ATP on intracellular $Ca^{2+}$ levels was estimated using Indo-1 fluorescence (Fig. 3 A). In voltage-clamped cells, ATP elicited a transient rise in $[Ca^{2+}]_i$ of $88 \pm 14$ nM ($n = 5$). No increase in $Ca^{2+}$ was observed in $Ca^{2+}$-free solution ($n = 4$), indicating that the rise is dependent on extracellular $Ca^{2+}$. For $Ca^{2+}$-free experiments, extracellular $Mg^{2+}$ was raised (to 5 mM) to compensate for surface charge effects. Under these conditions, current amplitude was decreased by $30 \pm 13\%$ ($n = 4$); in the presence of control $Ca^{2+}$ levels, addition of 5 mM $Mg^{2+}$ also reduced $I_{ATP}$ by $62 \pm 10\%$ ($n = 3$).

To determine if the ATP channels were directly permeable to $Ca^{2+}$, currents were activated in a solution containing $Ca^{2+}$ as the only cation (Fig. 3 B). In three cells, ATP evoked inward currents in 120 mM CaCl₂ which were 10%−20% the amplitude of currents recorded under control conditions.

### Effect of extracellular Zn²⁺ on $I_{ATP}$

Submillimolar concentrations of $Zn^{2+}$ had marked effects on $I_{ATP}$ (Fig. 4 A). At low concentrations (up to 10 μM) $Zn^{2+}$ enhanced current amplitude and duration. The potentiation was rapid, as illustrated in Fig. 4 B. In this cell $I_{ATP}$ was evoked and $Zn^{2+}$ was applied at the peak of the current. The amplitude of $I_{ATP}$ increased rapidly upon exposure to $Zn^{2+}$ and reversed upon its removal.

At higher concentrations, $Zn^{2+}$ reduced the amplitude of $I_{ATP}$. The dose/response relationship for $Zn^{2+}$ on $I_{ATP}$ amplitude is summarized in Fig. 4 C. The peak current amplitude was measured and the percentage enhancement by $Zn^{2+}$ plotted with respect to an initial control ATP current (no $Zn^+$ present). An increase in amplitude was detected with 500 nM $Zn^{2+}$. $Zn^{2+}$ maximally

**A**  control     10 µM Zn²⁺     wash     30 µM Zn²⁺

**B**     ATP

**C**
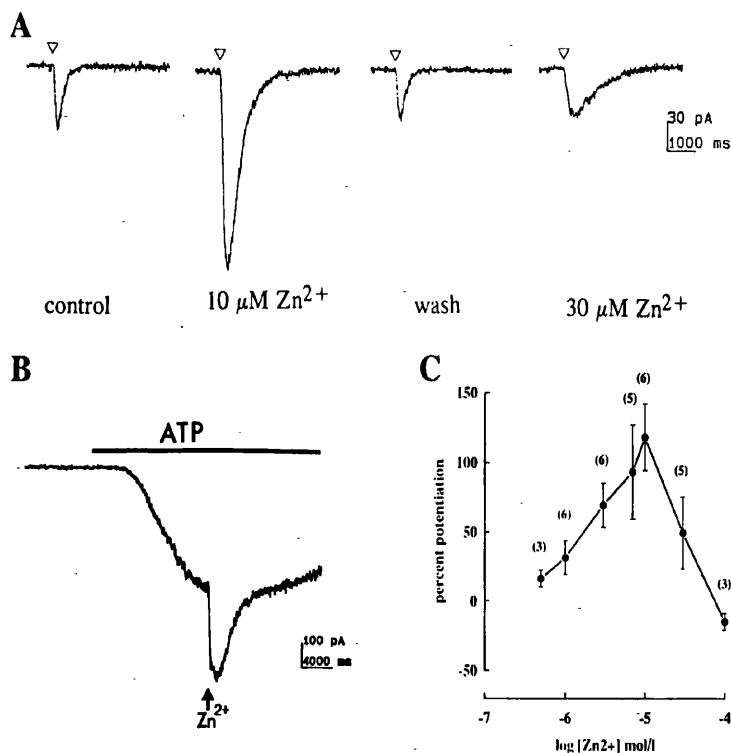


**Fig. 4A–C.** Effects of extracellular $Zn^{2+}$ on $I_{ATP}$. **A** Current responses to 1 mM ATP (20 ms, pressure ejection) in either control or $Zn^{2+}$-containing solutions. The current was enhanced by low concentrations of $Zn^{2+}$ and reduced by higher concentrations. **B** The current evoked by ATP (100 µM ATP, bath application) was rapidly potentiated by a short application of 100 µM $ZnCl_2$ (pressure ejection, 100 ms) applied at the peak of the current. **C** The percentage enhancement of ATP current amplitude compared to control plotted as a function of $ZnCl_2$ (0.5–100 µM) included in the bath. *Error bars* are SEM (number of cells listed above points)

enhanced $I_{ATP}$ at 10 µM, after which it reduced the current.

In addition to increasing current amplitude, extracellular $Zn^{2+}$ altered the kinetics of $I_{ATP}$. Figure 5 A shows $I_{ATP}$ in the absence and presence of 10 µM $Zn^{2+}$ normalized to illustrate the increase in current duration. The rate of rise of $I_{ATP}$ did not appear to change significantly in the presence of $Zn^{2+}$. Given the variability between cells (attributable to the method of ATP application), the onset kinetics were not examined further. The decay kinetics were more consistent and could be fit with a single exponential. The time constant of the decay of the current was 300–600 ms under control conditions and increased with increasing concentrations of $Zn^{2+}$. Above 10 µM $Zn^{2+}$, the decay was not fit with a single exponential. To illustrate the increase in current duration, the time from peak amplitude to half recovery was measured with increasing concentrations of $Zn^{2+}$ (Fig. 5 B). As the concentration of extracellular $Zn^{2+}$ increased, the duration of the current continued to increase despite the decrease in current amplitude.

The potentiation of $I_{ATP}$ by extracellular $Zn^{2+}$ was accompanied by an increase in conductance, indicating that it was not due to inhibition of an outward current (for example a $Ca^{2+}$-activated $K^+$ current). Also, blockers of outward currents such as tetraethylammonium (1 mM), apamin (100 nM), $d$-tubocurarine (100 µM) and charybdotoxin (10 nM) did not enhance $I_{ATP}$. It is unlikely that $Zn^{2+}$ is affecting ATPases, enzymes that break down ATP, because the response to the poorly hydrolysable ATP analogue, ATP[γS], was also potentiated by $Zn^{2+}$. Inclusion of 10 µM $Zn^{2+}$ in the patch pipette solution did not affect the mean amplitude or duration of $I_{ATP}$ ($n = 3$), suggesting that $Zn^{2+}$ acts at an external site to potentiate $I_{ATP}$.

**A**

**B**
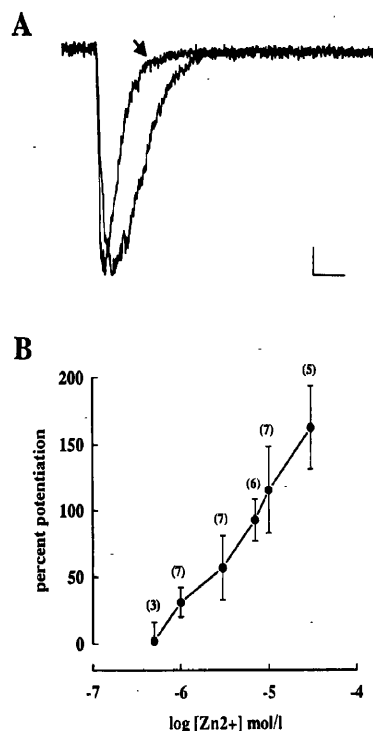


**Fig. 5 A, B.** Extracellular $Zn^{2+}$ increases $I_{ATP}$ duration. **A** Control (*arrow*) and potentiated (10 µM $Zn^{2+}$) ATP currents normalized to illustrate increase in current duration. *Scale bar* represents 30 pA for control current and 40 pA for potentiated current; 1000 ms. **B** Percentage increase in time from peak current amplitude to one-half recovery of $I_{ATP}$ compared to control current plotted as a function of $Zn^{2+}$ concentration. *Error bars* are SEM (number of cells listed above points)

Changes in the rate of "desensitization" of $I_{ATP}$ by $Zn^{2+}$ were examined. Currents were evoked with long applications of ATP in the presence and absence of $Zn^{2+}$

**A**



**B**
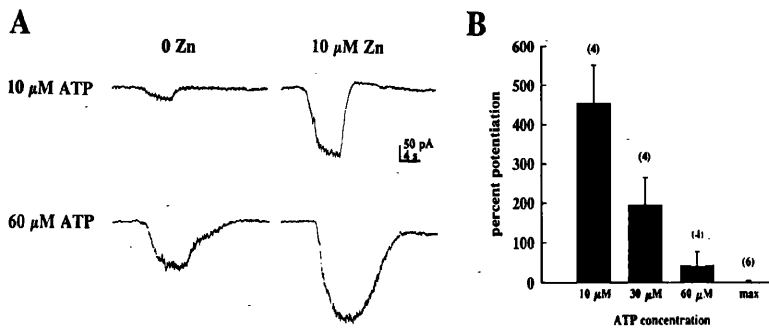


Fig. 6A, B. Potentiation by $Zn^{2+}$ is dependent on ATP concentration. A $I_{ATP}$ activated by two concentrations of ATP (bath application, 5 s exposure) in the presence and absence of $Zn^{2+}$ (10 μM). B Percentage potentiation by $Zn^{2+}$ (10 μM) of $I_{ATP}$ activated by increasing concentrations of ATP (bath application, 5 s exposure). Cells were exposed to one concentration of ATP in the presence and absence of $Zn^{2+}$ and data were pooled ($n = 4$ for each point). The maximum was obtained by pressure ejection of ATP (100 mM) for increasing durations until the current did not increase with longer durations

and the half-time of decay was measured. The half-time did not change ($n = 4$), indicating that the potentiation of $I_{ATP}$ is distinct from an effect on the slow decline during long applications. It is possible that $Zn^{2+}$ affects a fast component of desensitization that is not resolved within the time course of our application. Currents continued to run down with repeated exposure to ATP in the presence of $Zn^{2+}$.

### $Zn^{2+}$ potentiation is dependent on agonist concentration

The potentiation of $I_{ATP}$ by $Zn^{2+}$ was dependent on the concentration of agonist used to elicit the current. Figure 6 A shows the current evoked by two concentrations of ATP in the presence and absence of $Zn^{2+}$. The potentiation was greater at low concentrations and decreased as the agonist concentration increased. Figure 6 B shows the percentage enhancement by $Zn^{2+}$ of currents evoked by increasing concentrations of ATP. Because of the run-down of $I_{ATP}$, a full dose/response curve of control and potentiated currents was not feasible. Cells were therefore exposed to only one concentration of ATP in the presence and absence of $Zn^{2+}$ and the data pooled. In four cells, ATP (6–10 μM) elicited a response in the presence of $Zn^{2+}$ while there was no response under control conditions (data not shown).

To examine whether the maximum of the dose/response curve was potentiated, a supramaximal concentration of ATP (100 mM) was applied by pressure ejection to the cell. The duration of application was increased until the current amplitude reached a plateau and this was taken to be the maximal response of the cell. The maximum amplitude did not significantly change in the presence of $Zn^{2+}$ (control: $-397 \pm 61$ pA; 10 μM $Zn^{2+}$: $-389 \pm 53$ pA; $n = 6$).

### Effect of $Zn^{2+}$ on $[Ca^{2+}]_i$

In addition to potentiating $I_{ATP}$, extracellular $Zn^{2+}$ also potentiated the accompanying rise in intracellular $Ca^{2+}$. Figure 7 shows the changes in $[Ca^{2+}]_i$ for an ATP current that was strongly potentiated by $Zn^{2+}$. Data from four cells showed that $Zn^{2+}$ enhanced $I_{ATP}$ amplitude ($128 \pm 78\%$) and peak $Ca^{2+}$ rise ($132 \pm 45\%$) *pari passu* compared to control conditions.

### Effect of other divalent cations

The effect of $Zn^{2+}$ on $I_{ATP}$ was mimicked by some other divalent cations. $Ni^{2+}$ potentiated the current response to ATP but at higher concentrations than $Zn^{2+}$. 100 μM $Ni^{2+}$ maximally enhanced $I_{ATP}$ ($123 \pm 48\%$; $n = 7$). At higher concentrations, $Ni^{2+}$, like $Zn^{2+}$, blocked the current. $Cd^{2+}$ (100 μM) potentiated $I_{ATP}$ but to a smaller degree than either $Ni^{2+}$ (100 μM) or $Zn^{2+}$ (10 μM) ($38 \pm 19\%$; $n = 2$). $Ba^{2+}$ and $Mg^{2+}$ (10–100 μM) did not affect the current. Reducing external $Ca^{2+}$ from control conditions (2.5 mM) to nominally zero $Ca^{2+}$ (no added $Mg^{2+}$) increased $I_{ATP}$ amplitude by $61 \pm 20\%$ ($n = 9$). Addition of low concentrations of $Ca^{2+}$ (10–100 μM) did not potentiate $I_{ATP}$ and in fact slightly inhibited the current.

### Discussion

The principal new observations reported in this paper are that (a) ATP activates a cation current ($I_{ATP}$) in rat superior cervical ganglion neurons, which induces a substantial rise in intracellular $Ca^{2+}$, and (b) both $I_{ATP}$ and the rise in $Ca^{2+}$ are strikingly potentiated by low concentrations of $Zn^{2+}$. (A preliminary abstract noting the effect of $Zn^{2+}$ on $I_{ATP}$ has been published [28].)

The rise in $Ca^{2+}$ induced by ATP was dependent on extracellular $Ca^{2+}$. This contrasts with the effects of ATP on intracellular $Ca^{2+}$ in PC12 [10] and NG108-15 cells [20], which are not dependent upon extracellular $Ca^{2+}$. The dependence on extracellular $Ca^{2+}$, as well as the ability to record currents under conditions in which $Ca^{2+}$ is the only external cation, indicate that the $I_{ATP}$ channels in SCG cells are directly permeable to $Ca^{2+}$, as has been reported in other neuronal preparations [5, 16, 37].

$Zn^{2+}$ decreases the threshold for activation of $I_{ATP}$ so that lower concentrations of ATP are required to elicit the current, but it does not change the maximum current amplitude. At higher concentrations, $Zn^{2+}$ blocked $I_{ATP}$, leading to a prolongation of the current with a reduction in current amplitude. Blocking effects of $Zn^{2+}$ on a variety of membrane currents have previously been reported: $I_{Ca}$ [8]; $I_{KCa}$ [35]; GABA$_A$ ($\gamma$-aminobutyrate) [9, 27, 36]; NMDA ($N$-methyl-D-aspartate) [32, 38], but potentiation is much more unusual. Interestingly, non-NMDA receptors expressed in *Xenopus* oocytes are af-
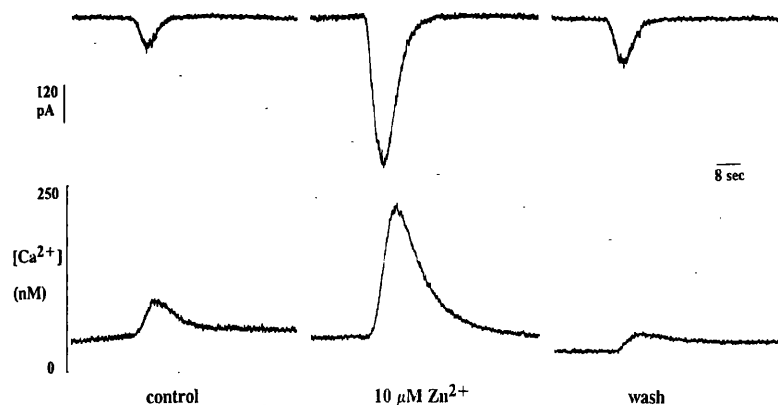
Fig. 7. $Zn^{2+}$ potentiates $[Ca^{2+}]_i$ levels during $I_{ATP}$ activation. *Top traces* show $I_{ATP}$ and *bottom traces* show intracellular $Ca^{2+}$. $I_{ATP}$ was evoked by bath application of ATP (100 µM, 5 s) under control conditions and in the presence of 10 µM $Zn^{2+}$, leaving 2 min between exposures to ATP. Traces are filtered 330 Hz

fected by $Zn^{2+}$ in much the same way as $I_{ATP}$, though at higher concentrations [32, 33, 38].

The concentration of free $Zn^{2+}$ is reportedly quite low (0.2 nM in blood plasma) [29] and below the threshold necessary to increase $I_{ATP}$. However, in several brain areas $Zn^{2+}$ is sequestered in vesicles in presynaptic terminals [11, 17] and can be released during excitatory stimulation [2, 21]. If the synaptic concentrations reached levels sufficient to augment $I_{ATP}$, then the large increase in current and most especially in $Ca^{2+}$ entry suggest that it might have important physiological consequences.

# References

1. Allen TGJ, Burnstock G (1990) The actions of adenosine 5'-triphosphate on guinea-pig intracardiac neurones in culture. Br J Pharmacol 100:269−276

2. Assaf SY, Chung S (1984) Release of endogenous $Zn^{2+}$ from brain tissue during activity. Nature 308:734−736

3. Bean BP (1990) ATP-activated channels in rat and bullfrog sensory neurons: concentration dependence and kinetics. J Neurosci 10:1−10

4. Bean BP, Friel DD (1990) ATP-activated channels in excitable cells. In: Navahashi T (ed) Ion channels. Plenum, New York, pp 169−203

5. Bean BP, Williams CA, Ceelen PW (1990) ATP-activated channels in rat and bullfrog sensory neurons: current-voltage relation and single-channel behavior. J Neurosci 10:11−19

6. Burnstock G (1972) Purinergic nerves. Pharmacol Rev 24:509−581

7. Burnstock G, Kennedy C (1985) Is there a basis for distinguishing two types of $P_2$-purinoceptor? Gen Pharmacol 16:433−440

8. Busselberg D, Michael D, Evans ML, Carpenter DO, Haas HL (1992) Zinc ($Zn^{2+}$) blocks voltage gated calcium channels in cultured rat dorsal root ganglion cells. Brain Res 593:77−81

9. Celentano JJ, Gyenes M, Gibbs TT, Farb DH (1991) Negative modulation of the gamma-aminobutyric acid response by extracellular zinc. Mol Pharmacol 40:766−773

10. Clementi E, Scheer H, Raichman M, Meldolesi J (1992) ATP-induced $Ca^{2+}$ influx is regulated via a pertussis toxin sensitive mechanism in a PC12 cell clone. Biochem Biophys Res Commun 188:1184−1190

11. Crawford IL, Connor JD (1972) Zinc in maturing rat brain: hippocampal concentration and localization. J Neurochem 19:1451−1458

12. Dunn PM, Blakeley AGH (1988) Suramin: a reversible $P_2$-purinoceptor antagonist in the mouse vas deferens. Br J Pharmacol 93:243−245

13. Dvergsten CL, Fosmire GJ, Ollerich DA, Sandstead HH (1983) Alterations in the postnatal development of the cerebellar cortex due to zinc deficiency. I. Impaired acquisition of granule cells. Brain Res 271:217−226

14. Edwards FA, Gibb AJ, Colquhoun D (1992) ATP receptor-mediated synaptic currents in the central nervous system. Nature 359:144−147

15. Evans RJ, Derkach V, Surprenant A (1992) ATP mediates fast synaptic transmission in mammalian neurons. Nature 357:503−505

16. Fieber LA, Adams DJ (1991) Adenosine triphosphate-evoked currents in cultured neurones dissociated from rat parasympathetic cardiac ganglia. J Physiol (Lond) 434:239−256

17. Friedman B, Price JL (1984) Fiber systems in the olfactory bulb and cortex: a study in adult and developing rats, using the Timm method with the light and electron microscope. J Comp Neurol 223:88−109

18. Grynkiewicz G, Poenie M, Tsien RY (1985) A new generation of $Ca^{2+}$ indicators with greatly improved fluorescence properties. J Biol Chem 260:3440−3450

19. Hamill OP, Marty A, Neher E, Sakmann B, Sigworth FJ (1981) Improved patch-clamp techniques for high-resolution current recording from cells and cell-free membrane patches. Pflügers Arch 391:85−100

20. Hirano Y, Okajima F, Tomura H, Majid MA, Takeuchi T, Kondo Y (1991) Change of intracellular calcium of neural cells induced by extracellular ATP. FEBS Lett 284:235−237

21. Howell GA, Welch MG, Frederickson CJ (1984) Stimulation-induced uptake and release of zinc in hippocampal slices. Nature 308:736−738

22. Hoyle CHV (1992) Transmission: purines. In: Burnstock G, Hoyle CHV (eds) Autonomic neuroeffector mechanisms. Harwood, Reading, pp 367−407

23. Hurley LS, Shrader RE (1972) Congenital malformations of the nervous system in zinc-deficient rats. Int Rev Neurobiol [Suppl] 1:7−51

24. Itoh M, Ebadi M (1982) The selective inhibition of hippocampal glutamic acid decarboxylase in zinc-induced epileptic seizures. Neurochem Res 7:1287−1298

25. Jahr CE, Jessel TM (1983) ATP excites a subpopulation of rat dorsal horn neurones. Nature 304:730−733

26. Krishtal OA, Marchenko SM, Pidoplichko VI (1983) Receptor for ATP in the membrane of mammalian sensory neurones. Brain Res 41−45

27. Legendre P, Westbrook GL (1991) Noncompetitive inhibition of gamma-aminobutyric acid channels by zinc. Mol Pharmacol 39:267−274

158

28. Li C, Peoples RW, Li Z, Weight FF (1992) Zinc potentiates ATP-activated inward current in rat nodose ganglion neurons. Soc Neurosci Abstr 18:1503

29. Magneson GR, Puvathingal JM, Ray WJ Jr (1987) The concentrations of free $Mg^{2+}$ and free $Zn^{2+}$ in equine blood plasma. J Biol Chem 262:11 140−11 148

30. Marrion NV, Smart TG, Brown DA (1987) Membrane currents in adult rat superior cervical ganglia in dissociated tissue culture. Neurosci Lett 77:55−60

31. Nakazawa K, Fujimori K, Takanaka A, Inoue K (1990) An ATP-activated conductance in pheochromocytoma cells and its suppression by extracellular calcium. J Physiol (Lond) 428:257−272

32. Peters S, Koh J, Choi DW (1987) Zinc selectively blocks the action of $N$-methyl-D-aspartate on cortical neurons. Science 236:589−593

33. Rassendren FA, Lory P, Pin JP, Nargeot J (1990) Zinc has opposite effects on NMDA and non-NMDA receptors expressed in Xenopus oocytes. Neuron 4:733−740

34. Robbins J, Trouslard J, Marsh SJ, Brown DA (1992) Kinetic and pharmacological properties of the m-current in rodent neuroblastoma × glioma hybrid cells. J Physiol (Lond) 451:159−185

35. Sim JA, Cherubini E (1990) Submicromolar concentrations of zinc irreversibly reduce a calcium-dependent potassium current in rat hippocampal neurons in vitro. Neuroscience 36:623−629

36. Smart TG (1992) A novel modulatory binding site for zinc on the GABA receptor complex in cultured rat neurones. J Physiol (Lond) 447:587−625

37. Ueno S, Harata N, Inoue K, Akaike N (1992) ATP-gated current in dissociated rat nucleus solitarii neurons. J Neurophysiol 68:778−785

38. Westbrook GL, Mayer ML (1987) Micromolar concentrations of $Zn^{2+}$ antagonize NMDA and GABA responses of hippocampal neurons. Nature 328:640−643

39. Wright DM (1984) Zinc: effect and interaction with other cations in the cortex of the rat. Brain Res 311:343−347